NASw-4435

Design of a Vehicle Based System to Prevent Ozone Loss

by

1993-94 NASA/USRA Advanced Senior Design Team

Final Report

June 1, 1994

Matthew D. Talbot, Leader
Steven C. Eby
Glen J. Ireland
Michael C. McWithey
Mark S. Schneider
Daniel L. Youngblood

Freshman Contributors
Matt Johnson
Chris Taylor

Prepared at Virginia Polytechnic Institute and State University
for the NASA/Universities Space Research Association
Aeronautics Advanced Design Program

W.H. Mason & N. Kirchbaum, Faculty Advisors, VPI

Department of Aerospace and Ocean Engineering
Virginia Polytechnic Institute and State University
Blacksburg, VA 24060

Design of a Vehicle Based System to Prevent Ozone Loss

Abstract

PURPOSE: This project is designed to be completed over a three year period. Overall project goals are:

1) To understand the processes that contribute to stratospheric ozone loss.
2) To determine the best scheme to prevent ozone loss.
3) To design a vehicle based system to carry out the prevention scheme.

The 1993/1994 design objectives included:

1) To review the results of the 1992/1993 design team, including a reevaluation of the key assumptions used.
2) To develop a matrix of baseline vehicle concepts as a candidates for the delivery vehicle.
3) To develop a selection criteria and perform quantitative trade studies to use in the selection of the specific vehicle concept.

OZONE HOLE: Chlorine liberated from Chlorofluorocarbons (CFCs) and natural sources initiates the destruction of stratospheric ozone though a free radical chain reaction. Reduced quantities of ozone in the atmosphere allow greater levels of ultraviolet light (UV) radiation to reach the earth's surface. High levels of UV radiation are known to cause skin cancer and mutations.

PREVENTION SCHEMES: A scheme proposed by R.J. Cicerone, Scott Elliot, and R.P. Turco in late 1991 was used for the design because of its research support and economic feasibility. This scheme uses hydrocarbon injection into the Antarctic ozone hole to form stable compounds with free chlorine, thus reducing ozone depletion. Because most ozone depletion takes place during a 3-4 week period each year, the hydrocarbon must be injected during this time window.

MISSION ANALYSIS: A mission analysis model was developed to analyze a vehicles capability to fulfill the requirement set forth by Cicerone. This model utilizes three airports and has provisions for multiple mid-air refueling of the aircraft. The critical factors in the mission model are the vehicle range, the volume of the polar vortex, the maximum propane injection plume radius achievable and the maximum propane payload for a vehicle.

PROPANE DELIVERY AND STORAGE: Propane delivery and mixing techniques were investigated to determine the best mixing technique available. This led to the exploration of blooming jet technology. However, due to the uncertainty of the jets effectiveness at

supersonic speeds and the potential for failure, the classical diffusion theory was used to determine the mixing requirements. In addition, a multi-tank storage system was designed and details of the tank and support structures integration with the aircraft were discussed.

SELECTION CRITERIA: The mixing problem, propane storage, and mission analysis studies were used to compile a set of baseline vehicle requirements and a baseline mission profile. A selection criteria was generated based on assessment of applicable existing and proposed designs in conjunction with the developed baselines.

AIRCRAFT CONFIGURATION STUDIES: Selected concepts were modeled in an aircraft synthesis code (ACSYNT). An HSCT 2.4E model and a dedicated aircraft model were developed and optimized using ACSYNT. The concepts were then further optimized using a productivity index with respect to the requirement set forth in the mission analysis code and mixing analysis details (i.e. propane injection plume radius)

ACKNOWLEDGMENTS

The authors wish to express their gratitude and appreciation to Dr. William H. Mason and Mr. Nathan Kirchbaum for their guidance and support throughout the design process. We would also like to thank Dr. Roger Simpson and Dr. Joseph Schetz for their direction and contribution to the mixing analysis.

TABLE OF CONTENTS

LIST OF FIGURES

LIST OF TABLES

NOMENCLATURE

Symbol	Definition
a	Injection nozzle radius
# of A/C	Aircraft Fleet Size
c	Mixing constant
C_{cl}	Concentration at center of plume
C_{dw}	Coefficient of Wave Drag
C_i	Concentration of propane
C_{Lmax}	Coefficient of Lift
F.S.	Factor of safety
L/D	Lift to Drag Ratio
Mean AC	Mean Aerodynamic Chord
P	Internal tank pressure
r	Plume radius
R	Internal tank radius
ρ	Density
ρ_i	Injection density
ρ_∞	Free-stream density
$\rho_{material}$	Density of tank structure material
$\rho_{propane}$	Density of propane
SFC	Specific Fuel Consumption
σ_{yield}	Yield stress
t	Propane storage tank wall thickness
t/c_{root}	Thickness to Chord Ratio at Wing Root
t/c_{tip}	Thickness to Chord Ratio at Wing Tip
TOGW	Takeoff Gross Weight
T/W	Thrust to Weight Ratio
V_{stall}	Stall Velocity
W	Weight of Aircraft
W/S	Wing Loading
x	Plume distance behind aircraft
U_i	Injection velocity
U_∞	Free-stream velocity

1.0 INTRODUCTION

Since the discovery of the Antarctica ozone hole in the late 1970's, there has been much research to determine the causes and global effects of this hole. This research has yielded a much better understanding of the factors that are its cause. With a better understanding of the causes of the hole comes a moral responsibility to work to eliminate these causes. As ozone depletion intervention schemes are researched and proven to be potentially successful, their implementation also becomes the responsibility of scientists and law-makers alike.

The project, currently in the second of a three year program, is highly multidisciplinary with significant interactions between a range of technologies and the environment. The overall goal of the NASA/USRA Advanced Design Program project is to respond to the threat of ozone. This is accomplished by 1) defining the process which contributes to stratospheric ozone loss, 2) examining possible prevention schemes and determining the best scheme to prevent ozone loss, and 3) designing a vehicle-based system to carry out the prevention scheme. Included in the 1993/1994 design objectives are a review of 1992/1993 design team results including a reevaluation of key assumptions and development of selection criteria for vehicles that potentially fulfill the baseline mission requirements.

One of the main concerns of the implementation of an active intervention scheme is the belief that human intervention into the environment is ethically wrong and at first glance the notion of injecting a compound into the atmosphere, whose reactive nature is still of some debate, may appear premature. However, the design of a vehicle that can accomplish the mission of injecting a compound into the Antarctic Ozone Hole, in a constricted time period, regardless of the chemical agent, is the main thrust of this research. The 1992/1993 design team provided this year's team with general mission guidelines and requirements. The 1993/1994 team has further refined these guidelines and requirements by making the

idea and process much more reasonable and achievable. In addition, the nature of this project is to identify or develop an aircraft that can accomplish the mission while minimizing the enormous expense required in undertaking such a global task.

The broad array of multidisciplinary design technologies may appear, at the onset, to be unrelated to one another. However, regardless of the first impression, they are intricately connected and highly dependant on one another. Figure 1-1.1 illustrates the dependence of each discipline on the others.

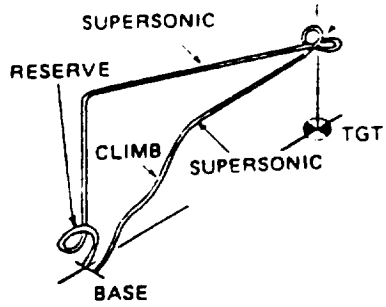

Mission Profile Model

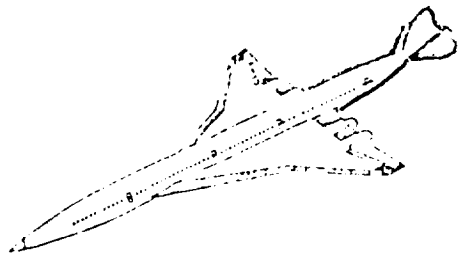

Aircraft Configuration Studies

Ozone Hole

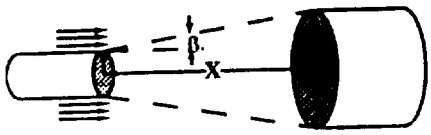

Propane Mixing Analysis

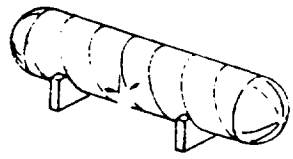

Propane Storage

Figure 1.1-1 Multidisciplinary Design

The chemical properties of ozone and the lack of ozone in the upper atmosphere above the Antarctic are at the heart of the problem, and serve as a basis for all other aspects of the design. All other aspects of the design are dependent upon these factors, and on one another. The mission analysis addresses the optimization of the parameters of the mission such that the intervention scheme can be accomplished in the efficient and cost effective manner. This optimization relies heavily on the results of the mixing analysis, the aircraft configuration studies, and to some extent, the injection compound storage system.

Prevention schemes that will be discussed later require precise concentrations of propane to be injected and mixed into the atmosphere. The mixing analysis defines a method to ensure that the proper propane concentrations are acheived in the polar vortes. This method also determines the attainable propane plume radius which in turn dictates the payload required for each mission. Propane storage then plays a pivotal role in the aircraft configuration by requiring a specific storage volume due to the chemical composition of ozone, the amount required for a proper mixture between chlorine and propane, and the duration of the mission (determined using the mission profile model).

The storage system for the injection compound is intimately dependent upon the volume over which injection is to take place (i.e., the Antarctic ozone hole), the rate of injection, and the size and range of the delivery vehicle. These factors all define the necessary storage capacity for the tank system.

Aircraft configuration studies are used to research possible delivery vehicle concepts, select a concept with respect to baseline delivery vehicle parameters and selection criteria, and size a concept. The aircraft configuration studies depended on the storage tank studies to find out the volume and mass of the tanks a delivery vehicle would have to carry for a given propane payload. The mission analysis provided the aircraft configuration analysis the most appropriate mission scenario for a delivery vehicle with respect to its payload capability. Using this data, a delivery vehicle concept may be sized and evaluated with respect to its mission performance and its cost effectiveness. Thus, although the

different aspects of this design appear to be individualistic and isolated from one another, they are uniquely connected and dependent on one another.

The cyclical process of ozone production and destruction is described in the second chapter of the report, where the chemical processes specific to the Antarctic ozone hole are also described. In addition, it discusses the consequences of ozone depletion future predictions. In the third chapter, possible active intervention schemes are explained, and the selected technique described.

Chapter four addresses the mission analysis. Using the requirements set forth by the Cicerone method of propane injection, it discusses shortcomings of last year's mission analysis and discusses new techniques utilized in the current mission analysis. Note that the mission analysis does not select the delivery vehicle, rather it provides a method for determining the relative capability of an aircraft to complete the defined mission. Chapter five discusses the airport requirements, location, and availability for the mission analysis as well as refueling requirements.

The injection and mixing strategies are discuss in chapter six. Once again some of the shortcomings of the previous year's assumptions are discussed as well as new techniques for improved injection and mixing. Although new alternative mixing techniques were investigated (i.e. Blooming Jets), the current analysis focuses on the utilization of classical diffusion theory. In conjunction with propane injection, the storage of the propane is discussed in chapter seven. A preliminary multiple tank storage system is designed, and a construction material investigation was conducted to minimize weight while maximizing storage capacity. In addition, details of the storage tank and support structures integration with the vehicle are discussed.

Chapter eight investigates vehicle concepts that may fulfill the requirements of the mission. In addition, a selection criteria is developed based on the mission profile, technology standards of the year 2006, the requirements set forth by the propane storage and mixing analysis, and the physical capabilities of current and proposed aircraft designs.

These investigations examine the aircraft's ability to complete the mission and compare the delivery vehicle's capabilities to a selection criteria. Finally, chapter nine discusses conclusions drawn from the analyses and provides multiple alternatives that are capable of completing the mission.

2.0 ATMOSPHERIC OZONE

2.1 Introduction

Ozone (O_3) is a natural atmospheric gas, which is found in its highest concentration in the stratosphere at an altitude between 15 and 30 km (49,000-98,000 ft) (Hamill, 1991). This concentration of ozone, approximately 90% of the total atmospheric ozone, is essential to maintain a livable environment, as it shields the surface of the Earth from incoming ultraviolet radiation. Without this protective ozone "layer", it would not be possible for life as we know it to exist.

2.2 The Ozone Cycle

Ozone is continuously generated, and destroyed, during its natural cycle as it absorbs harmful UV radiation from the sun of wavelengths between 240 and 320 nm. Ozone is produced in the upper stratosphere, where incoming UV radiation of wavelengths less than 240 nm, splits molecular oxygen into atomic oxygen as in reaction (1). This atomic oxygen can then react with another oxygen molecule, to form an ozone molecule as in reaction (2).

$$O_2 + hV \text{ ---> } O + O \qquad \text{(wavelength < 240 nm)} \qquad (1)$$

$$O + O_2 \text{ ---> } O_3 \qquad (2)$$

Ozone is destroyed as it absorbs incoming UV radiation in the stratosphere before it reaches the earth's surface (3).

$$O_3 + hV \text{ ---> } O_2 + O \qquad \text{(wavelength < 320 nm)} \qquad (3)$$

The ozone cycle then begins again as the new atomic oxygen formed in reaction (3), can react with another oxygen molecule to produce another ozone molecule.

Other important reactions in the cycle are:

$$O + O_3 \text{ ---> } O_2 + O_2 \quad (4)$$

$$O + O \text{ ---> } O_2 \quad (5)$$

Reaction (4) chemically destroys ozone, and reaction (5) prevents the formation of ozone from the atomic oxygen. However, these reactions are not favored because the amount of molecular oxygen present in the stratosphere is much greater than that of either atomic oxygen or ozone. As a result, ozone formation, reaction (2), is more likely to occur.

About thirty years ago, it was predicted that the ozone cycle would result in much greater levels of ozone than had been measured. It was concluded that an additional type of ozone reducing process must naturally occur. The process is described by reactions (6) and (7).

$$X + O_3 \text{ ---> } XO + O_2 \quad (6)$$

$$XO + O \text{ ---> } X + O_2 \quad (7)$$

Net: $O + O_3 \text{ ---> } 2O_2$

In this reaction the X term corresponds to either ClO, NO, OH, or BrO (Zurer, 1993). These species are naturally present, and are capable of reducing many ozone molecules because of their catalytic reaction in which ozone is destroyed while the X molecule remains. However, they do not do so, because they are naturally present only in trace amounts.

The combination of the above reactions, (1) through (7), maintains the ozone balance in the atmosphere.

2.3 The Chlorine Connection

The wide spread use of chloroflourocarbons has resulted in an increase in the levels of Cl radicals in the atmosphere. Over 80% of the chlorine now present in the stratosphere, is a result of man-made sources such as CFCs (Chipperfield, 1993). Normally, CFCs are very stable, and inert. However, when they rise into the stratosphere and are exposed to high doses of UV radiation, a chlorine atom is released (Zurer, 1993). Figure 2.3-1 gives a representation of this process. Reactions (8) and (9) are examples of this process for the two most common commercial CFCs, which together contribute about 47% of the chlorine in the atmosphere (Prather, 1990).

CFC-11 $CF_2Cl_2 + hV \rightarrow CF_2Cl + Cl$ (8)

CFC-12 $CFCl_3 + hV \rightarrow CFCl_2 + Cl$ (9)

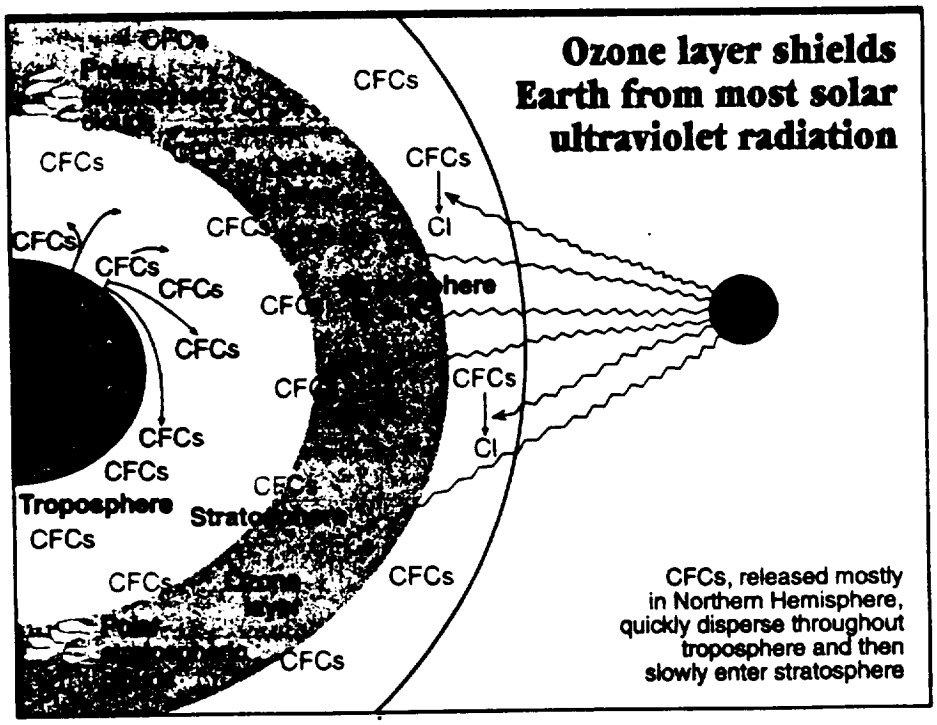

MAY 24, 1993 C&EN

Figure 2.3-1 CFC Distribution in the Atmosphere

The majority of these active chlorine atoms, which are now capable of catalytically destroying ozone as in reactions (6) and (7), react with either hydrogen, nitrogen, or oxygen compounds in the stratosphere and are tied up in unreactive, stable forms termed reservoirs. Most often the chlorine atoms end up in either hydrochloric acid (HCl), or chlorine nitrate ($ClONO_2$) (Popular Science, 1992).

As a result of the increase in chlorine levels, more ozone is catalytically destroyed by reactions (6) and (7) than would occur naturally. The increase of chlorine loading and corresponding increase in catalytic reactions in the atmosphere explains, in part, the reduction of the ozone layer. However, it does not explain the dramatic decrease in the ozone layer over Antarctica during austral spring.

2.4 The Antarctic Ozone Hole

Since the early 1970's scientists stationed in Antarctica have been recording significant decreases in atmospheric ozone during September, and October. Almost all the ozone at certain altitudes is destroyed as the sun rises during the Southern hemisphere's spring. In October of 1992, the hole in the ozone layer over Antarctica covered an area of 9 million square miles, and spread to include the tip of South America (Svitil, 1993).

James G. Anderson, a professor of chemistry and earth science at Harvard University, makes the connection between CFCs, and ozone when he says "We know unequivocally that CFCs are responsible for ozone destruction in the Antarctic." The reason for the extreme depletion of ozone over Antarctica, while a milder depletion is occurring elsewhere, is the extreme atmospheric conditions specific to Antarctica during the winter.

2.4.1 The Antarctic Atmosphere during Winter

As the Southern hemisphere moves into its winter, strong westerlies encircle the polar region, essentially isolating the air over the pole from the rest of the atmosphere. As

the air cools, contracts, and descends, a cyclonic system termed the polar vortex is formed. Since the region is in complete darkness, and there is no incoming energy, the air inside the vortex becomes extremely cold. In fact, the air drops to a temperature of 193 K, at which time particles of nitric acid ($ClONO_2$) condense (type I polar stratospheric clouds) . As the temperature drops even further to about 187 K, ice particles form (type II polar stratospheric clouds) (Hamill, 1991). Figure 2.4-1 gives a representration of these conditions.

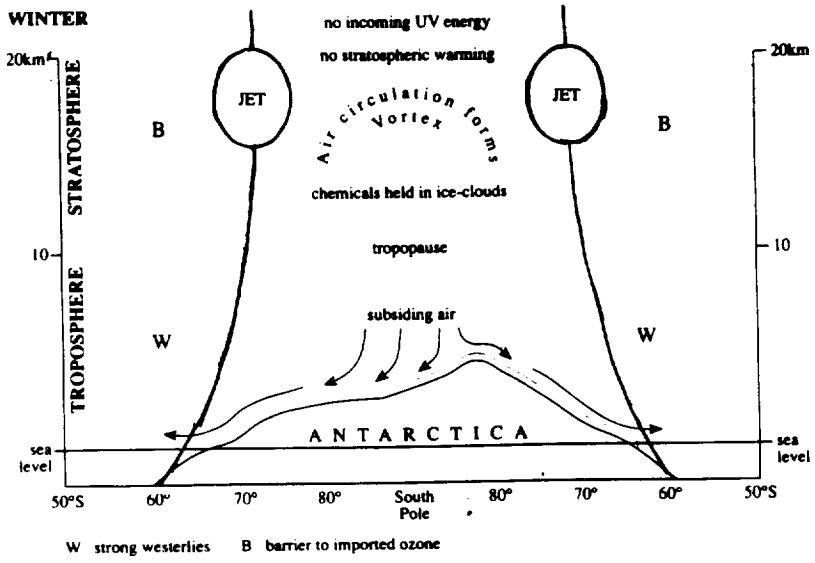

Figure 2.4-1 - Winter Atmospheric Conditions Over Antarctica Which Result in Extreme Ozone Loss (Money, 1993)

The importance of the polar stratospheric clouds (PSCs) is that they provide a surface on which chemical reactions can occur. On the PSCs, heterogeneous reactions convert stable chlorine reserves of hydrogen chloride (HCl), and chlorine nitrate ($ClONO_2$), to photolytically reactive molecular chlorine (Cl_2), and hypochlorous acid (HOCl) as in reactions (10) and (11). (Hamill, 1991)

$$HCl + ClONO_2 \text{ ---> } Cl_2 + HNO_3 \quad (10)$$

$$H_2O + ClONO_2 \text{ ---> } HOCl + HNO_3 \quad (11)$$

As the polar winter ends with the rising of the sun, the incoming solar radiation releases chlorine atoms from the molecular chlorine (Cl_2) and hypochlorous acid (HOCl) as in reactions (12), and (13), freeing them to react catalytically with the ozone as in reactions (6) and (7) (Zurer, 1993).

$$Cl_2 + hV \quad ---> \quad 2Cl \qquad (12)$$

$$HOCL + hV \quad ---> \quad OH + Cl \qquad (13)$$

This occurs over a three week period during which the active chlorine destroys the ozone in the polar vortex. This ozone accounts for approximately 3% globally of total stratospheric ozone (Hamill, 1991).

With the rising of the sun, the incoming solar energy eventually causes the vortex to break down in austral spring (Autumn in the Northern Hemisphere). Without the necessary winter atmospheric conditions, ozone destruction essentially ceases until the next year.

2.4.2 The Future of the Ozone Hole

The hole in the ozone layer first occurred in the 1970's when the level of chlorine in the atmosphere reached 2 ppb. Since then, chlorine levels have continued to rise to reach approximately 3.5 ppb. today, and are predicted to rise further until they reach about 5 ppb in 2010.(Prather, 1990) Figure 2.4-2 gives an indication of the increase in chlorine levels over the past thirty years, and predicts future levels under the restrictions of the Montreal protcol.

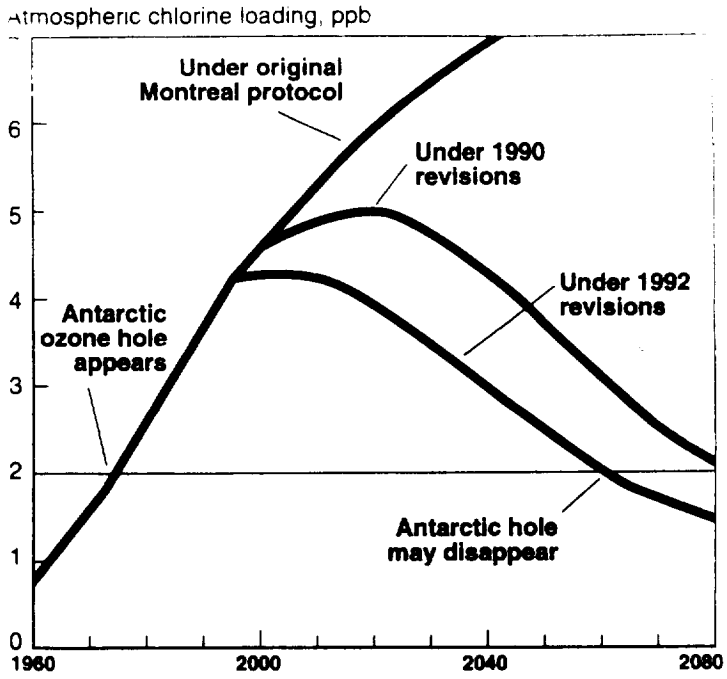

Note: Measured (1960–90) and projected (from 1990 on) abundances of chlorine in the atmosphere under the terms of the original 1987 Montreal Protocol on Substances That Deplete the Ozone Layer and under its 1990 London and 1992 Copenhagen revisions.
Source: World Meteorological Organization

Figure 2.4-2 Prediction of Future Atmospheric Chlorine Concentrations (Prather, 1990)

Since the hole first occurred when chlorine reached a concentration of 2 ppb in the atmosphere, it is predicted that the hole will reoccur until the levels again drop to 2 ppb. Under the 1992 revisions of the Montreal protocol which calls for the complete phase out of CFCs by 1996, the 2 ppb. level of chlorine is not predicted to occur until about the year 2060.(Zurer, 1993)

2.5 Global Ozone Depletion

After the polar vortex breaks down, and the air inside is no longer isolated, ozone rich air from surrounding latitudes moves in and partially replenishes the ozone layer over Antarctica. As a result, the surrounding region's ozone layer is decreased. This surrounding region consists of populated areas of South America, and Australia. In 1990 the extreme loss of ozone over Antarctica resulted in a decrease in ozone over the mid-latitudes of the Southern hemisphere during the spring and summer of as great as 10% (Prather, 1990).

In addition to the ozone "sink" of the hole, which reduces levels of ozone throughout the southern hemisphere during the spring, and summer, there has been a general overall global reduction of the ozone layer during the past years. In the past fourteen years, the ozone layer over both North America, and Europe has decreased by approximately 4-7% (Madronich, 1993). Figure 2.5-1 shows the ozone loss for the past ten years over Europe and North America.

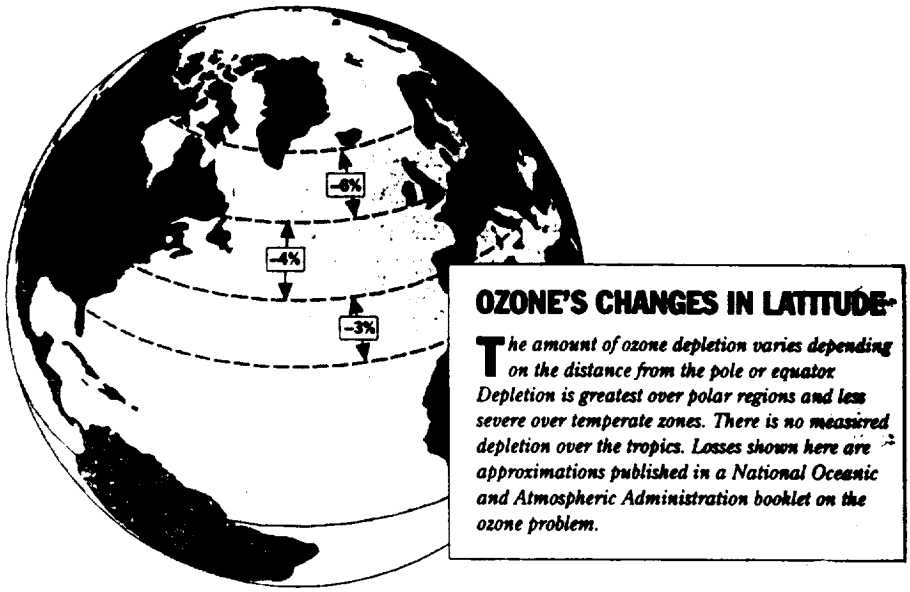

The Washington Post, April 15, 1993

Figure 2.5-1 Approximation of Northern Hemisphere Ozone Reduction for the Past Decade

It should be noted that there are natural seasonal variations, as well as year-to-year variations in ozone levels. In fact, ozone levels vary slightly with time of day. These variations generally correspond to changes in incoming amounts of solar radiation, as the destruction/production process of the ozone cycle is dependant on the amount of incoming radiation. However, the losses in ozone are generally calculated on a yearly average to account for seasonal variations, and the reduction in ozone that has occured over the past years, falls far outside of the range of the natural variation.(Parsons,1994)

It is often stated that natural phenomenon, specifically volcanic eruptions, result in ozone loss. Although volcanoes due inject chlorine compounds into the atmosphere, direct measurments taken on both El Chichon, the largest eruption in the 1980's, and on Pinatuba, the largest since 1912, have shown that the overall contribution of the eruptions to both chlorine concentration, and ozone loss was minor.(Parson,1994)

2.6 Consequences of Ozone Depletion

The result of the worldwide reduction in ozone is an increase in levels of UV-b radiation. For every percent decrease in ozone, there is an approximate increase of 1.3% in UV radiation (Solomon, 1992). The consequences of increasing UV radiation are somewhat uncertain. However, it is predicted that a 10% loss of ozone would result in 1.75 million more cases of cataracts a year, and a 26% increase in non-melanoma skin cancer, or an additional 300,000 cases worldwide per year (Lipske, 1992). It is also thought that UV increases will cause damage to the immune system. Table 2.6-1 provides predicted rates of increase for carcinoma skin cancers, of which more than 90% of cases in the past have been atributed to UV-b exposure (Wayne,1991)

Table 2.6-1 Expected Increases in Skin Cancer Rates
Due to Ozone Depletion between 1979 and 1992 (Madronich,1992)

Latitude	% Ozone Loss 1979-1992	%Increase in rate basal cell carcinoma	%increase in rate squamous cell carcinoma
75N	9.0 +/- 2.9	15.4 +/- 5.8	29.1 +/- 11.5
55N	7.4 +/- 1.3	13.5 +/- 5.3	25.4 +/- 10.3
35N	4.8 +/- 1.4	8.6 +/- 4.0	16.0 +/- 7.6
15N	1.5 +/- 1.1	2.7 +/- 2.4	4.8 +/- 4.4
15S	1.9 +/- 1.3	3.6 +/- 2.6	6.5 +/- 4.8
35S	4.0 +/- 1.6	8.1 +/- 3.6	14.9 +/- 6.8
55S	9.0 +/- 1.5	20.4 +/- 7.4	39.3 +/- 15.1
75S	19.5 +/- 2.6	50.6 +/- 21.4	107.7 +/- 52.0

In addition to human consequences, it is predicted that percentage increases in UV radiation will correlate to equal percentage reductions in crop yields, at an almost one to one reduction. Similarly, ozone thinning can curb tree height and mass in our forests.(Lipske, 1992) Of even more concern to scientists is the reaction of photoplankton in Antarctic waters to the increase in UV radiation.

Photoplankton is the bases for the marine food chain in the region, and a change in its makeup could alter the population balance of the animals which feed on them. In 1992, the production of photoplankton was reduced by 6 to 12 percent in Antarctic waters. (Svitil, 1993) This means that UV radiation increases are threatening a critical food source, and could disrupt the entire marine food chain.

Generally, it is predicted that the continued thinning of the ozone layer will lead to major changes in the Earth's ecosystem. These impending problems are what initiated, and are what motivate research in the scientific community to repair/reduce the damage.

3.0 ACTIVE INTERVENTION SCHEMES

3.1 Introduction

To prevent further damage to the environment, and specifically the ozone layer, a number of active intervention schemes have been proposed by the scientific community. These proposals range from the deflection of UV radiation by mechanical means, to man-made generation of ozone, to cleanup of the CFCs by chemical means. The main problem inherent in any of these proposals is the lack of a thorough understanding of the atmosphere, and the dynamics of atmospheric constituents, energy transfer, and global circulation. As a result, any analysis can only be done on a limited scale model, and therefor cannot accurately predict the reaction of the environment to the intervention scheme. Even so, a number of intervention plans are being pursued. They have been researched by Jacob Kay in a paper entitled "A Review of the Stratospheric Ozone Depletion Problem and Considerations for the Development of Vehicle-Based Intervention Scemes" and are briefly described below.

3.2 Ethics of Intervention

There are a number of concerns over the implementation of an active intervention scheme. Most of which stem from the fact that there is an incomplete understanding of the behavior of environmental systems. Without understanding the full mechanics of the system, any predictied response to perturbations in it would lack a basis. Therefor any large-scale intervention sceme would have inherent risks. The risks include possible side effects, or negative reactions, as well as the wasting of time and resources.

These scemes are being considered because of the environmental danger faced by the world due to the depletion of the ozone layer. It is predicted that the whole Earth ecosystem could be disrupted, the number deaths due to skin cancer increased, and unknown health problems resulting from increased untraviolet radiation exposure

encountered. With possible preventive technology available, another question arises: Is it ethical to knowingly allow people, and the ecosystem, to be subjected to dangerous UV radiation levels when it could be prevented? There will always be some controversy, but if action is not taken and the predictions are proved to be accurate, the consequences to the environment and to the human lifestyle will be significant. While the opportunity exists to restore the natural ozone cycle, and prevent the consequences of misuse, it should be seized.

3.3 *in situ* Ozone Generation

Generation of man-made ozone by photolysis, or electric discharge to replace that lost due to CFCs would be ideal. Ozone can be generated by emulating the natural ozone production process described in equations (1) and (2) by disassociation of molecular oxygen. However, the amount of energy required to photolyse oxygen and produce ozone is excessive; to produce 1% of global ozone, over 10 gigawatts of power must be supplied to the atmosphere for an entire year (Kay, 1992). A nuclear plant produces 3 gigawatts.

The creation of ozone by electric discharge has a similar problem. Electric discharges of several kilovolts can generate molecular oxygen and thereby ozone, as in reaction (14).

$$e^- + O_2 \text{ ---> } 2O + e^- \qquad (14)$$

Unfortunately, ozone is only generated at a rate of 150 g ozone/kWh (Fowler, 1988). This translates into a power requirement of 30 gigawatts. These power requirements of 10 and 30 gigawatts are far to high for the scheme to be reasonably implemented. In addition, although ozone protects us from UV radiation when it is in the stratosphere, ozone is a poisonous gas. As a result it can not simply be produced by a ground based system and released into the atmosphere in high concentrations, but would require containment, and distribution into the stratosphere. And finally, although the

overall rate of ozone production would increase, the chlorine which was destroying the ozone to begin with would keep on attacking it and might completely negate the effect.

3.4 Removal of PSCs

As explained in the chapter on ozone, polar stratospheric clouds are necessary for the chemical heterogeneous processes to occur, and for the formation of the ozone hole. By either removing them, or preventing their formation, the ozone hole would be prevented. It is theorized that 5.5 GW of microwave radiation at 22 GHz produced by a low Earth orbit satellite, could evaporate the PSCs in 38.8 days. (Kay, 1992)

Although this process would dissipate the PSCs, the remaining molecules can reform into new PSCs because of the persisting extreme cold. Also the fate of the chemical species contained in the PSCs after being liberated is unknown. In addition, spill over microwave radiation would reach both the troposphere, and the surface of the Earth with unknown consequences. This plan requires further, and complete knowledge of the PSC cycle, and research into possible side effects of spillover radiation to be implemented.

3.5 NOx Injection

The introduction of an NOx species into the atmosphere, could restore the active chlorine to its stable reservoirs by reaction (15) (Kay, 1992), thereby preventing the catalytic destruction of the ozone by free chlorine.

$$ClO + NO_2 + M \text{ ---> } ClONO_2 + M \qquad (15)$$

Unfortunately, data on the injection of NOx into the atmosphere is lacking. Also, while the reaction of NOx with chlorine forms stable reservoirs, NOx on its own, is a known catalytic ozone destroyer. The unpredictability of this method makes it unfeasible.

3.6 Chemical Adsorbent

A permanent solution for the prevention of ozone reduction would be the removal of the chlorine introduced into the atmosphere by CFCs. It has been proposed that the addition of zeolite chemical sieves (minerals with extensive molecular pores) into the atmosphere could "soak up" the unwanted atmospheric chlorine. (Kay, 1992)

These sieves are presently used industrially to absorb Freon-12, and certain chlorinated molecules. However, the introduction of them into the atmosphere raises a question of their selectivity. It is quite possible that the sieves would remove a number of species from the atmosphere, and not just the chlorine. Also, the sieves would have to be introduced as a powder which might settle towards the ground before having time to achieve the desired outcome. In addition, the recovery and disposal of the sieves would be extremely costly and difficult. Finally, the reaction of the sieves to high doses of UV radiation is unknown, and it is quite possible that they would be rendered useless. As with the other active intervention schemes, further understanding is required.

3.7 Injection of Alkali Metals

Disruption of the conversion process of chlorine reserves into active chlorine atoms by the addition of an alkali salt/metal would prevent the ozone hole from occurring. It has been proposed that by the addition of an alkali metal, sodium hydroxide (NaOH) for example, the hydrochloric acid (HCl) in the atmosphere could be dissolved on the PSCs before it reacts to release atomic chlorine (Kay, 1992), as in reaction (16).

$$NaOH + HCl \quad ---> \quad NaCl + H_2O \qquad (16)$$

If the resulting NaCl remains stable, and does not re-release the chlorine, it would then settle out of the atmosphere. Whether or not it will has not yet been determined, and is the major drawback. As with the other chemical intervention schemes, there is the concern

of unknown reactions in the atmosphere with the chemical additive, and as before more extensive experiments, and modeling needs to be done.

3.8 Blocking UV Radiation

A different idea for preventing the consequences of the thinning ozone layer, is partial shielding of the Earth from the UV radiation. A number of ideas have been considered, such as the placement of a system of mirrors in Earth orbit to deflect some of the incoming radiation. The most simple and sound idea is the induced formation of stratus clouds, as they have been found to provide significant protection against UV radiation (Kay, 1992).

The idea is simple and introduces no reactive chemicals into the atmosphere (H_2O). However, there is no known process by which cloud formation can be achieved. In addition, this is a restricted, short term, local solution, which even if generated would dissipate quickly.

3.9 Hydrocarbon Injection

The atmospheric intervention scheme that has had the most experimental testing, is the injection of hydrocarbons into the polar vortex with the intent of scavenging the atomic chlorine there. It is proposed by R. J. Cicerone, Scott Elliott, and R. P. Turco in a paper entitled "Reduced Antarctic Ozone Depletion in a Model with Hydrocarbon Injections" (Cicerone,1991), and appears to be the most promising proposal due to the accompanying research. As a result, hydrocarbon injection is the intervention scheme that has been selected for implementation.

3.9.1 The Injection Concept

It is proposed that by the injection of a hydrocarbon into the polar vortex, during the time period of catalytic ozone destruction by atomic chlorine, the amount of ozone that is destroyed could be minimized by the immobilization of the active chlorine through its rapid reaction with a hydrocarbon (Cicerone, 1991). The intention is to inject a hydrocarbon, specifically either propane or ethane, to react with the chlorine and tie it up in a reservoir until the polar vortex breaks down, and atmospheric conditions no longer exist for the release of atomic chlorine. The general reaction of a hydrocarbon with atomic chlorine is equation (17).

$$Cl + C_xH_y \text{ ---> } HCl + C_xH_y \qquad (17)$$

The use of propane is recommended as it does a better job of entrapping the active chlorine. The propane reacts at a 1:1 ratio with the active chlorine, and the amount required is therefor dictated by the amount of active chlorine in the stratosphere. As of 1991, the concentration of atomic chlorine present during the optimum injection time period was 2 ppb.(Cicerone, 1991).

Under analysis, the injection of 1.8 ppb. of propane did not accomplish the desired results, and in some cases actually increased ozone reduction. The injection of 3.6 ppb. of propane though, provided the desired outcome of minimal ozone reduction. (Cicerone, 1991)

3.9.2 The Atmospheric Model

The computer model used in the Cicerone analysis was based on a tested model of stratospheric gas-phase photochemistry (Turco, 1985) with the addition of atmospheric knowledge of the south polar region. It included data (as of 1991) for both the Antarctic atmospheric composition, and the ozone chemistry reduction reactions. It included 130 stratospheric gas-phase photochemistry equations, all known heterogeneous PSC

reactions, as well as the corresponding reaction rates for both the gas-phase reactions, and the heterogeneous reactions. For specifics on the chemical reactions included in the analysis see Cicerone 1991.

The model parameters are as follows:

Parameter	Baseline Input
Altitude	15 km
Latitude	80 S
Calculations begin	8 August
Sunrise	15 August
PSC evaporation	1 September and 1 October

(Cicerone, 1991)

This model is a simulation, and as a result there are simplifications inherent in it. These simplifications may result in inaccuracies, and provide misleading results. Unfortunately, until a completly accurate model of the atmosphere is developed, or experimental testing is done on the actual atmosphere, there is no way in which to quantify the error involved in the model.

3.9.3 Implementation

The major constraint on the implementation of the hydrocarbon injection scheme is the time period; approximately three weeks. For the scheme to work as predicted, approximately 100,000 tons of propane needs to be distributed throughout the polar vortex in the region of 15 to 20 km (47,000-65,000 ft) covering an area of 2×10^7 km^2.

In addition to the small delivery window, the mixing of the propane is crucial, as there is little natural atmospheric mixing, and the entire scheme is dependent on achieving the correct distribution. As a result, a detailed analysis of both the mixing scheme, and mission is required so that the propane would be evenly distributed at an average concentration of 3.6ppbv. throughout the entire polar vortex.

4.0 MISSION ANALYSIS

4.1 Introduction

Several types of delivery systems were investigated to implement the Cicerone method, including lighter-than-air (LTA) vehicles, missiles, and aircraft. These investigations were performed by the 1992-93 Virginia Tech USRA/NASA Advanced Design team and are detailed in their final report. LTA's were ruled out because of their low speed, altitude restrictions (propane delivery altitudes will be as high as 66,000 feet), and susceptibility to damage from the high winds present in the operational area. Missiles were also ruled out, based on their low payload to gross weight ratio and debris problems. It was decided that aircraft were the most appropriate delivery vehicle due to their high payload capacity and high speed.

The proposed mission profile calls for a fleet of aircraft flying through the polar vortex region while injecting propane into the atmosphere. This propane delivery scheme assumes uniform coverage of the entire polar vortex area by overlapping the propane injection plumes created behind the aircraft. Propane will be delivered on two or three levels (depending on plume radius) to ensure coverage over the entire polar vortex thickness.

This chapter details the work done to optimize the delivery pattern and parameters such that the number of aircraft required (and therefore cost) is as low as realistically feasible. The mission analysis schemes developed are multidisciplinarily linked to the other aspects of this project; mainly to the mixing analysis studies and the aircraft configuration studies performed.

As detailed later in this chapter, the number of aircraft required to implement the Cicerone method is highly dependent on the plume radius attainable as determined by the mixing analysis. As the plume radius increases, however, the payload capacity required of

the aircraft also increases. Furthermore, payload considerations must be taken into account when considering the possibility of mid-air refueling to reduce the number of aircraft required. The mission analysis is therefore dependent on the payload capacity determined by the aircraft configuration studies portion of this project (see Chapter 8).

4.2 Mission Parameters

Critical factors for this mission include the delivery time window, the volume of the delivery area, the assumed injection plume diameter, the maximum aircraft payload, and the mission range for each aircraft. Propane injection rate is taken into account in the plume diameter assumption. The assumed plume diameter along with the aircraft's velocity dictate the injection rate. The injection rate therefore does not have to be explicitly specified.

Cicerone specified a three week delivery window, although Kay suggested this could be increased to four weeks if necessary. This analysis assumes a three week window thus allowing for any unanticipated problems which may increase the time required.

Although the exact volume of the polar vortex changes from year to year, it was assumed constant in this analysis for simplicity. The polar vortex covers an area of approximately 20 million sq. km (5.83 million sq. nm) and has a height of 5 km (2.7 nm) as specified in the 1992-93 Virginia Tech NASA/USRA Advanced Design Team's final report. This equates to a volume of 100 million km^3 (15.73 million nm^3). The proposed delivery scheme assumes propane injection whereby the plumes are overlapped to minimize the number of untreated areas.

The mission modeling is highly dependent on the assumed plume diameter. (This will be discussed in greater detail in section 4.6). With a plume radius of less than 1428 m (0.77 nm), treatment over the entire height of the polar vortex requires delivery at three altitude levels, as shown in Figure 4.2-1. If a plume radius of greater than 1428 m (0.77

nm) can be attained, the number of required delivery levels is decreased to two. This reduces the number of missions required immensely. Increasing the plume diameter also increases the horizontal spacing between flight paths, and thus greatly decreases the required number of missions required to cover the entire polar vortex volume. Hence, it is desirable to have the largest plume diameter that can realistically provide the required propane concentration of 3.0 parts per billion.

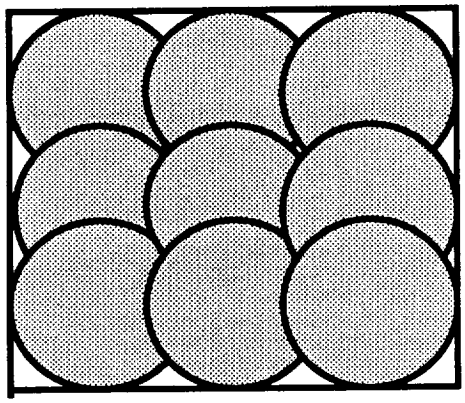

Figure 4.2-1 Sample cross sectional area of delivery scheme.

4.3 1992-93 Mission Model

The mission model proposed by the 1992-93 team is shown in Figure 4.3-1. This model was designed so that aircraft would fly out of two airport regions, located in South America and Australia. Each aircraft would fly at Mach 2.4 in concentric arcs around the South Pole until the fuel or payload were expended and the aircraft had to return to base. The arc radius would decrease by 1,732 m (5,682 ft) whenever a mission reached the dividing line between the two airport regions. This decrease in radius is determined by the assumed plume diameter taking plume overlap into account. Each new mission would begin where the previous mission ended. A FORTRAN program implementing this

method was developed by the 1992-93 Virginia Tech NASA/USRA Advanced Senior Design team which output the number of missions required and the total mission range. This enabled the determination of the number of aircraft required.

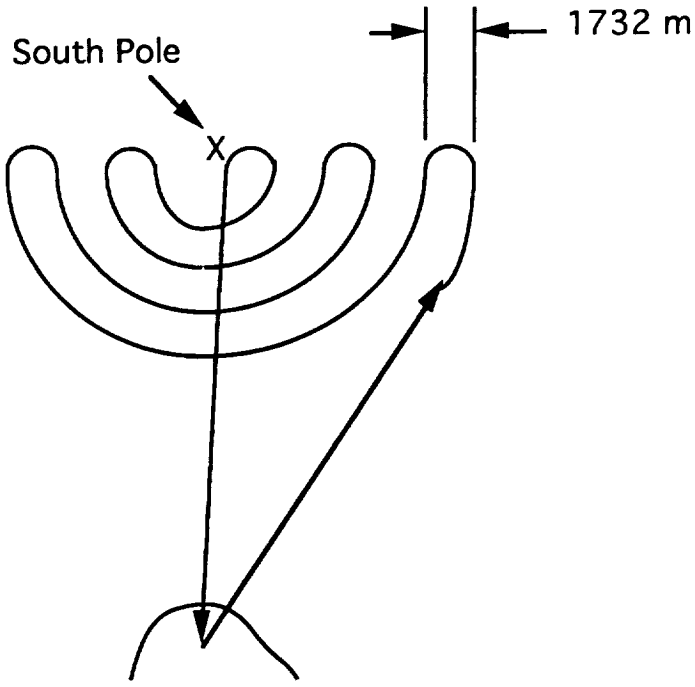

Figure 4.3-1 Schematic of the proposed 1992-93 mission model.

Further investigation of this model revealed several drawbacks. The range of each aircraft must be nearly 15,000 km (8,000 nm) or the number of aircraft required becomes prohibitive. Even at this range, 130 aircraft were required to complete the mission in the allotted time window. The current design team deemed a 15,000 km (8,000 nm) range unrealistic. No Mach 2.4 aircraft in existence or in development possess a range this large.

A proposed option of using tankers to increase effective aircraft range was investigated by the 1993-94 team. This option decreased the number of aircraft required, but still required an aircraft range of 15,000 km (8,000 nm) due to the proposed delivery pattern. This option required refueling before and after propane injection. Therefore, if a plane was unable to refuel, it would be lost.

Another drawback of the previous mission model was the inefficient use of aircraft range. Each aircraft returned to base when the remaining range equaled the range to the base or when the aircraft ran out of propane. Using this model, virtually every aircraft reached its return point somewhere inside the vortex. The aircraft would potentially have to fly a considerable distance through areas of the vortex already covered. The next mission would then have to fly through this same area before beginning injection. This led to a large increase in total mission range, total number of missions, and number of aircraft required.

An simplification made in the FORTRAN code developed was neglecting the turning radius of the aircraft when decreasing the arc radius. The code decreased the arc radius by 1,732 m (5,682 ft), but for the proposed velocity of Mach 2.4, the minimum turning diameter, based on a 2-G load, is 67.6 km (36.5 nm). The distance consumed in turning is 106.25 km (57.37 nm). When multiplied over the 4000+ missions required, this adds 425000 km (229480 nm) to the total mission which would require the addition of about one aircraft. The addition of this aircraft seems almost insignificant. However, because of this approximation, the pattern that was modeled could not actually be flown.

It was determined that the problems in the 1992-93 proposed mission model, namely the high range of the vehicle, the inefficient use of vehicle range, and the absence of the turning distance, necessitate the development of a more detailed model.

4.4 1993-94 Mission Models

Several new mission models were developed by the 1993-94 team to address the deficiencies in the 1992-93 model. The driving factors for the development of the new models were to keep down the range of the aircraft, reduce the number of aircraft required, and ensure that each aircraft has enough fuel to return to base at every point in the mission.

4.4.1 The Through-and-Back Model

The first mission model developed requires the use of three airports from only one airport region. South America was chosen for its closer proximity to the polar vortex. (The airports will be discussed in Chapter 5.) Each aircraft would fly out from its airport and rendesvous with a tanker on the way to the polar vortex, adding approximately 1,500 km (800 nm) to its effective range. The aircraft would then accelerate to Mach 2.4 and travel from one side of the vortex to the other while injecting propane. Mach 2.4 was chosen as the delivery velocity because it is the highest realistically attainable Mach number for the aircraft being considered for delivery vehicles as discussed in Chapter 8. After executing a 2-G turn, the aircraft travels back along a path parallel to the first, once again delivering propane all the way through the vortex. Using this technique, the aircraft would have enough fuel left over to return to base without refueling. For the 256 km (138 nm) wide strip at the top and bottom edges of the polar vortex, each plane would execute a turn of radius 128 km (69 nm) on the turn-around to allow coverage to the edge of the polar vortex while minimizing the number of missions.

Figure 4.4-1 depicts one sortie for the proposed mission model. Each flight path overlaps several on either side during turn-around. This should cause no problem, as the aircraft will be staggered at take-off and while refueling. The plume diameter was assumed to be 2000m (the same as for the 1992-93 model), but adjacent plumes are not created by a single aircraft. The plumes from a single aircraft are separated by the turning diameter. By dividing the turning diameter by the assumed plume diameter, it is determined that 36 missions are required to make one sweep of planes flying through the vortex and back in parallel paths.

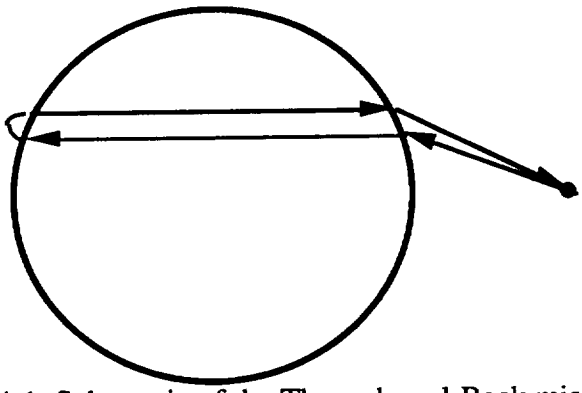

Figure 4.4-1 Schematic of the Through-and-Back mission model.

A FORTRAN program was developed to implement this model. The program ran in blocks of 36 missions (to cover a strip of one turning diameter's width through the vortex and one turning diameter's width back through the vortex), fully covering a strip of the vortex 135 km (73 nm) wide. For the outer edge, a block of 69 missions was run to cover the remaining portion of the vortex. This entire procedure was done for half the area of the vortex at one altitude. The results from this were then doubled to account for both sides of the vortex and tripled to account for all three delivery altitudes. The number of aircraft and the number of sorties per day per aircraft were calculated based on the total mission range, number of missions, Mach number, and ground time. The time required for refueling and climbing to altitude were also taken into consideration. Finally, the program assumed that ten percent of the fleet was grounded to take into account any repairs, maintenance, etc. that might be necessary.

The results from the "Through-and-Back" model were very encouraging. Using the same parameters as the 1992-93 team, the number of aircraft required for the *baseline mission* (Mach = 2.4, Plume Radius = 1000 m , Ground Time = 4 hours) was reduced from 130 to 99. Approximately 20 tankers would be required to accomplish the refuelings. (Tanker requirements are discussed further in Chapter 5.) Despite the advantages of this new model, the model had a few shortcomings that needed to be addressed. The first and most significant of these shortcomings is that due to a lack of foresight, the FORTRAN

code did not provide a convenient way to test the effects of changes on the mission parameters such as delivery velocity, plume radius, and ground time. It was therefore very difficult to perform sensitivity studies on these and other variables. The second drawback of this model is that it did not allow for a second or third refueling such that the aircraft could make a second or third run through the vortex and back without returning to base. These issues were addressed by the "Modified Through-and-Back" model which is discussed in section 4.4.3.

4.4.2 The Quartered Vortex Model

At the suggestion of Dr. S. C. Sarin, a pattern optimization specialist in the Industrial Systems Engineering Department at Virginia Tech, a new model was developed in an attempt to decrease the distance to and from the point at which delivery begins and ends, respectively. The pattern, which is pictured in Figure 4.4-2, divides each delivery level into quarters. Two quarters on one side of the vortex would be covered by aircraft from a South American airport while the other two quarters would be covered by aircraft from an Australian airport. After reaching the entry point of the vortex, the delivery aircraft would fly to the center of the vortex. After making a 90 degree turn, the aircraft would fly to the outer edge of the vortex and then fly along a path parallel to the circumference of the vortex until it reached its point of entry. The aircraft would then return to its airport. Each subsequent aircraft would then follow a path one plume diameter inside the previous aircraft's path until the quarter is filled in. The results of this quarter would then be multiplied by four to obtain the results for one level of the vortex. This number would then be multiplied by two or three (depending on the plume diameter) to cover all levels of the vortex.

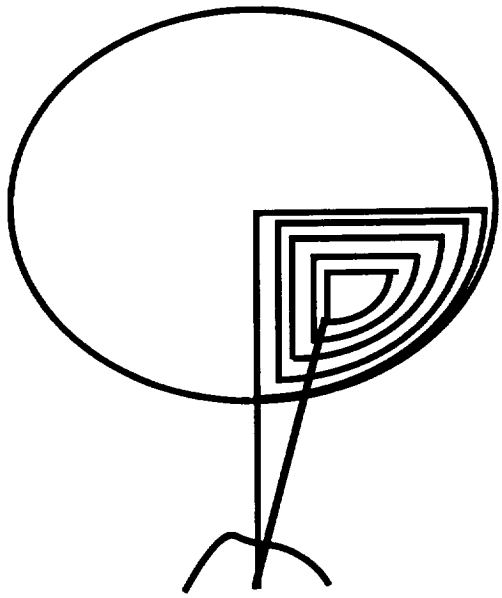

Figure 4.4-2 Quartered Vortex Model

While this pattern did originally show potential, the need to utilize airports on both side of the vortex negates any possible advantages. Since the aircraft from the Australian airport would have to fly an additional 926 km (500 nm) to and from the vortex (1852 km per mission), this results in an increased range of 926km (500 nm) for the average mission. A FORTRAN program was written to simulate this pattern. Using *baseline mission* parameters (Mach = 2.4, Plume radius = 1000m, Ground Time = 4 hrs), the program revealed that this pattern would require approximately twice as many aircraft as the "Through-and-Back" model (196 compared to 99). Due to these preliminary results, no more work was put into this model.

4.4.3 Modified Through-and-Back Model

To expand upon the "Through-and-Back" model and address its shortcomings, a new mission model was developed and a FORTRAN program was written. This new model shares the same approach as the Through-and-Back model. Aircraft based at a

South America airport fly to the vortex at subsonic speeds refueling by tanker just before they reach the vortex. They then accelerate and climb to injection velocity and altitude and begin delivering propane. The aircraft fly through the vortex, turn around, and fly back through the vortex again delivering propane.

Several modifications were made to the old model. The first modification allows each aircraft to be fully refueled in the air after making each pass through the vortex and back such that the aircraft can make another round trip through the vortex without returning to base (See Figure 4.4-3). This takes advantage of the fact that the aircraft proposed for the mission (see Chapter 8) are capable of carrying enough propane payload for more than one round trip through the vortex thus cutting down on the number of required trips to and from the vortex.

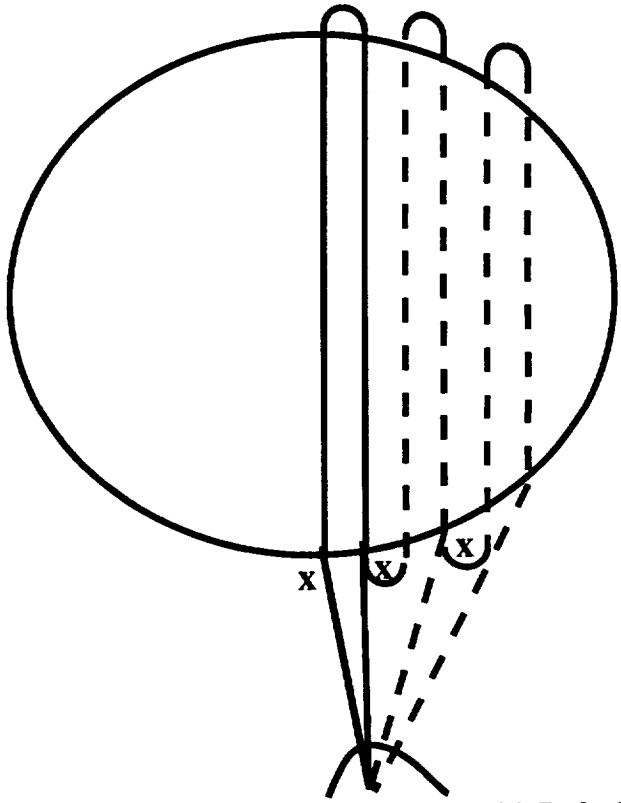

Figure 4.4-3 Modified Mission Pattern with Refueling
(Refueling location marked by x)

A second modification to the model was the adjustment to the turning radius. In the old model, each aircraft made a 2-G turn after one pass through the vortex. This determines the distance between the aircraft's trip through the vortex and the trip back. With the turning radius specified, however, a block of the vortex at either end is left that must be covered with one trip through the vortex (not making use of the return trip). In the new model, the turning radius is determined such that the radius is the lowest possible (for a 2-G or less turn) such that the entire vortex is covered without the need for an extra trip through the vortex to cover the outer edge. The number of refuelings is taken into account in determining this radius.

The third and most important modification to the old model is the fact that all mission parameters can be easily varied in the FORTRAN program to perform sensitivity studies on all relevant parameters. This has also allowed the examination of all reasonable mission configurations such that the optimum configuration (fewest required aircraft) could be determined. A feature was added to the program that tabulates the thirty best mission configurations for given payload restrictions. This feature was used as part of the aircraft configuration study and will be discussed further in Chapter 8. A copy of the FORTRAN code is included as Appendix B.

Investigations of this model showed that it yields the smallest number of aircraft required of the models investigated. This proved the model to be the best available.

4.5 Model Assumptions and Details

It was necessary to make certain assumptions for simplification of each of the models. Though the shape of the vortex actually changes from year to year, it was taken to be a cylinder of diameter 160 km (86.4 nm) and height 5 km (2.7 nm), as specified by Cicerone. The speed of sound used for the determination of flight velocity was taken to be

295 m/s (968 ft/s), which is the standard day value over the altitudes at which the aircraft will be flying.

The final assumption was that some way of maintaining the distance between injection paths will be available. It was assumed that global positioning satellites combined with the inertial navigation system have the capacity to deliver accurate positioning data to the aircraft during flight.

The current mission model requires only one airport region, as opposed to two required for the 1992-93 mission model. Based on distance from the polar vortex and the South Pole, South America was chosen as the best region from which to base missions. The average distance to the polar vortex for the three closest airports in this region is approximately 1,670 km (900 nm).

The possibility of using Antarctica as a base for missions was investigated by the 1992-93 Virginia Tech NASA/USRA Advanced Design team, but severe weather conditions during the delivery window have the potential to severely restrict flight operations. The possibility of using Antarctica as a mission base was therefore dismissed; however, in the event of an emergency landing of one of the delivery aircraft, a rescue mission could be mounted from one of the several scientific stations located on the continent.

Each aircraft will cruise from the airport to the tanker at Mach 0.8, and refueling will also occur at this speed. The time required for refueling was incorporated into the logic of the model.

4.6 Sensitivity Studies

The FORTRAN program written for the Modified Through-and-Back model made it very simple to vary as many variables as desired while holding the others constant.

Several studies were therefore performed to determine which variables had the biggest impact on the mission. The object was to minimize the number of aircraft required.

Figure 4.6-4 illustrates that it is desirable to deliver the propane at the highest Mach number possible while utilizing the most refuelings possible. The graph shows the dependency of the number of aircraft on the delivery Mach number. As expected, the number of aircraft is greatly reduced as the delivery Mach number increases. At higher Mach numbers, however, the change in number of aircraft as Mach increases is not nearly as significant as it is at lower Mach numbers. This graph also emphasizes the advantage of using multiple refuelings. As the number of refuelings is increased from 1 to 2, the number of aircraft required is reduced by almost 30%. As the refuelings increases from 2 to 3, the number of aircraft required is only reduced by about 15%.

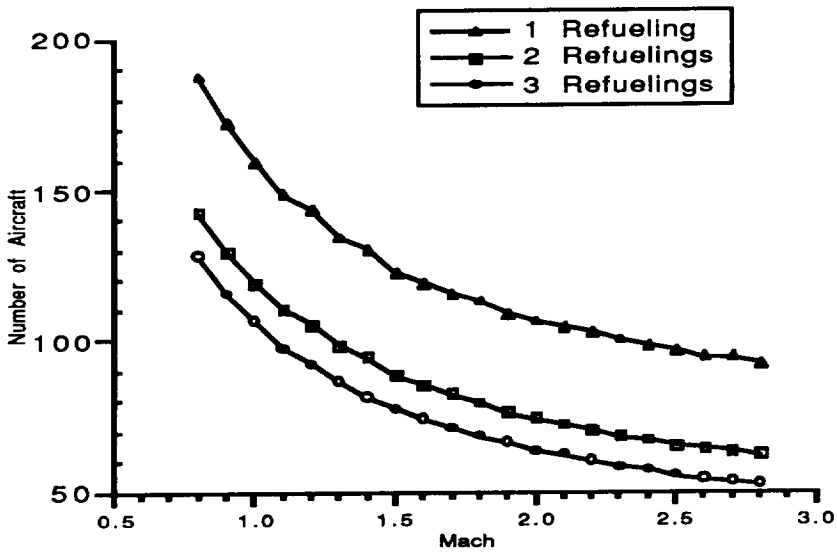

Figure 4.6-4 Effects of Mach Number on the Number of Aircraft Required
(Plume radius = 1000 m and 4 hours Ground Time)

Figure 4.6-5 is a graph of the number of aircraft required as a function of the plume radius. It illustrates that the larger the plume radius, the lower the number of aircraft required. The sudden drop in aircraft required from a plume radius of 1400 m to 1500 m is because for a plume radius of greater than 1428 m, the number of altitude layers of propane delivery required to cover the vortex is decreased from 3 to 2. This graph reemphasizes the advantages of utilizing as many refuelings as the payload capacity will allow.

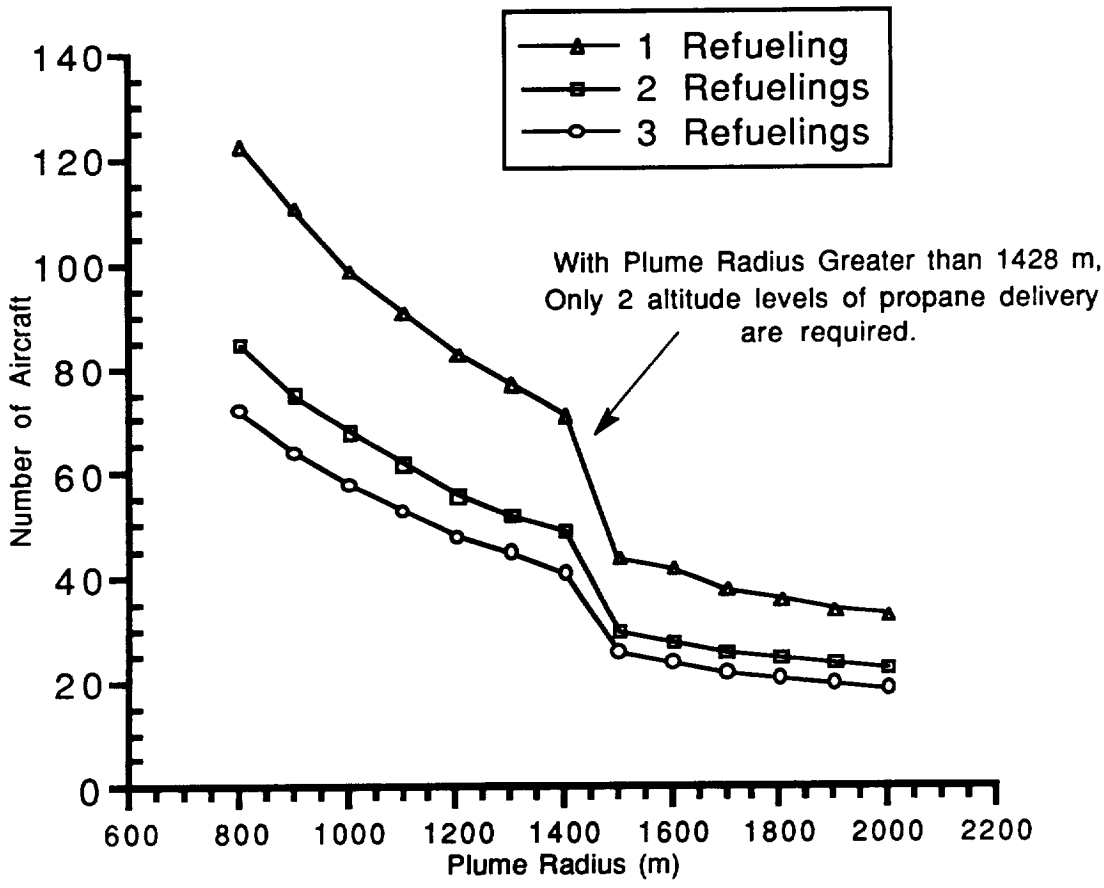

Figure 4.6-5 Effect of Plume Radius on the Number of Aircraft Required (Mach = 2.4 and 4 hours Ground Time)

As the plume radius in increased to cover more of the vortex per sortie, the required payload capacity is increased as well. With multiple refuelings, the required propane capacity increases to unreasonable numbers very quickly. This is illustrated in Figure 4.6-6.

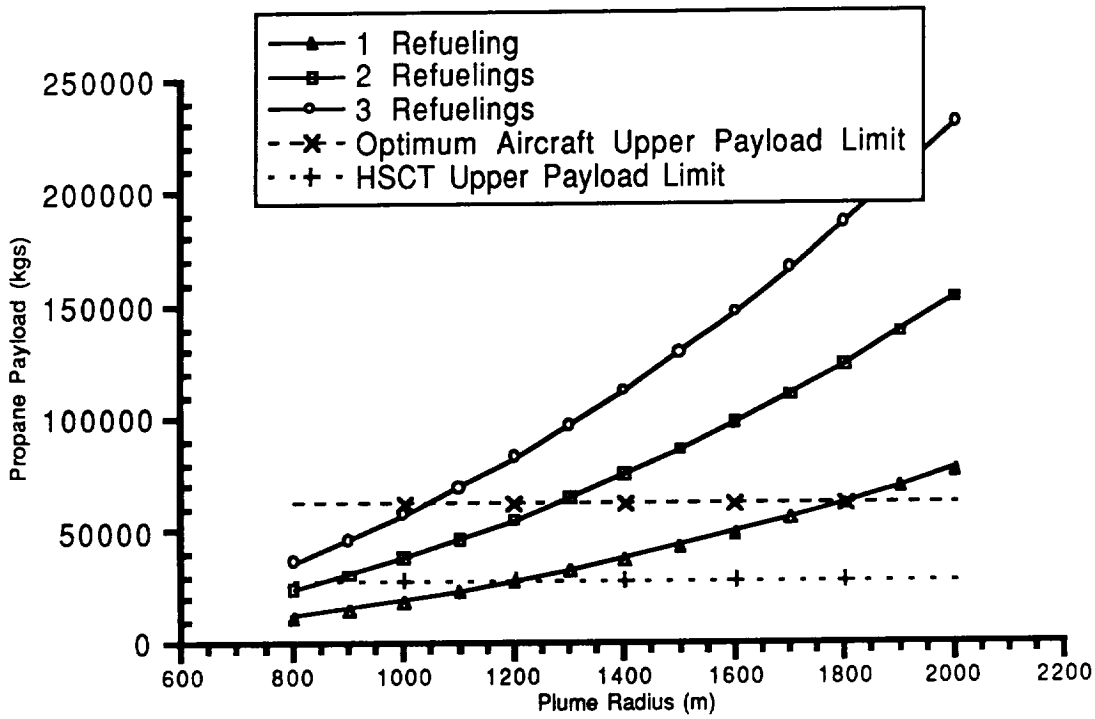

Figure 4.6-6 Effect of Plume Radius on Payload Required
(Mach = 2.4 and 4 hours Ground Time)

4.9 Summary

The mission models developed by the 1993-1994 team have provided a much greater insight into the different aspects of the mission development. Through the exploration of several different patterns, one has been chosen as the most efficient pattern while still maintaining the mission's feasibility. The use of the FORTRAN code of the "Modified Through-and-Back" model has revealed the interdependencies of all the relevant

mission parameters aiding the team in the mission profile optimization. The code has also allowed the team to explore every reasonable combination of parameters to determine which combinations yield the optimum mission (lowest required number of aircraft) while maintaining feasibility as determined by the other aspects of this project.

5.0 BASES OF OPERATION AND REFUELING

5.1 Introduction

The location of the airports from which missions are based is of vital importance to the development of a mission model. The current model requires only one airport region, hence it utilizes airports only on the South American continent. This region was selected due to its proximity to the polar vortex. The average range to the polar vortex for three airports in this region was used for analysis. The three airports investigated for use as bases for the delivery vehicles were Porvenir, Chile; Mount Pleasant, Falkland Islands; and Rio Gallegos, Argentina. Two additional South American airports were investigated for use as bases for tanker operations. Information for two airports (Christchurch, New Zealand and Avalon, Austrilia) on the Australia side of the polar vortex were investigated as emergency landing bases in case of problems with the delivery vehicle while on the far end of the delivery run.

5.2 Existing Airports

Table 5.2-1 lists the locations of the three airports used in the mission analysis, as well as locations for other airports in the South America region.

Due to the number of take-offs and landings necessary each day, the possibility exists that one airport may not be able to handle the amount of extra traffic required while still maintaining normal commercial operations. In this case, more than one airport could be used for staging sorties. The *baseline mission* analysis , discussed in the previous chapter, determined that 71 operations per day per airport are required to stay within the three week delivery window.

Table 5.2-1 Airport Locations.
Civilian airports with minimum field length of 2440 m (8,000 ft.)
Source: Boeing Aircraft Company, 1992

Airport	Latitude (deg)	Longitude (deg)	Range to Polar Vortex (km)	Range to South Pole (km)	Length (m)	LCN
Porvenir, Chile	-53.27	70.33	1563.41	4084.77	2501	39
Mount Pleasant, Falkland Islands	-51.82	58.45	1724.65	4246.01	2591	72
Rio Gallegos, Argentina	-51.62	69.28	1746.88	4268.23	3551	66
Puerto Montt, Chile	-41.43	73.10	2879.33	5400.69	2651	114
Buenos Aires, Argentina-Pistari	-34.82	58.53	3615.06	6136.42	3301	80
Christchurch, New Zealand	-43.48	-172.53	2654.15	5178.19	2443	80
Avalon, NSW, Australia	-38.03	-144.47	3260.83	5784.86	3049	95

The 1992-93 team reported that a single runway can support 47 operations per hour under visual flight rule (VFR) conditions and 30 operations per hour under instrument flight rule (IFR) conditions. This equates to 1,128 operations per day under VFR conditions and 720 operations per day under IFR conditions. A typical daily demand for an airport servicing larger aircraft is approximately 310 to 350 operations per day (Airport Capacity and Delay, 1983). This would suggest that the entire delivery operation could be based out of a single airport without unduly disrupting the normal airport schedule. Tankers, however, would have to be based out of a separate airport. Since the KC-10A can operate at a distance 3,540 km (1,910 nm) from its base it could therefore operate out of any of the airports listed in Table 5.2-1, including the airports not primarly used in the mission analysis.

In the event of an in-flight emergency on the far side of the polar vortex, the delivery aircraft could abort the return leg of the delivery run and divert to one of the alternate airports located in Christchurch, New Zealand and Avalon, NSW, Australia.

5.3 Field Length

A field length of 2,438 m (8,000 ft) was used as a baseline figure for airport consideration. Further analysis revealed that a field length of 3,048 m (10,000 ft) may be required for operation of a large supersonic aircraft. The tankers used in the mission profile also require a field length greater than 2,438 m (8,000 ft). Jane's (1989) quotes the

critical field length for the KC-10A at 3,124 m (10,250 ft). Of the airports listed in table 5.2-1, only Rio Gallegos, Argentina has the required field length for the delivery vehicles. The airport in Buenos Aires, Argentina - Pistari also has sufficient runway length, but should be limited to tanker operations due to its distance from the polar vortex. To accommodate the delivery and tanker aircraft, it may be possible to increase the runway lengths and possibly strengths, a requirement due to the low Load Classification Number (LNC) number at these airports, at one or more of the remaining airports (a LCN value of 90 was deterimed to be sufficient for the delivery vehicle and tankers.)

5.4 Other Airport Considerations

Routine on-site maintenance of the delivery aircraft and of the tankers is unavoidable. The airports must have adequate maintenance facilities to deal with this demand. Due to the proximity of the airports to one another, it may be possible to concentrate the repair facilities at one location and fly all aircraft needing major repairs into that airport. This would alleviate some of the burden on the other airports.

The airports must have sufficient space for aircraft storage. It was assumed that the airports have this capacity; most of the aircraft will be in the air at any given time.

Approximately 100,000 metric tons of propane is required for the entire operation. A large amount of storage space will be necessary for this amount of propane, and this space may be limited by safety concerns to areas far from airport facilities. It may be necessary to truck the propane from a remote storage facility to the airport for loading onto the delivery aircraft.

The possibility of building new airports to meet the mission requirements was investigated as an alternative to using existing airports. The cost of building an entirely new airport, however, is substantial. However, the cost of upgrading facilities at existing airports could be offset by allowing the airport to use them for other purposes during the 42

weeks between delivery periods (i.e., HSCT landing site and increased aircraft storage area).

5.5 Refueling Concerns

The main concern with mid-air refueling was ensuring that each aircraft has enough fuel to return to base at all points in the mission. By refueling before entering the polar vortex, this problem was prevented. If an aircraft cannot refuel, it can abort the mission and return to base. After refueling, the aircraft has enough fuel to complete delivery and return to base.

Another concern with using tankers was the capabilities of the tankers to provide fuel without overcrowding the primary airports used for the design vehicle. The KC-10A Extender can deliver 90,718 kg (200,000 lb) of fuel to a receiver 3,540 km (1,910 nm) from its home base, and return to base (Jane's, 1989). Therefore, according to Table 5.2-1, the airports selected as primarly tanker support airports (Puerto Montt, Chile and Buenos Aires, Argentina-Pistari) are within the operational range of the KC-10A. Realizing the limited number of KC-10A tankers built (60) and the lower number of tankers that will be available, an analysis into the number of tankers required was conducted. For this analysis, fuel requirements for the delivery vehicle were estimated at 143,182 kg of fuel (315,000 lbs. of fuel). Using these estimates and the max payload of the KC-10A, the ability to determine the number of tankers required was incorporated into the mission analysis code. A key assumption in calculating the number of tankers required was that initial refueling (required to ensure a safe airfield could always be reached) for the delivery vehicle was only 42,727 kg of fuel (94,000 lbs. of fuel). For the *baseline mission* case, since the only refueling was the initial refueling, a total of 50 tanker aircraft are required for the *baseline mission.* This number is within the number of tankers available and will not disrupt the normal operating schedules at airports used for bases of tamker operations.

5.6 Integration of Refueling Apparatus

A Universal Aerial Refueling Receptacle-Slipway System will be used in the refueling process. Figure 5.6-1 provides a detailed schematic of the system. The relatively small size (92 x 37 x 35 cm) of the system allows some flexibility into the placement of the system. Both the nose cone and back bone locations were investigated to determine the most effective and practical location for the refueling system.

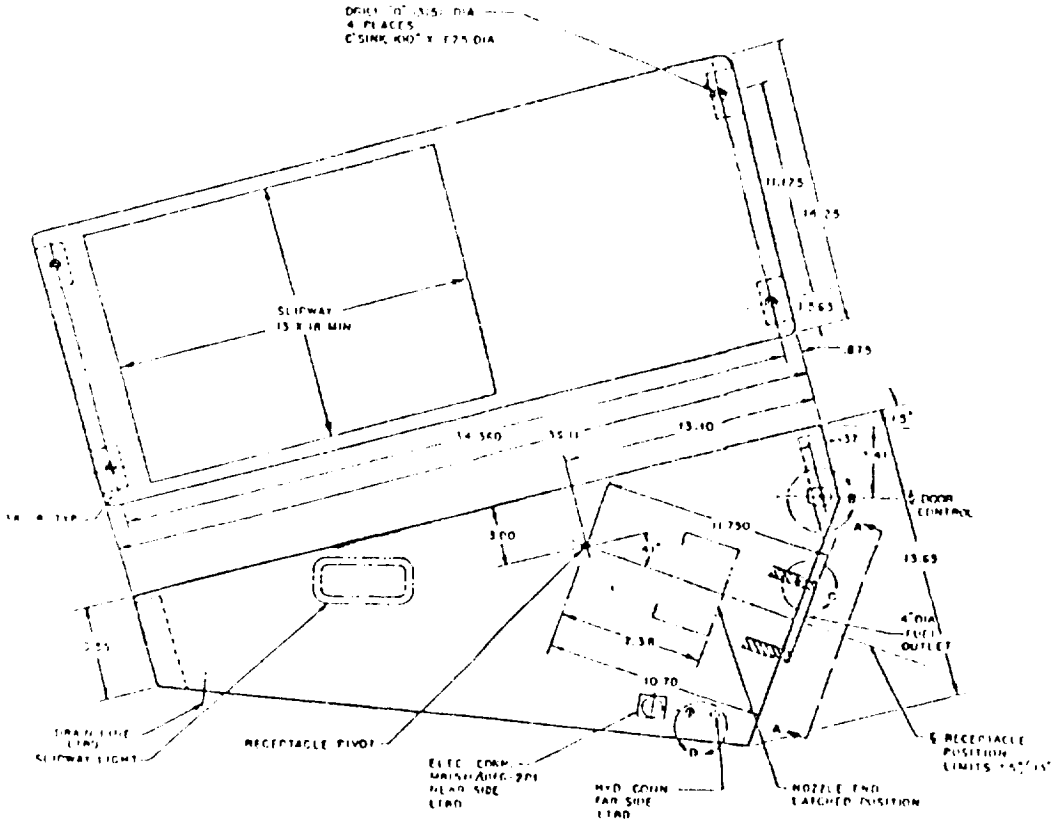

Figure 5.6-1 Universal Aerial Refueling Receptacle-Slipway System Schematic
Source: Mil-F-38363B (USAF)

Placement of the refueling system in the nose cone provides several advantages. Using this location, pilots are provided with an excellent view of the refueling tanker during hook-up, in addition, installing the system in the nose decreases the flowfield disturbance due to the tanker by keeping the aircraft as far away from the tanker as possible, thus increasing the stability and ease of hook-up and refueling. However, along with the penalty of a larger moment due to the refueling process, the nose cone is often congested with avionics and radar equipment, and therefor lacks sufficient area for even this small of a system.

Although placing the refueling system along the backbone of the aircraft (approximately 3 m. behind the flight cabin) provides plenty of installation room and a smaller moment due to the intake of the fuel, it is not without penalties. In addition to not providing the pilots with any visual cues during hook-up and the difficulty of running fuel lines from the ceiling to the floor of a pressurized cabin, this placement subjects the aircraft to an increase in flowfield disturbances due to the tanker. However, considering the relative size of the delivery vehicle, the effects of the tanker's flowfield on the aerodynamic characteristics of the delivery vehicle were determined to be acceptable.
Thus, provisions for the installation of the refueling system along the backbone of the aircraft will be required in the final design.

5.7 Summary

The use of existing airports was determined to be the most cost effective choice for this mission. The cost of extending existing runways and building new storage and repair facilities is more easily offset than the cost of building entirely new airports.

The distance of existing airports in Australia and Africa from the polar region requires an unrealistic range requirement for the delivery aircraft. Antarctica was ruled out

as an operational base due to the severity of the weather during the delivery period. Airport locations in South America were chosen due to their proximity to the polar region.

A method was developed to determine the number of tanker aircraft required (20) to support the *baseline mission* prescribed by the mission analysis. A Universal Aerial Refueling Receptacle-Slipway System will be used in the refueling process. In addition, investigations indicate the most effective location for a refueling system is along the backbone of the aircraft.

6.0 HYDROCARBON INJECTION AND MIXING

6.1 Introduction

The proper injection and efficient mixing of the selected hydrocarbon in the polar vortex cone is of prime importance to the implementatation of the injection sceme. If the required hydrocarbon concentration of 3.6 ppbv. is not achieved, the scheme will be ineffective.

The injection scheme defines the mass of propane injected into the atmopshere per kilometer traveled which is a function of plume radius and required propane concentration. Since the propane concentration is constant, the mass of propane injected per kilometer was purely a function of plume radius. This parameter was used by the mission analysis designer to determine the amount of propane required to complete differing missions with various plume sizes. The mission analysis designer then found the optimum mission using a payload constraint defined by the aircraft configuration designer. The optimum mission defined, among other parameters, the required plume radius. Using this requirement, the nozzle was then designed to achieve the desired plume radius. It is therefore extremely important that the injection and mixing techniques are developed so that they can be analyzed and implemented. Figure 6.1-1 gives a basic representation of the desired nozzle to plume model.

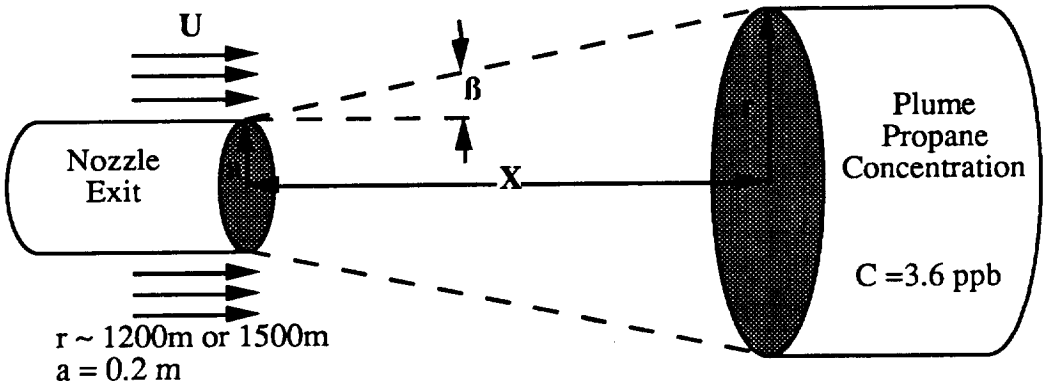

Figure 6.1-1 Nozzle to Plume Diagram (adapted form USRA,1993)

6.2 Mixing Technique

Several options were considered to mix the propane into the polar vortex. An oscilating nozzle which uses the interaction of annular vorticies along multiple axis to increase the dispersion angle (β in Figure 6.1-1) of the jet, called the blooming jet (Reynolds) was under consideration. However, since the jet is relatively new technology, there is no existing method by which empirical analysis can be performed on it. In addition, due to the uncertainty of the jet's effectiveness at supersonic speeds and the potential for mechanical failure, a nozzle with swirl vanes was decided to be the most economical and feasible mehtod for mixing the propane. Such nozzles have been in widespread use, and have been found to be both reliable and effective for mixing. Also, analylitical analysis can be perfomed on the nozzle using classical diffusion theory to reliably predict the results of the mixing downstream.

The nozzle to be employed is represented in Figure 6.2-1. It uses vanes to induce mixing by initiating a swirl effect which dramitacally improves the mixing. The swirl effect simply adjusts a constant defined in classical diffusion theory as the mixing constant, "c", as desribed in the next section (eq 6.3-3).

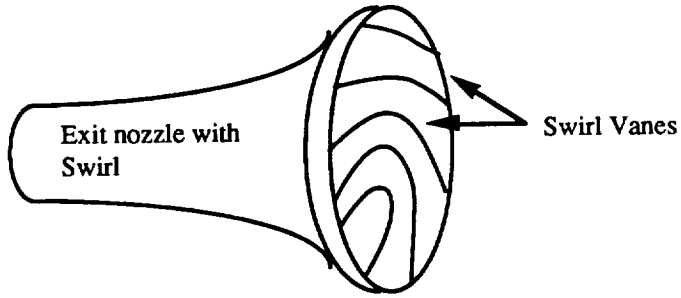

Figure 6.2-1 Injection Nozzle Diagram (Adapted form USRA,1993)

6.3 Input Parameters

From the vehicle selection section of the report (chapter 8), it was determined that the optimum plume radii for which a 3.6 ppbv. concentration should be achieved are 1200 and 1500 meters. Each of these radii require different amounts of propane to be injected, and therefore different injection mass flow rates. The parameter used to determine and describe this is the mass propane per plume unit length. These values were obtained from the required 3.6ppbv. average concentration, the desired plume radii, and the speed of the aircraft.

To achieve the most rapid mixing and distribution of the hydrocarbon as possible, the largest reasonable injection should be used. The largest nozzle is required because it allows for the lowest injection velocity and therefore produces the most turbulent mixing. Through consultation with Prof. Kirschbaum it was determined that a nozzle with a 20 cm. radius would be the largest allowable without producing large drag effects. Appendix A shows sample calculations of input variables needed to analyze propane distribution using Classical Diffusion Theory. Table 6.3-1 lists these input parameters for the two desired plume radii cases.

Table 6.3-1 Input Parameters

plume radius (m)	1200	1500
propane conc.(ppbv.)	3.6	3.6
mass prop./unit length plume (kg/m)	0.0030	0.0047
nozzle radius (m)	0.20	0.20
injection velocity (m/s)	94.4	147.5
injection Mach #	0.32	0.50
injection mass flow (kg/s)	2.12	3.32

6.4 Diffusion Theory Explanation

Classical diffusion theory (Carslaw & Jager, 1959) was used to determine the effectiveness of the mixing. The theory, analogous to heat conduction, was used to determine the mixing time required to attain the appropriate propane concentration over the plume area. Sample calculations using this theory are also shown in Appendix A.

The initial equation used for gas diffusion, eq. 6.4-1, was adapted from the differential equation for heat conduction, eq. 3-62 in *Boundary Layer Analysis*, (Schetz, 1993) with the help of Dr. Joseph Schetz.

$$U_\infty * (\partial C_i/\partial x) = (v_t/s_{ct}) * (\partial^2 C_i/\partial r^2 + \partial C_i/r\partial r) \qquad \text{(eq. 6.4-1)}$$

where:

$$v_t/s_{ct} = (0.025/0.8) * U_\infty * a * | 1 - (\rho_i U_i / \rho_\infty U_\infty) | \qquad \text{(eq. 6.4-2)}$$

rearranging,

$$(v_t/s_{ct}) * (1/U_\infty) = (0.025/0.8) * a * | 1 - (\rho_i U_i / \rho_\infty U_\infty) |$$

define the mixing constant c as,

$$c \equiv (v_t/s_{ct}) * (1/U_\infty) = (0.025/0.8) * a * | 1 - (\rho_i U_i / \rho_\infty U_\infty) |$$

This definition of the mixing constant allows simplifications later in the analysis.
Next, analyze the swirl effect by redefining the mixing constant by multiplying the original mixing constant by the swirl factor.

$$c = c * \text{Swirl Factor} \qquad \text{(eq. 6.4-3)}$$

Considering the analogous heat transfer equation for an infinite region with an initial temperature given by f(1) in cylindrical coordinates, the equation becomes eq. 6.4-4 (Carslaw & Jeager, 1959):

$$u = (V/2kt) * \exp(-r^2/4kt) \int_o^a \exp(-(r')^2/4kt) * I_0 * (rr' / 2kt) * r' dr' \qquad \text{(eq. 6.4-4)}$$

After performing variable substitutions to change a heat transfer problem to a mass diffusion problem, equation 6.4-4 becomes equation 6.4-5.

$$C_i = (1/2cx) * \exp(-r^2/4cx) \int_o^a \exp(-(r')^2/4cx) * I_0 * (rr' / 2cx) * r' dr' \qquad \text{(eq. 6.4-5)}$$

A set of tables called the P-function tables was then used to evaluate this integral. Joseph Masters shows how the P-function tables can be used to evaluate the integral in "Some Applications In Physics of the P-Function" (Masters, 1955).

Masters defines the P-function as follows:

$$P(Z/\sigma, R/\sigma) = \exp(-R^2/2\sigma^2) \int_o^z \exp(-r^2/2\sigma^2) * I_0 * (rR/ \sigma^2) * rdr \qquad \text{(eq. 6.4-6)}$$

Equating variables for diffusion analysis from eq. 6.4-5 to variables from Masters' P-function in eq. 6.4-6 gives:

diffusion var.	P-function var.
2cx	σ^2
a	Z
r	R
r'	r

We can then define the P-function in terms of diffusion analysis variables as follows:

$$C_i(a/\sigma , r/\sigma) = P(Z/\sigma, R/\sigma)$$

where

$$\sigma^2 = 2kt = 2cx$$

This definition allows one to evaluate the propane concentration at a specific point based on the nozzle radius, the distance behind the aircraft, and the distance from the centerline.

However, we can calculate the plume radius for a desired concentration at a given distance behind the aircraft using the following definition from Masters

$$P^* \equiv P(a/\sigma, r/\sigma) / P(a/\sigma, 0)$$

which in terms of diffusion variables is

$$P^* = C_i(a/\sigma , r/\sigma) / C_{\text{center line}}$$

Masters gives an equation for evaluation along the centerline (r=0) dependent upon nozzle design (a and c) and distance behind the aircraft (x). The expression follows.

$$C_{\text{center line}} = (1 - \exp(-a^2/2\sigma^2))$$

Since the desired concentration ($C_i(a/\sigma , r/\sigma)$) and centerline value are known, then P* is also known. Table II of the P-function tables lists P* based on r/σ and a/σ, leaving r as the only unknown. The calculated P* value is then matched to a tabulated P* value in the appropriate a/σ row and the value of r/σ read off. Then solve for r. An example of this calculation is made in Appendix A.

6.5 Diffusion Results

Analyzing propane dispersion using Classical Diffusion Theory reveals how a propane plume expands over time. Figure 6.5-1 shows the radius at which a concentration of 3.6 ppbv is achieved for mixing times up to two hours. This graph shows the plume radius increasing rapidly at first and then increasing slowly as mixing time increases for both the case of a 1200m desired radius and a 1500m desired radius. A mixing time of two hours was chosen to analyze the plume's propane concentration profile because the plume expansion has leveled off, while the results are not to far downstream to be questionable.

The propane concentration variations with distance from the plume's centerline after two hours of mixing time are shown in Figure 6.5-2. The case of a desired plume radius of 1500 meters is represented by a propane injection Mach number of 0.50 and the 1200 meter case is represented by a propane injection Mach number of 0.32.

The amount of propane injected into the atmosphere is enough to provide for a 3.6ppbv average concentration over the desired plume areas. Although the outer parts of the plumes have less than the desired concentrations after two hours of mixing, with time natural diffusion will even out the concentration profile to provide the desired average concentrations for both of the plumes.

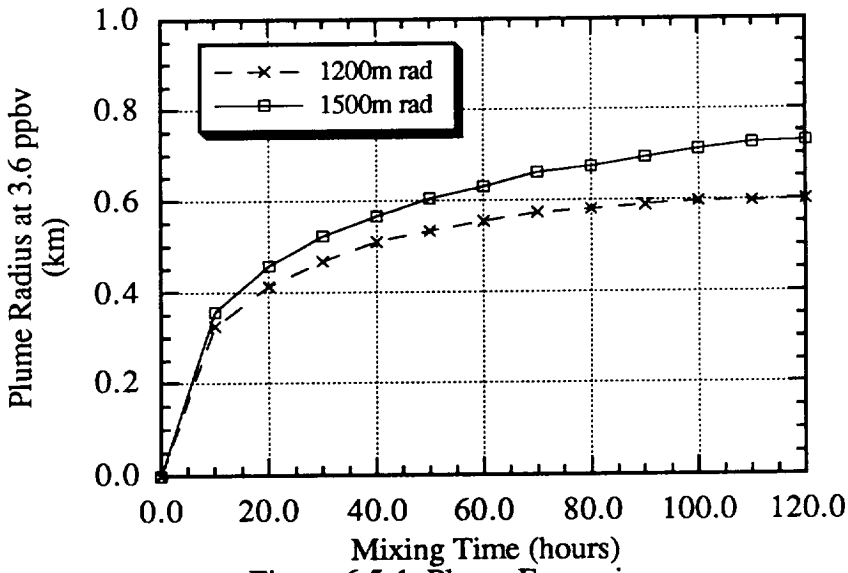

Figure 6.5-1 Plume Expansion

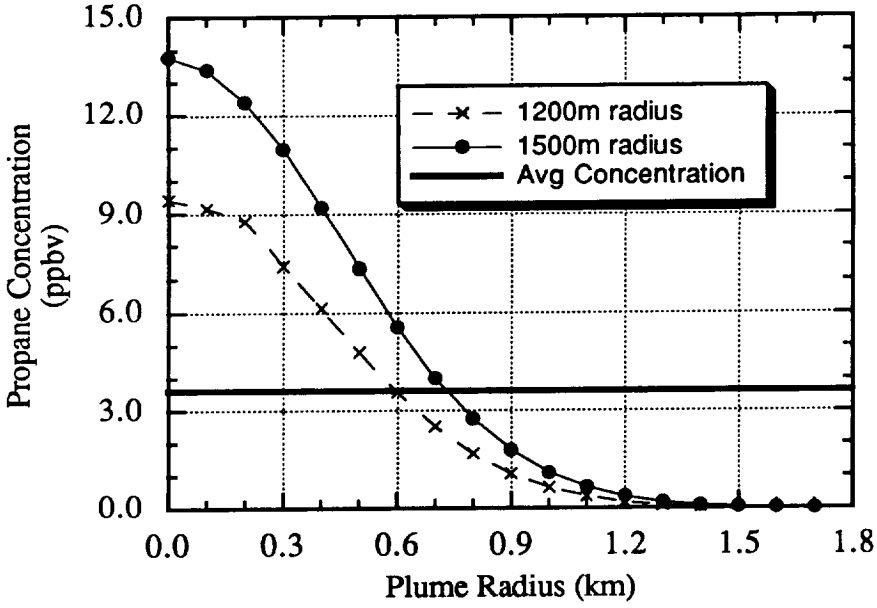

Figure 6.5-2 Plume Concentration Profile

Adjacent plumes were overlaped to compensate for the low propane concentration at the plume's outer edge, as shown in figure 6.5-3. For the 1.2 kilometer radius plume, overlap occurs in the region from 1 kilometer to 1.4 kilometers from the centerline. This occurs because the centerline of the two plumes are 2 kilometers apart, while each plume radius is 1.2 kilometers. This means that the concentrations at the edge of each plume will be increased by the propane at the edge of the adjacent plume. Figure 6.5-3 shows the propane concentrations at increasing radii from the centerline of one plume. In the 1.2 kilometer case, the concentration decreases to a minimum at 1.2 kilometers and then increasing again. The increase is due to the adjacent plume.

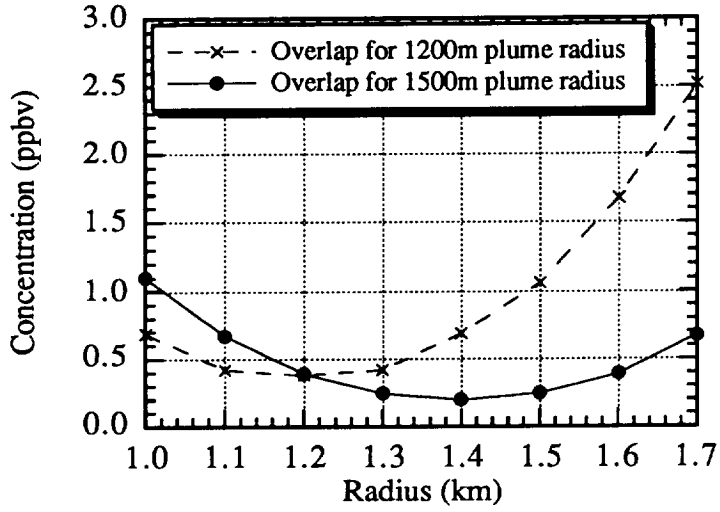

Figure 6.5-3 Propane Concentration Profile as the Plumes Overlap

6.6 Conclusion

The desired plume radii can be achieved through the use of turbulent mixing with induced swirl . The average concentration in the plume is 3.6ppbv as determined by Cicerone. All calculations were developed using Classical Diffusion Theory for a two hour mixing time, after which point natural diffusion will take over so as to finish distributing the propane throughout the vortex.

7.0 PROPANE STORAGE

7.1 Introduction

The aircraft propane storage system is an integral part of the delivery scheme. The propane will be stored in multiple identical, individual pressure vessels. A multiple vessel system is utilized to minimize center of gravity shifts, reduce in-flight stresses due to aircraft deflections, and provide safety in case of failure with a redundant system. The pressure vessels will be equipped with a relief valve exhausting to the atmosphere in case an emergency evacuation is required. The tank dimensions and mounting system presented in this analysis are for a delivery vehicle similar to the HSCT.

The size of the storage tanks is determined by both the amount of propane required and the size of the aircraft structure where the tanks will be mounted. The amount of propane required is a function of propane mass flow rate and propane injection range. The propane mass flow rate was determined in the mixing analysis, while the propane injection range was determined in the mission analysis. After determining the mass of propane, the volume was calculated, providing the required tank storage capacity. The size of the aircraft structure limits the maximum dimensions for each tank, as well as the overall dimensions of the entire storage system. Information on the aircraft structure was obtained from the aircraft configuration designer to determine the best location for storage system loading and mounting. The tank mounting system size was limited not only by the size of the cabin interior, but also by the size of the cargo door through which tank installation will occur. These dimensions were all obtained from the aircraft configuration design.

After determination of tank size and weight, this information was given to the configuration designer to incorporate into the overall aircraft design. If the desired propane payload could not be carried by the current aircraft configuration, the mixing analysis, mission analysis and configuration designers were all required to revise their respective designs to fit the new requirements.

7.2 Pressure Vessel Design

The pressure vessel is designed to be a cylindrical tank (length L and radius R) with spherical end caps (radius R). This tank provides the best balance of maximum space utilization and minimum stress. The propane will be stored at a gage pressure of 10 atmospheres in order to keep the propane at approximately 85% liquid state by volume (Southwest Virginia Gas Service Corp.). As a design requirement, the tanks must hold 19,270 kg (42,500 lbs) of propane to allow sufficient propane for the longest delivery mission.

An investigation of construction materials was conducted to determine the lightest and most durable material that would fulfill the design criteria. For each material investigated, the tanks were designed so they would not fail due to internal pressure and weight of the propane at a 2.5 g load, which is standard for air transports. A factor of safety of 2.0 was used. Failure would occur along the center line on the bottom of the tank when the tank is full, due to maximum weight concentration and high internal pressure. The tanks will be equipped with emergency relief valves exhausting to the atmosphere in case of tank failure. These relief valves will be set to open if internal tank pressure exceeds the optimum gage pressure of 10 atmospheres by more than 10%. The construction materials investigated in this analysis included:

1) Steel ASTM-A514
2) Aluminum 6061-T6 (1% Mg)
3) S-glass / epoxy composite
4) E-glass / epoxy composite
5) Aramid / epoxy composite
6) Graphite / epoxy composite
    - unidirectional and ±45° fiber direction
    - high strength and high modulus

A minimal thickness was calculated for the homogenous materials using Tresca's failure theory for 2-D stresses (Beer and Johnson), and Tsia-Hill failure criteria was used for the composite materials. Calculations are based on material properties shown in Table 7.2-1.

Table 7.2-1 Material Properties

Material	**σ_{yield} (MPa)**	**X (MPa)**	**Y (MPa)**	**$\rho_{material}$ (kg/m^3)**
Steel	690.0			7860.0
Aluminum	255.0			2710.0
S-glass/epoxy		1511.1	51.1	2043.3
E-glass/epoxy		1380.0	29.7	1960.4
Aramid/epoxy		724.5	70.38	1435.8
Graphite/epoxy *High Strength*				
0° Fiber direction		1242.0	55.2	1546.3
45° Fiber direction		160.1	160.1	1546.3
Graphite/epoxy *High Modulus*				
0° Fiber direction		759.0	27.6	1546.3
45° Fiber direction		116.6	116.6	1601.5

Homogenous materials: steel and aluminum

$$t = \frac{(0.8660254)\,(P)\,(R)\,(F.S.)}{\sigma_{yield}}$$

Non-homogenous materials: composite materials

$$t = (P)\,(R)\,(F.S.)\,(X^{-2} - 0.5X^{-2} + 0.25Y^{-2})^{0.5}$$

where:

$P = \rho_{propane} * 2R * g + 10$ atm.

$\rho_{propane} = 497.2$ kg/m^3

The material that produced the lightest tank structure and fulfilled the design criteria was the graphite / epoxy high strength ±45° fiber direction composite, and this was chosen as the material for storage tank construction. The necessary tank wall thickness for this material was determined to be 5.507 mm (0.2168 in). It may be necessary to provide some protection for the tanks during loading and unloading to protect them from puncture or denting caused by negligence of the tank handlers. This may be in the form of a protective foam or polyurethayne coating placed around the tanks. Depending on the size and weight of this coating, it could be removed after tank installation or left on to provide further protection.

The radius of the tank was set to be 0.5 meters (1.64 ft) to allow a three tank, stacked pyramid mounting system inside the pressure cabin of the delivery vehicle. The length of the tanks was found by using the preset tank radius along with the required mass of the propane payload per tank. The length of each tank was limited by the size and location of the cargo door used for loading. A maximum door size of 2.0 meters (6.56 ft) in length was set to prevent large structural loads and airframe weight penalties. For the specified propane payload capacity, storage systems ranging from 3 to 18 tanks were investigated. Individual tank length was then used to determine the necessary cargo door length. Figure 7.2-1 illustrates how the required entrance door size decreases as the number of tanks increases. These numbers are for a cargo door located aft of the pressure cabin and below the tail cone of the aircraft.

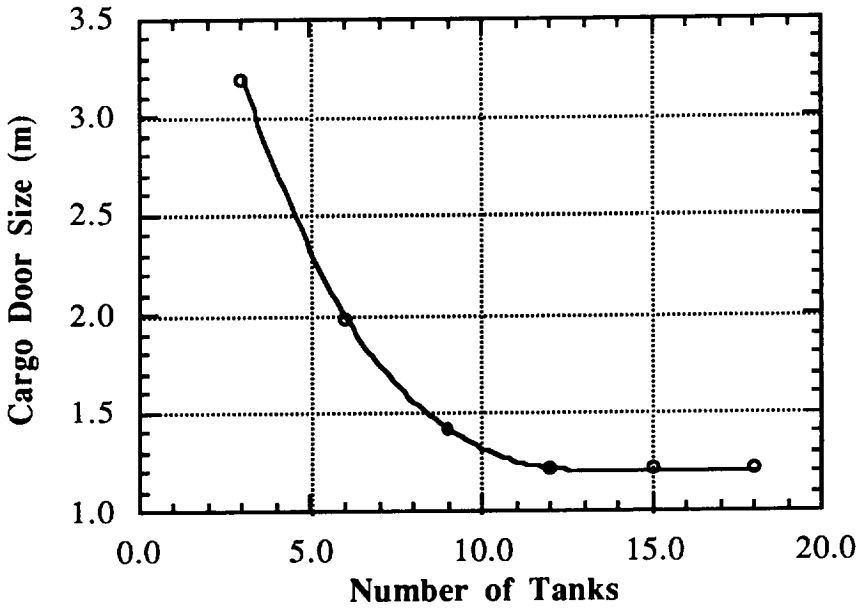

Figure 7.2-1 Cargo Door Dimension Along Fuselage Length

The trade-off for decreasing the necessary door size is an increase in the total mass of the tank system. The increase in storage tank mass with number of tanks is minimal, but the support system for each three-tank set has an estimated mass of 700 kg. (1,500 lb); this greatly increases the total mass of the storage system (Fig. 7.2-2).

To minimize the three-tank support system mass and provide ease of tank installation, a six tank system was chosen for propane storage, with the length of each tank being 7.557 m (24.8 ft). By placing the loading door at the rear of the pressure cabin, beneath the uprising tail cone (Figure 7.2-3), the required door height was 1.977 m (6.5 ft), with a door width of 1.5 m (4.9 ft). The tanks will be loaded individually into the aircraft through this loading door and into the support frame. The tanks will not be filled with propane until after being securely mounted in the aircraft so as to minimize loading weight and maximize safety during installation. Filling of the tanks is facilitated by running a hose in through the cargo door and connecting it to the tank valves.

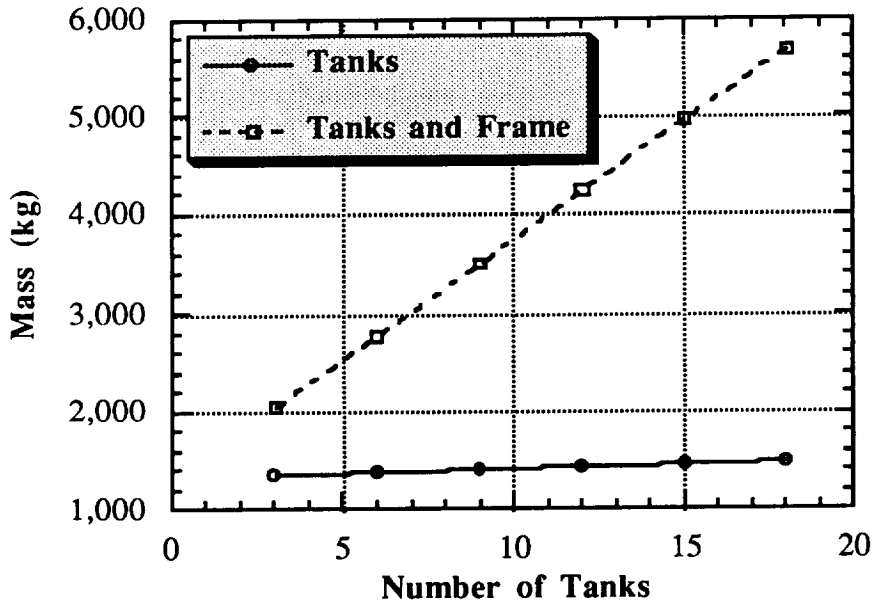

Figure 7.2-2 Storage System Mass

For the required payload capacity of 19,270 kg (42,500 lbs). and a delivery vehicle similar to the HSCT, six cylindrical pressure vessels with spherical end caps will be utilized. The overall dimensions and weight per tank are provided in Table 7.2-2.

Table 7.2-2 Pressure Vessel Specifications

Dimensions	Proposed 1993-1994
Material	Graphite/epoxy
Payload (kg)	19,269
Length (m)	7.557
Radius (m)	0.5
Wall Thickness (mm)	5.507
Mass (kg)	230.35

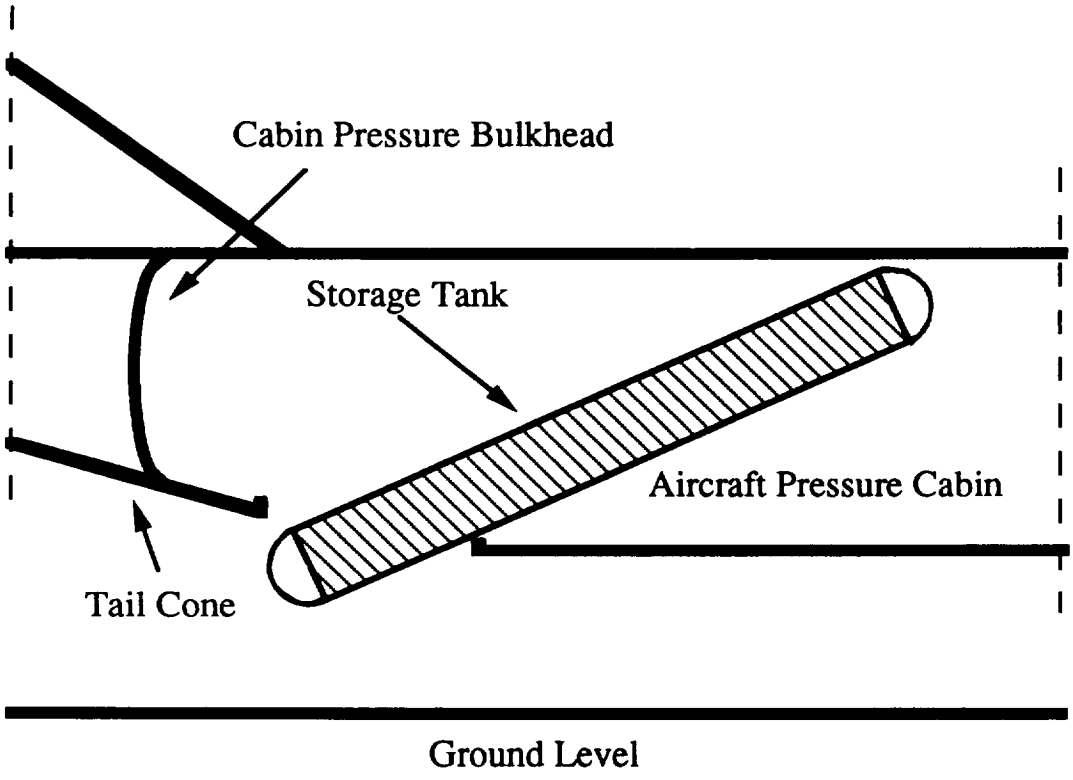

Figure 7.2-3 Propane Tank Loading

7.3 Mounting System

A mounting system was developed for an HSCT type delivery vehicle. The propane tanks must be able to withstand the torsional and bending moments imparted by the aircraft as well as the weight of the propane and tanks. It is also necessary to construct a modular mounting system that will allow the individual tanks to be removed with ease. If an HSCT type passenger aircraft is used for propane delivery, the tanks must be interchangeable with the normal passenger seating arrangements.

The previous year's USRA design team determined that the tanks should be placed in a support system which is rigidly fixed yet easily attached and detached to the airframe at one end, while the other end should be relatively free in order to reduce the torsional and bending moments and to allow for fuselage expansion at the delivery Mach number. The three tanks are rigidly fixed to one another, and also attached to the supports with a non-rigid support. The tank system will be equipped with tracks which move along airframe

mounted ball bearings so that each tank may be easily removed from the aircraft. The supports will be constructed from rolled steel to maximize strength while minimizing size. A simple schematic of the mounting system is illustrated in Figure 7.3-1. The mounting system will be dismantled for installation and removal. Loading will be through the rear cargo door.

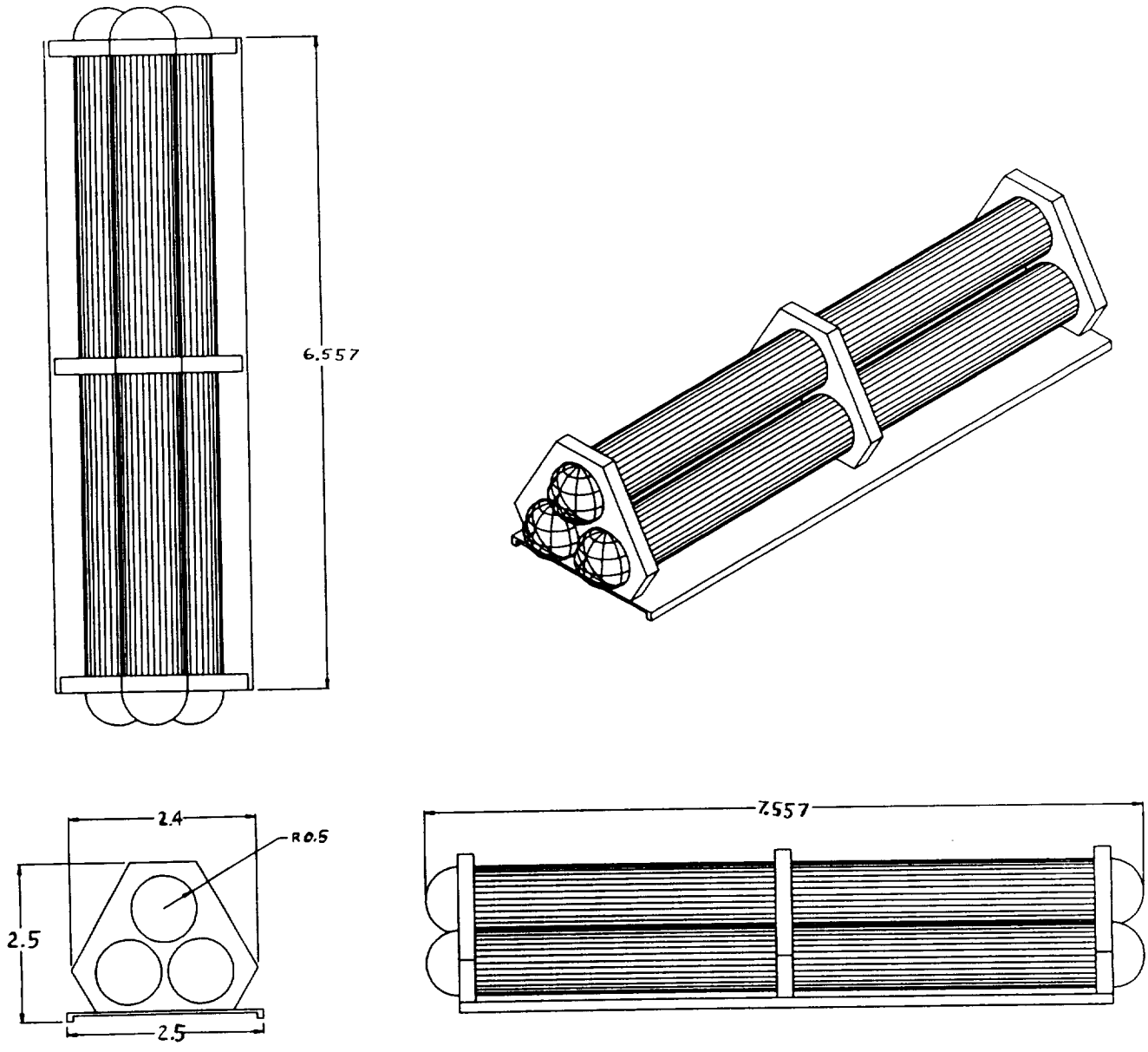

Figure 7.3-1 Propane Storage Tanks

7.4 Summary

The aircraft propane storage system will consist of six identical, individual, interconnected pressure vessels. The total propane capacity for the six tanks will be 19,270 kg (42,500 lbs) stored at 10 atmospheres gage pressure. The six vessel, stacked system is utilized to minimize center of gravity shifts, reduce in-flight stresses due to aircraft deflections, provide safety through redundancy in case of tank failure, and facilitate ease of tank installation. The tanks will be constructed of graphite / epoxy high strength 45° fiber direction composite material to minimize tank weight. The empty storage tanks will be loaded through a cargo door placed in the rear of the aircraft, beneath the uprising tail cone. Loading of propane into the tanks will take place by way of hoses entering through the cargo door of the aircraft.

8.0 AIRCRAFT CONFIGURATION STUDIES

The Virginia Tech USRA Advanced Design Team has set forth its latest iterations of mixing problem, mission analysis, and tank configuration studies in this report. The mixing problem studies showed an obtainable plume radius was 1500 meters (4,920 ft) or less in size. The mission analysis computed all the possible mission variations with respect to Mach, refuelings per mission, obtainable mixing plume radius, and aircraft payload capability. The tank configuration analysis showed how much storage volume and payload capability an aircraft would need for tanks that store a specific propane payload. These studies were used to derive a set of baseline parameters for researching delivery vehicle candidates.

Utilizing the established baseline parameters, nine aircraft designs were researched. The designs were then compared to identify their relative performance with respect to the baseline parameters, and the resulting comparison were used to formulate a set of selection criteria. After assessing the nine designs with respect to the selection criteria, the HSCT 2.4E design was selected for the ozone depletion prevention mission (from herein "the USRA mission.")

Upon selection of the HSCT 2.4E design, aircraft configuration studies were initiated to analyze how effectively it could perform the USRA mission. The HSCT 2.4E design was modified and optimized for the USRA mission using the AirCraft SYNThesis computer modeling code at Virginia Tech (ACSYNT, 1994.) ACSYNT is a parametric design tool that provides computer aided drawing (CAD) and aircraft sizing optimization capabilities. In addition to modifying the HSCT 2.4E design for the USRA mission, a dedicated aircraft concept, a conceptual aircraft specifically configured for flying the USRA mission, was modeled and optimized using ACSYNT. The dedicated aircraft concept was formulated to provide a reference point for determining how well the modified HSCT 2.4E design (from herein the "HSCT variation") could perform the USRA mission.

In addition to modeling and optimizing the HSCT variation and dedicated aircraft concepts using ACSYNT, USRA mission scenarios were selected for these aircraft concepts using the mission analysis code described in Section 4.0. Initial mission selections were conducted to provide a starting point for the ACSYNT modeling process, and final mission selections were made after the aircraft concepts were optimized using ACSYNT.

To conclude the aircraft configuration studies performed on the HSCT variation, sensitivity studies were done on the HSCT variation and the dedicated aircraft concepts with respect to cost and USRA mission performance. Doing so provided clear evidence that the HSCT variation would be able to perform the USRA mission effectively.

8.1 Baseline Aircraft Design Studies

8.1.1 Baseline Aircraft Parameters

A baseline set of aircraft and mission parameters was developed for the purpose of assessing aircraft design data. The parameters were derived from the results of the mixing problem, mission analysis, and tank storage studies. The aircraft and mission parameters are listed in Table 8.1.1-1.

Table 8.1.1-1 Baseline Aircraft and Mission Parameters

Aircraft Parameters	
Cruise Mach	2.4
Cruise L/D	<= 11
Cruise SFC	>= 1.3
Storage Volume	147 m^3 (5,200 ft^3)
Payload	30,180 kg (66,700 lbs)
Mission Parameters	
Range	12,030 km (6,500 nmi)
Cruise Altitude	20,122 m (66,000 ft)
Refuelings	1
Ground Time	4 hrs
Propane Payload	24,660 kg (54,500 lbs)
Plume Radius	1000 m (3,228 ft)
KC-10s Required	25
Aircraft Fleet Size	99

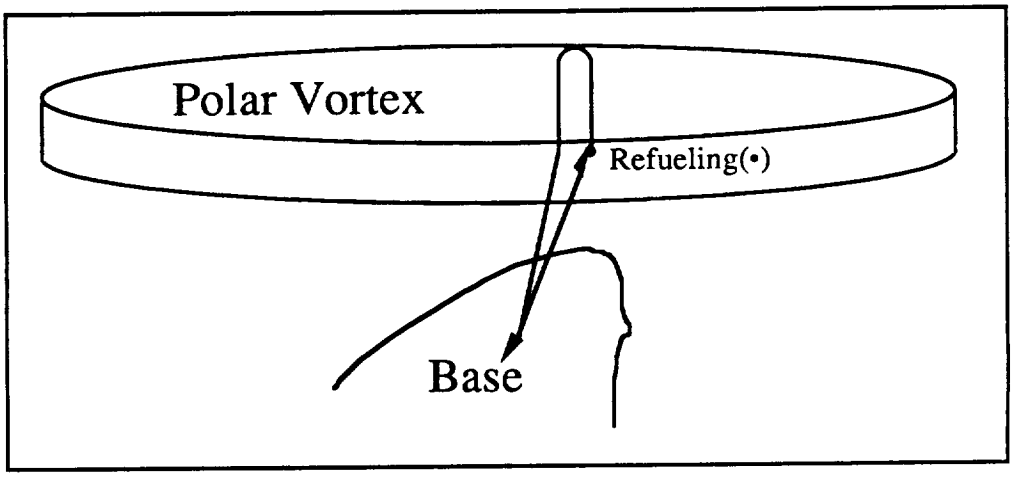

Figure 8.1.1-1
Baseline Mission Diagram

The mission analysis shows a fleet of 99 aircraft would be required to complete the USRA mission using an aircraft with the baseline parameters. The mission would assume a mixing plume radius of 1000 meters (3,280 ft) since the mission analysis showed this was the best mixing radius for baseline payload capability. The aircraft meeting the baseline parameters would also have to be refueled once prior to entering the polar vortex to

perform propane injection. A diagram of the baseline mission is shown in Figure 8.1.1-1 and illustrates this refueling regime.

8.1.2 Matrix of Designs Considered

The matrix shown in Table 8.1.2-1 shows the designs researched and compared to the baseline aircraft and mission parameters. The aircraft fell into three major categories. The first were moderate Mach and range vehicles capable of meeting USRA mission payload requirements. These aircraft were all commercial supersonic transport designs.

The second category of aircraft were low Mach and high range vehicles. These vehicles were both supersonic bombers. Supersonic bombers have the payload capability required for the USRA mission but their storage volume capability is conducive to warheads much denser in mass than liquid propane. Also, the cruise Mach of these supersonic bombers is less than half of the baseline cruise Mach (see Table 8.1.1-1.)

The third category of aircraft assessed were high Mach and low payload vehicles. The vehicles in this grouping are both Mach 3 aircraft. The XB-70, designed to be a supersonic bomber, only has a payload capability of 4525 kg (10,000 lbs.) The SR-71 was a reconnaissance aircraft with very low payload capacity also. In addition, the SR-71 does not have the range required for the USRA mission.

Assessing the three categories of aircraft in Table 8.1.2-1 showed the only grouping of aircraft capable of completing the USRA mission were commercial supersonic transport designs. These were the only designs assessed with anywhere near the storage and payload capabilities needed to match the baseline parameters in Section 8.1.1. All, the designs in Table 8.1.2-1 are evaluated with respect to a set of selection criteria outlined in Section 8.1.3.

Table 8.1.2-1 Existing Aircraft Design Data

Aircraft Design	First Flight	Cruise Mach	Range	Altitude	Payload	Storage	TOGW	Fleet Size	Takeoff Thrust
	Date		km (nml)	m (ft)	kg (lbs)	m^3 (ft^3)	kg (lbs)		kN st (lbs st)
Baseline Vehicle Presented in Table 8.1.1-1									
Baseline	-	2.4	12,220 (6,500)	20,121 (66,000)	24,660 (54,500)	147 (5,200)		-	
Moderate M and Range Vehicles									
HSCT[1] 2.4E	-	2.4	10,180 (5,500)	16,770 (55,000)	35,430 (78,300)	442 (15,600)	256,000 (565,760)	-	871 (196,000)
Tupolev Tu-144[2]	6/5/69	1.9	6,480 (3,500)	17,990 (59,000)	14,960 (33,000)	195 (6,880)	179,560 (396,800)	~15	783 (176,360)
Concorde 2	12/6/73	2.04	6,220 (3,360)	18,290 (59,990)	12,670 (28,000)	168 (5,930)	184,620 (408,010)	16	676 (152,200)
Boeing SST[2]	-	2.7	7,410 (4,000)	19,510 (64,000)	32,760 (72,400)	400 (14,115)	297,180 (656,770)	-	1067 (240,000)
Lockheed L-2000[2]	-	2.7	N/A	>20,120 (>66,000)	22,620 (50,000)	323 (11,400)	226,250 (500,000)	-	889 (200,000)
Low Mach and High Range Vehicles[2]									
Rockwell Intl. B1-B	10/18/84	.9	11,990 (6,475)	18,290 (60,000)	28,960 (64,000)	62 (2,188)	215,840 (477,000)	100	533 (120,000)
Tupolev Tu-160	12/19/81	.8	13,980 (7,550)	18,290 (60,000)	16,290 (36,000)	74 (2,611)	274,330 (606,300)	~40	>400 (90,000)
High Mach and Low Payload Vehicles[2]									
North American XB-70	9/21/64	3.0	14,070 (7,600)	21,340 (70,000)	4,530 (10,000)	Minimal	239,820 (530,000)	1	827 (186,000)
Lockheed SR-71	12/22/64	3.0	5,550 (3,000)	24,010 (78,750)	2,260 (5,000)	Minimal	65,610 (145,000)	~35	289 (65,000)

[1]Hutchinson, M.G., Mason, W.H., Grossman, B., and Haftka, R.T., "Aerodynamic Optimization of an HSCT Configuration Using Variable-Complexity Modeling," AIAA Paper 93-0101, 1993.

[2]*Jane's All The World's Aircraft*, 1968-69, 77-78, 80-81, 88-89, Jane's Publishing Company Inc., New York, New York.

In the process of researching existing aircraft designs, subsonic vehicles were also considered. However, no subsonic vehicle design capable of transporting even half of the baseline payload and cruising at 20,120 m (66,000 ft) was found. Subsonic vehicles capable of cruising at 20,120 m (66,000 ft), such as the Lockheed U-2 are designed to transport a minimal payload of less than 340 kg (750 lbs) (Gourley, 1991.) Subsonic commercial transports which can carry the baseline propane payload, such as the Airbus

340-200 and Boeing 767-200, are designed to cruise at an altitude of approximately 33,000 ft (*Janes*, 1989.)

Since no subsonic designs are capable of carrying the baseline payload and cruising at the baseline altitude, the feasibility of designing a subsonic transport that cruises at 20,120 m (66,000 ft) from scratch was assessed. To determine the feasibility, a Boeing 767-200 of wing span 156 ft and an aspect ratio of 12 was sized to fly the baseline range and payload presented in Section 8.1.1 (*Janes*, 1989.) Using a Nicolai method code calibrated with an Airbus 320, MD-80, and Boeing 737-200, an aircraft with the following characteristics resulted (Nicolai, 1975):

Table 8.1.2-2 Subsonic Vehicle Sizing Results

Aircraft Parameter	Boeing 767-200-P[1]	USRA Subsonic Aircraft[2]
Cruise Mach	0.8	0.8
Cruise Altitude	10,610 m (34,800 ft)	20,122 m (66,000 ft)
L/D[2]	18	18
TOGW	135,747 kg (300,000 lbs)	170,135 kg (376,000 lbs)
Wing Area	283 m^2 (3,050 ft^2)	650 m^2 (7,000 ft^2)
Range	10,663 km (5,760 nmi)	12,220 km (6,500 nmi)

[1] *Jane's All The World's Aircraft*, 1991-92, Jane's Publishing Company Inc., New York, New York.
[2] Calculated with the Nicolai method code.

The resulting vehicle configuration represents a subsonic transport with an excessively large wing area to allow it to fly at high altitudes. This large wing area would demand a large structural wing weight (reflected in the 170,135 kg (376,000 lbs) total gross weight.) A Boeing 767-200 capable of traveling 12,220 km (6,500 nmi) weighs 135,750 kg (300,000 lbs) at takeoff. In addition, the mission analysis code showed that a fleet of 165 aircraft would be required to complete the USRA mission flying at Mach 0.8. This is 33% more aircraft than specified by the baseline mission parameters in Section 8.1.1.

Even if a subsonic aircraft capable of flight at 20,120 m (66,000 ft) could transport the required baseline propane payload, the aircraft would not be capable of handling the polar vortex environment. In the vortex, gusts exceed 360 km/h (195 knots) at the end of the polar winter, which coincides with the proposed time window for the USRA mission (Wayne, 1991.) An aircraft traveling at Mach 0.8, which equates to 850 km/h (459 knots) at 20,120 m (66,000 ft), encountering a forward gust of 360 km/h (195 knots) would be pushed past the speed of sound to a resultant velocity of Mach 1.14 (1210 km/h (655 knots.)) The control surfaces on a subsonic or transonic vehicle flying at Mach 1.14 would be rendered temporarily ineffective by the occurrence of shocks. If the aircraft encountered a tail gust of 360 km/h (195 knots) and had a C_{Lmax}=1.2 at 20,120 m (Raymer, 5-19), the aircraft will slow to a resultant speed of 490 km/h (265 knots), according to Equation 8.1.2-1, which is below its stall speed of 794 km/h (429 knots.) Therefore, a subsonic aircraft encountering a typical polar winter tail gust in the vortex would stall.

$$C_{Lmax}=1.2= W / {}^{1}/_{2}\rho V_{stall}{}^{2}S \qquad \text{[Equation 8.1.2-1]}$$

The stall speed calculation was performed using the vehicle parameters determined for the Boeing 767-200 type vehicle sized in Table 8.1.2-2.

A supersonic aircraft flying at Mach 2.4 (2547 km/h (1,379 knots)) that encounters a tail gust of 360 km/h (195 knots) would only be slowed to Mach 2.06 which would be well in its cruise envelope. Due to the stall speed problem encountered by subsonic designs in the polar vortex environment, only supersonic designs were considered for the USRA mission.

8.1.3 Selection Criteria

In addition to comparing existing aircraft designs to a set of baseline parameters, a set of selection criteria were developed for making a final concept selection. The selection criteria were the following:

[1] Mission profile can take any form as long as the mission objectives are accomplished in the 3 week delivery time window.

[2] Vehicle technology must be available by the year 2006.

[3] If an existing aircraft is selected, no more than 20% of the vehicle should be re-designed to complete the mission. This is an industry standard.

[4] Aircraft must have a viable alternative use it performs efficiently and cost effectively when not flying the USRA mission (e.g. commercial transport.)

[5] The vehicle performance envelope must be able to handle the polar vortex environment (e.g. gusts in excess of 360 km/h (195 knots.))

[6] The mixing process dictates a propane payload / injection range ratio of at least 2.08 kg/km (8.38 lb/nmi) must be achievable by the delivery vehicle to complete the baseline mission presented in Section 8.1.1.

[7] The vehicle has sufficient range to reach the closest base from the center of the vortex (6850 km (3700 nmi)) without tanker support.

[8] The noise suppression regulations of the selected airports must be obeyed.

[9] NOx emissions should be less than 5 g/kg (.005 lb/lb) (Kandebo, 1993.)

[10] Vehicle configuration must be conducive to mixing process.

[11] The vehicle must be able to be serviced and loaded with propane in 4 hours to perform the baseline mission in Section 8.1.1.

[12] If an existing vehicle, resuming production of the vehicle must be feasible.

[13] The number of sorties the vehicle requires to complete the mission profile must not exceed the capabilities of the selected airports.

The above criteria provide detailed constraints for aircraft selection. The criterion that apply to logistical aspects of the mission, specifically criterion 8, 9, 11, 12, and 13, are not going to be assessed at this stage of the project.

8.1.4 Concept Selection

The concept selected from the matrix in Table 8.1.2-1 with respect to the baseline parameters and the selection criteria was the HSCT 2.4E. A top view of the HSCT 2.4E design is in Figure 8.1.4-1. The HSCT 2.4E, comes closer to meeting the baseline range than the Tupelov 144, Boeing or Lockheed supersonic transport designs in Table 8.1.2-1. The HSCT 2.4E design will also meet NOx emission and takeoff noise regulation selection criteria (criteria 8 and 9) as compared to the Concorde (Taylor, 1989.) The Tupolev 160 and Rockwell International B1-B do not have the storage capacity or cruise Mach to complete the USRA mission in accordance with criterion 6. The SR-71 and XB-70 do not have the payload and storage volume capabilities to satisfy criterion 6 as well.

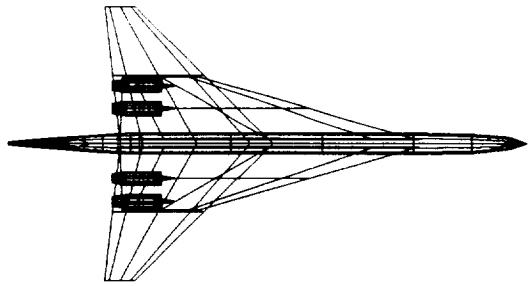

Figure 8.1.4-1
Top View of HSCT 2.4E Class Aircraft Design

The HSCT 2.4E design has capabilities equivalent or better than the baseline payload, storage volume, and cruise Mach. However, the HSCT 2.4E design does not quite meet the baseline range or cruising altitude requirements of the USRA mission. Therefore, it was decided that upon selection of the HSCT 2.4E concept, that a HSCT variation concept would be sized for the USRA mission.

8.1.5 Dedicated Aircraft Concept

In order to assess how effectively the HSCT variation would perform the USRA mission, a dedicated aircraft concept was formulated. This concept, by definition, would be an aircraft configured explicitly for the USRA mission and is herein referred to as the "dedicated aircraft." Deriving the dedicated aircraft concept provided a quantitative means to determine the penalty for using an aircraft designed to be a commercial transport to perform the USRA mission.

The dedicated aircraft was derived from and essentially represents a HSCT 2.4E optimized for the USRA mission. The HSCT 2.4E design has more than enough storage volume required to perform the USRA mission, but it does not have the capability to haul an exceptional mass of propane payload. The HSCT 2.4E is configured to carry a much less dense payload than liquid propane stored at 10 atmospheres which has a density of 0.41 kg/m^3 (32 lb/ft^3.) The fuselage on the dedicated aircraft concept was shortened and loaded with a large mass of propane since its smaller fuselage had significantly less friction drag and wave drag than the HSCT 2.4E design.

8.2 ACSYNT Model Construction

After determining what concepts to model to perform USRA mission aircraft configuration studies, the parameters of each concept, the HSCT variation and dedicated aircraft, were loaded into ACSYNT (ACSYNT Institute, 1993.) Since an ACSYNT model already existed for the HSCT 2.4E, this model was duplicated and modified in order to build the HSCT variation and dedicated aircraft models. However, prior to building these ACSYNT models, USRA mission scenarios were selected for each concept by entering their proposed propane payload capabilities into the mission analysis.

8.2.1 Initial Mission Selection

The USRA mission scenarios selected for HSCT variation and dedicated aircraft concepts are in Table 8.2.1-1. These missions were not intended to be the optimum mission profiles for the concepts, but rather starting points around which to build ACSYNT model data files. After the models were optimized the resulting aircraft capabilities were put back into the mission analysis to calculate the best USRA mission scenario for the aircraft concept.

These missions are different from the baseline mission specification in Table 8.1.1-1. The HSCT variation mission was selected to fit the payload and storage capability of the HSCT 2.4E design (see Table 8.2.1-1.) The mission analysis determined the plume radius of 1000 meters (3,280 ft) would be best for an aircraft with an 38,461 kg (85,000 lb) payload capability utilizing two refuelings per mission.

The mission selected for the dedicated aircraft concept took advantage of the maximum refuelings allowed by the mission analysis. This mission was selected since the

mission analysis discussion in Section 4.0 indicates that the overall fleet size required for the USRA mission drops significantly when a plume radius of greater than 1500 m (4,920 ft) is selected. The amount of propane injection levels required drops from three to two for this plume radius.

Table 8.2.1-1 Mission Selection Data

Mission Parameter	***HSCT Variation***	***Dedicated Aircraft***
Range	12,030 km (6,500 nmi)	12,030 km (6,500 nmi)
Cruise Altitude	20,122 m (66,000 ft)	20,122 m (66,000 ft)
Refuelings	2	1
Ground Time	4 hr	5 hr
Propane Payload	38,461 kg (85,000 lbs)	57,470 kg (127,000 lbs)
Plume Radius	1000 m (3,280 ft)	1800 m (5,904 ft)
KC-10s Required	136[1]	20[2]
Aircraft Fleet Size	68	40

[1]The HSCT variation requires 42,530 kg (94,000 lbs) when refueling at the edge of the vortex, this is 1/2 the capacity of a KC-10. The HSCT variation requires the capacity of 2 KC-10s on its second refueling. It was assumed that the KC-10s doing the initial refueling could refuel and do the second.
[2]The dedicated aircraft requires 44,200 kg (97,690 lbs) when refueling at the edge of the vortex, this is 1/2 the capacity of a KC-10.

The mission diagrams for each of the mission scenarios presented in Table 8.2.1-1 are presented in Figures 8.2.1-1a-b. The mission diagrams illustrate the refueling arrangements. The first refueling in both of the mission scenarios occurs after the aircraft climbs to altitude and prior to entering the vortex to distribute propane (see Section 4.0.) The additional refueling in the HSCT variation mission occurs after the aircraft has made one propane distribution run through the vortex.

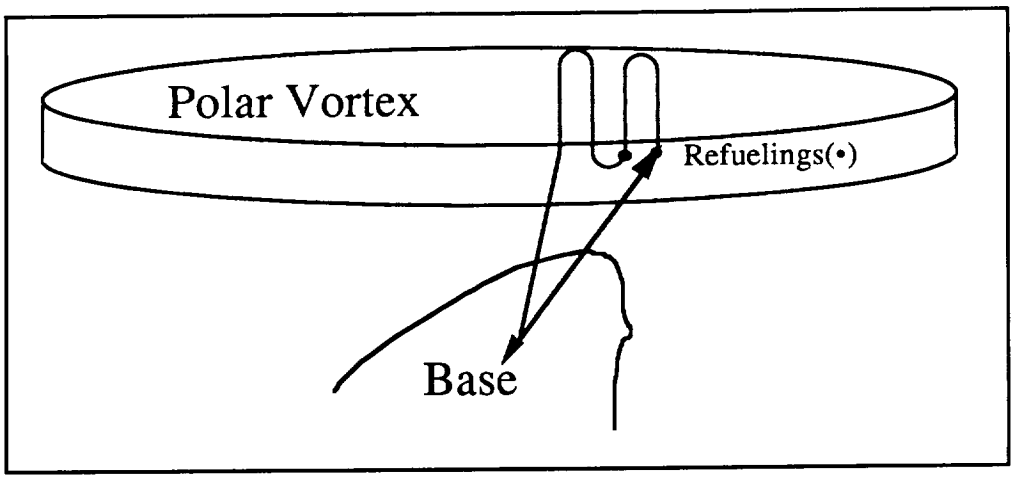

Figure 8.2.1-1a
HSCT Variation Mission Diagram

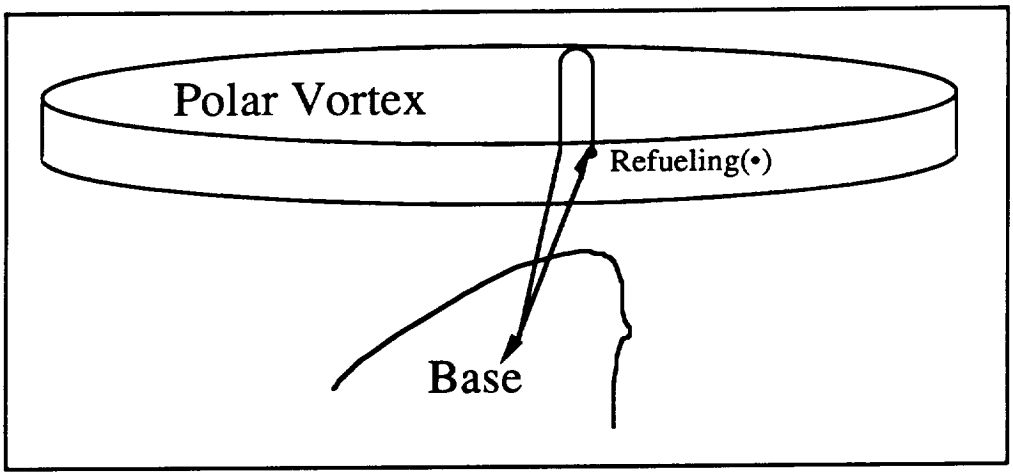

Figure 8.2.1-1b
Dedicated Aircraft Mission Diagram

8.2.2 Objective of ACSYNT Analysis

The objective of sizing the HSCT variation and the dedicated aircraft concepts was to find out the answers to the following questions:

1) How would the HSCT 2.4E design have to be varied to fly the USRA mission?

2) How would the USRA mission suffer by flying an HSCT variation instead of a dedicated aircraft?

This first question will be answered through by optimizing the HSCT 2.4E for the USRA mission and generating the HSCT variation concept. The characteristics and cost effectiveness of the HSCT variation will then be compared to the HSCT 2.4E design. An ACSYNT HSCT 2.4E model has been built by Brett Malone specifically for the purpose of HSCT class aircraft sensitivity studies (Malone, 1993.)

The second question will be answered through comparing how much better than the HSCT variation a dedicated aircraft can perform the USRA mission and also by assessing the cost of the dedicated aircraft. The essential question is whether or not the revenue earning capability of the HSCT variation concept justifies how ineffectively it flies the USRA mission when compared to the dedicated aircraft. An ACSYNT cost module has been built by Malone for calculating the cost and revenue earning capability of HSCT class aircraft. This cost module will be used to calculate costs for both the HSCT variation and dedicated aircraft concepts.

8.2.3 Carpet Plot of a HSCT Class Aircraft

Using the Malone HSCT 2.4E ACSYNT model configured for a USRA mission trajectory, the carpet plot of an HSCT class aircraft in Figure 8.2.3-1 was generated. The plot indicates that an HSCT class aircraft needs a landing thrust to weight ratio (T/W) of at least .25 and a wing loading (W/S) less than approximately 86.5. The resultant 362,000 kg (800,000 lbs) takeoff gross weight (TOGW) numbers indicate that aerodynamic drag, engine performance, or engine size must be optimized to have a feasible HSCT 2.4E variation that can fly the USRA mission. It was decided that a feasible HSCT 2.4E design variation would have a TOGW of 316,740 kg (700,000 lbs) or less. A heavier aircraft

requires a significant increase in total engine thrust above that specified in the HSCT 2.4E design in order to meet the T/W=.25 requirement set forth by the carpet plot in Figure 8.2.3-1.

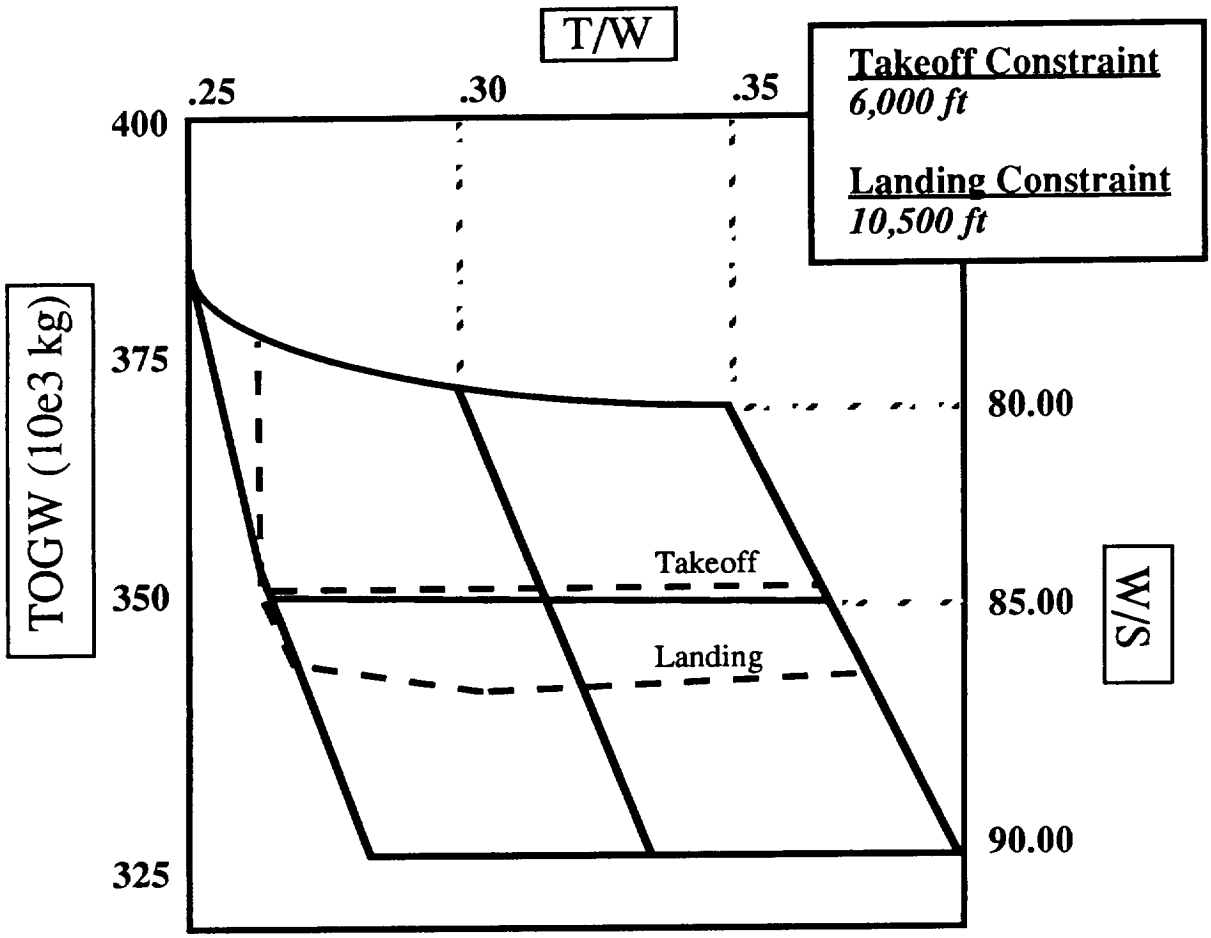

Figure 8.2.3-1
Carpet Plot of HSCT Class Aircraft

Since only the longest landing field at the airports considered for the USRA mission in Section 5.0 meet or surpass the landing field length requirements (3,353 m (11,000 ft)) in the HSCT carpet plot, a sensitivity study was done on landing field length. Figure 8.2.3-2 shows the result of this study. It indicates that the allowable wing loading decreases significantly for every 100 ft of landing field length is decreased. A decrease in wing loading, allows for a smaller wing area and a structurally lighter aircraft. Thus, the

runways at the airports intended to be utilized for the USRA missions should be lengthened instead of building an entire fleet of heavier-than-necessary aircraft.

The HSCT 2.4E design requires a landing field length of 3,353 m (11,000 ft) according to Malone's ACSYNT model. If a fleet of HSCT class aircraft were built for commercial transport, they would most likely be accommodated by the major airports of the world who currently have 3,353 - 3,963 m (11,000 - 13,000 ft) runways. Therefore, it will be assumed that present day USRA mission base configurations in Section 5.0 do not represent a landing field constraint that requires consideration in the sizing of the HSCT variation concept.

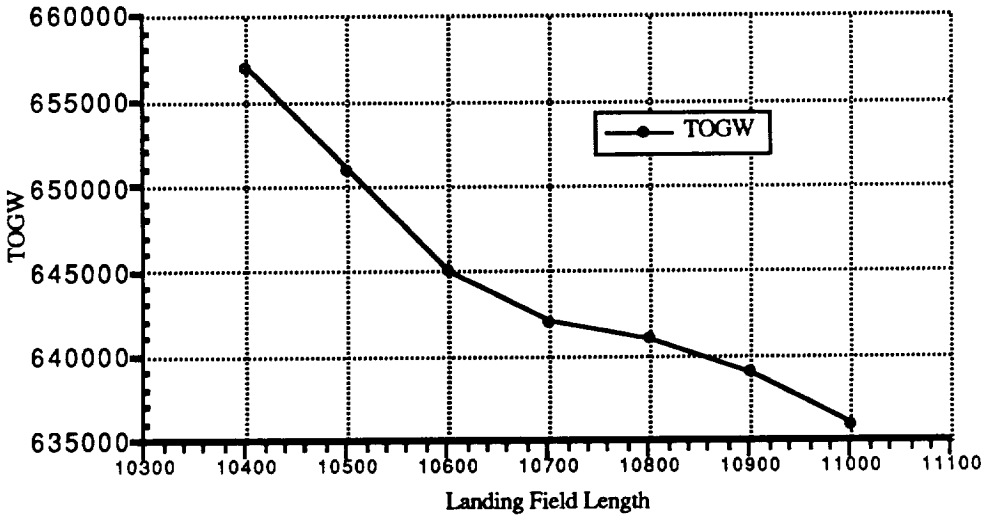

Figure 8.2.3-2
Landing Field Length Sensitivity Plot

8.2.4 ACSYNT Model Input

Using the mission selections in Section 8.2.1 and the carpet plot in Section 8.2.3, ACSYNT model input was derived for the HSCT variation and dedicated aircraft concepts. Table 8.2.4-1 shows this input data in comparison with the HSCT 2.4E design data in Malone's HSCT ACSYNT model (Malone, 1993.)

Table 8.2.4-1 ACSYNT Model Input Data

ACSYNT Parameter	*HSCT 2.4E*	*HSCT Variation*	*Dedicated Aircraft*
Cruise Mach	2.4	2.4	2.4
Range	10,180 m (5,500 nmi)	12,033 km (6,500 nmi)	12,033 km (6,500 nmi)
Cruise Altitude	16,770 m (55,000 ft)	20,120 m (66,000 ft)	20,120 m (66,000 ft)
Cruise SFC[1]	1.0	1.3	1.3
Wave Drag Factor[2]	1.0	1.0	1.0
Propane Payload	35,430 kg (78,300 lbs)[3]	38,460 kg (85,000 lbs)	62,440 kg (138,000 lbs)
Tank and Plumbing Weight[4]	N/A	8,326 kg (18,400 lbs)	11,824 kg (26,130 lbs)
Fuselage Length	86.59 m (284 ft)	86.59 m (284 ft)	41.67 m (137 ft)
Fuselage Diameter	3.66 m (12 ft)	3.66 m (12 ft)	3.05 m (10 ft)
Elevation of Mean AC	Bottom of Fuselage	Bottom of Fuselage	Middle of Fuselage
Wing Area	697 m^2 (7,500 ft^2)	790 m^2 (8500 ft^2)	679 m^2 (7300 ft^2)
Aspect Ratio of Wing	3.0	3.0	3.0
Wing Ref Sweep	38°	38°	38°
Taper Ratio of Wing	0.2	0.2	0.2
t/c_{root} of Wing	0.02	0.02	0.02
t/c_{tip} of Wing	0.02	0.02	0.02
Engine Weight *(per engine)*	3,167 kg (7,000 lb)	3,824 kg (8,450 lb)	3,462 kg (7,650 lb)
Engine Thrust *(per engine, w/o A/B)*	173 kN st (39,000 lb)	191 kN st (43,000 lb)	191 kN st (40,000 l)

[1]The cruise SFC was set to 1.0 in the Malone HSCT 2.4E model, but according to Peter Coen, the proper SFC setting for the 2006 technology factor specified in criterion 2 is 1.3 (Coen, 1993.)

[2]The wave drag factor was left at 1.0 during the model building process. The purpose of this factor is to adjust wave drag with respect to an optimum Sears-Haack since ACSYNT has no analysis that will perform this task.

[3]The payload of the HSCT 2.4E design equates to 250 passengers and baggage (22,624 kg (50,000 lbs) and 12,805 kg (28,300 lbs) of passenger accommodations cargo.

[4]The mass of the propane storage tanks, injection system plumbing, and refueling system plumbing was based on an estimate of 2,715 kg (6,000 lbs) for the plumbing systems and an estimate of 2,800 kg (6,200 lbs) of storage tanks for each 19,230 kg (42,500 lbs) of propane payload. The estimate for the tanks was based on data from Section 7.0.

The goal of modeling the HSCT variation concept was to generate the data required to determine the answer of the first question in Section 8.2.2. The basic aim of sizing an HSCT variation was to see if a feasible (316,742 kg (700,000 lbs) or less as specified in Section 8.2.3) commercial supersonic transport could fly the USRA mission scenario selected for the HSCT variation in Section 8.2.1.

All passenger accommodations were removed from the HSCT 2.4E to size the HSCT variation for the USRA mission. This amounted to approximately 3.5 % of the total gross weight of the aircraft or approximately 9,050 kg (20,000 lbs) (Moore, 1992.) The passenger accommodation weight was replaced with the tank, plumbing system, and injection equipment weight estimates. The passenger payload mass or 24,890 kg (55,000 lbs) was replaced with liquid propane which left no weight allowance for 13,560 kg (30,000 lbs) of the propane payload to be flown. Therefore, the payload of the HSCT 2.4E design was increased by 13,560 kg (30,000 lbs) in the HSCT variation ACSYNT model to accommodate the requirements of its USRA mission. Due to the extended duration which the aircraft will be in the air to complete the USRA mission scenario (approximately 10 hours), accommodations were allocated for two sets of two pilots, or a total crew of four in the HSCT variation ACSYNT model.

The ACSYNT input file developed for the HSCT variation concept was directly derived from the HSCT 2.4E model modified for a USRA mission trajectory. Since the altitude of the USRA mission requires a higher cruise altitude than for which the HSCT 2.4E was configured, the wing area of the aircraft had to be increased to attain an acceptable wing loading of 86 or lower. Since the weight of the aircraft increased due to HSCT variation USRA mission requirements and additional fuel was required to complete the USRA mission, engine size was increased by 20% to meet the minimum allowable landing thrust to weight ratio of 0.25.

The goal of modeling the dedicated aircraft concept was to generate the data required to determine the answer to the second question in Section 8.2.2. The philosophy behind sizing the dedicated aircraft concept was to start with the HSCT 2.4E ACSYNT model modified for the dedicated aircraft USRA mission scenario and shrink its internal volume down to the volume required by the mission payload (see Section 8.2.1.) Reducing internal volume significantly reduces surface area and thereby reduces friction drag.

The fuselage was shortened by 37 meters (120 ft) and the fineness ratio of the fuselage was set to 14. This made the fuselage diameter 3.05 meters (10 ft) whereas the HSCT 2.4E design has a fuselage diameter of 3.66 m (12 ft.) The fuselage and wing configuration was changed into a blended fuselage by raising the elevation of the mean aerodynamic chord of the wing from the bottom to the middle of the fuselage. This modification immediately cut 14,930 kg (33,000 lbs) off the total gross weight of the aircraft. The wing area was decreased by 18.6 m^2 (200 ft^2) to 697 m^2 (7,300 ft^2) to bring the wing loading up to 86. The HSCT 2.4E engines were sized up by 5% to give the dedicated aircraft a landing thrust to weight ratio of 0.25.

The mass of the plumbing and compressor equipment required for the propane injection and refueling systems was assumed to be 2,715 kg (6000 lbs.) The tank for the liquid propane carried in the dedicated aircraft concept was assumed to be the fuselage structure itself and no propane storage tank weight was included in the dedicated aircraft model. All the passenger and passenger accommodation payload was removed from the HSCT 2.4E model, and the payload represented by the liquid propane was set to 57,466 kg (127,000 lbs.) Due to the extended duration for which the aircraft will be in the air to complete the USRA mission scenario (roughly 10 hours), accommodations were made for two sets of two pilots or a total crew of four.

One-third of the propane payload loaded into the dedicated aircraft prior to takeoff was off-loaded as a bomb drop at three equally spaced increments during the aircraft's flight through the vortex. Propane was not dropped from the HSCT variation since the HSCT variation model was set up to model a commercial transport flying at the USRA baseline altitude. Commercial transports keep their payload on board for their entire mission.

8.3 Aircraft Configuration Optimization

8.3.1 Initial ACSYNT Modeling Results

When the input data presented in Table 8.2.4-1 was run through ACSYNT the aircraft in Table 8.3.1-1 resulted. Neither of the aircraft was able to achieve the altitude specified in their ACSYNT trajectory. The main reason for the aircraft concepts not doing so was that their wing configurations did not provide the necessary lift to fly at the USRA cruise altitude of 20,122 m (66,000 ft.) The concept's inability to generate sufficient lift can be linked to excessive friction drag, wave drag, and or an insufficient amount of engine thrust. The results in Table 8.3.1-1 illustrated the need for optimizing the wing configuration of each concept with Control Program for Engineering Synthesis (COPES) module of ACSYNT. An analysis of each concept using COPES is documented in Section 8.3.3.

The results in Table 8.3.1-1 also indicate that in addition to not achieving altitude, the HSCT variation concept could not handle its proposed mission scenario (see Section 8.2.1.) Its cruise SFC had to be lowered to 1.0 to keep the aircraft within the boundaries of the carpet plot presented in Section 8.2.3. When the SFC was set to 1.3, the HSCT variation TOGW increased to 390,226 kg (862,400 lbs), and the T/W ratio dropped below the T/W=.25 required by the carpet plot.

Table 8.3.1-1 Initial ACSYNT Modeling Results

ACSYNT Parameter	*HSCT Variation*	*Dedicated Aircraft*
Cruise Altitude	16,460 m (54,000 ft)	17,225 m (56,500 ft)
Cruise L/D	11.2	11.3
Cruise SFC	1.0	1.3
C_{dw}	.0028	.0036
Fuel Weight	166,360 kg (367,656 lb)	152,800 kg (337,685 lb)
TOGW	316,740 kg (700,000 lb)	270,280 kg (597,300 lb)
Takeoff Payload	46,790 kg (103,400 lb)	65,160 kg (144,000 lb)
W/S	82.1	84.2
T/W	0.25	0.26
Takeoff Field Length	1,826 m (5,990 ft)	1,814 m (5,950 ft)
Landing Field Length	3,175 m (10,415 ft)	3,200 m (10,500 ft)

8.3.2 Optimum Mission Selection

Prior to optimizing each concept with COPES, the mission analysis was run to re-analyze the mission scenarios of each concept with respect to the ACSYNT results obtained in Section 8.3.1. The HSCT variation mission scenario was modified to keep the total propane payload, tank weight, and plumbing weight at or below the payload capability of the HSCT 2.4E design in Table 8.1.2-1 (35,430 kg (78,300 lbs).) This was done since the SFC had to be lowered to 1.0 for the HSCT variation in Section 8.3.1 to size an aircraft that fell within the W/S and T/W constraints presented in the carpet plot in Figure 8.2.3-1. The mission analysis determined the optimum plume radius for an HSCT variation with the HSCT 2.4E design payload capability to be 1200 m (3,940 ft.) The mission analysis also determined the HSCT variation can only handle a payload that requires one refueling instead of two. The optimum mission scenario for the HSCT variation is presented in Table 8.3.2-1.

When re-evaluating the mission scenarios derived for the dedicated aircraft concept in Table 8.2.1-1, it was decided that a plume radius greater than the 1500 m (4,920 ft)

threshold (that lowers delivery levels from three to two) requires a much greater payload and does not lower the required fleet of aircraft significantly. Therefore, a dedicated aircraft was sized for the 1500 meters (5,580 ft) plume radius mission and it was found that cutting the payload of the aircraft by 14,216 kg (31,417 lbs) from the 1000 meter (3,280 ft) plume radius, three refueling mission in Table 8.2.1-1 cuts the total gross weight of the aircraft by 67,870 kg (150,000 lbs.) Even though the dedicated aircraft mission in Table 8.3.2-1 requires four more aircraft than the 1800 meter mission, a net of 1,920,000 kg (4,240,000 lbs) in fleet TOGW can be saved by flying the 1500 meter (4,920 ft) plume radius mission.

Table 8.3.2-1 Optimum Mission Selections

Mission Parameter	*HSCT Variation*	*Dedicated Aircraft*
Range	12,030 km (6,500 nmi)	12,030 km (6,500 nmi)
Cruise Altitude	20,122 m (66,000 ft)	20,122 m (66,000 ft)
Refuelings	1	1
Ground Time[1]	4 hr	5 hr
Propane Payload	27,680 kg (61,175 lbs)	43,250 kg (95,583 lbs)
Plume Radius	1200 m (3,940 ft)	1500 m (5,580 ft)
KC-10s Required	42[1]	15[2]
Aircraft Fleet Size	83	44

[1]The *optimized* HSCT variation requires 42,090 kg (92,300 lbs) when refueling at the edge of the vortex, this is 1/2 the capacity of a KC-10. This number was calculated after HSCT variation COPES optimization.
[2]The optimized dedicated aircraft requires 27,150 kg (60,000 lbs) when refueling at the edge of the vortex, this is 1/3 the capacity of a KC-10. This number was calculated after dedicated aircraft COPES optimization.

8.3.3 Optimization of ACSYNT Models

After building ACSYNT models for the HSCT variation and dedicated aircraft concepts and identifying their shortcomings, these models were optimized with the Control Program for Engineering Synthesis (COPES) module of ACSYNT. The target variable of the COPES optimization performed on the HSCT variation and dedicated aircraft concepts

was block fuel weight. Block fuel was selected since the main cost driver in commercial passenger transport as well as the USRA mission is fuel consumption. The optimization design variables used are in Table 8.3.3-1. The optimization constraints used to find minimum block fuel were takeoff and landing field length, and were derived from the carpet plot in Figure 8.2.3-1.

Table 8.3.3-1 COPES Optimization Design Variables

	Design Variables
1	Wing Area
2	Aspect Ratio
3	Wing Sweep
4	Taper Ratio
5	Wing Root t/c
6	Wing Tip t/c

The results of the COPES optimizations are in Table 8.3.3-2. The results are compared to the Malone HSCT 2.4E ACSYNT results. Top views of each aircraft generated by the optimization are presented and compared to the HSCT 2.4E design in Figure 8.3.3-1. Figures 8.3.3-2a-e show bar graphs of the optimization results presented in Table 8.3.3-2.

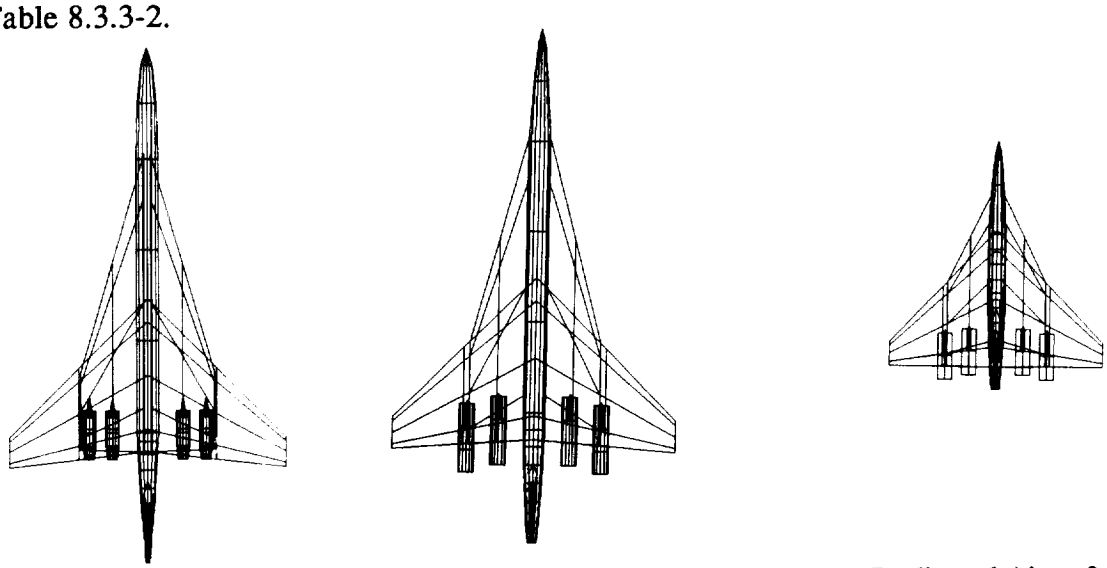

HSCT 2.4E HSCT Variation Dedicated Aircraft

Figure 8.3.3-1a-c
Top Views of Optimized Concepts Compared to HSCT 2.4E

Table 8.3.3-2 ACSYNT Results For HSCT Variation Optimization

Aircraft Parameter	*HSCT 2.4E*	*HSCT Variation*	*Dedicated Aircraft*
TOGW	288,110 kg (636,720 lbs)	321,225 kg (709,910 lbs)	199,610 kg (441,140 lbs)
Fuel Weight	143,080 kg (316,200 lbs)	169,567 kg (374,743 lbs)	93,850 kg (207,410 lbs)
Total Payload	35,430 (78,300 lbs)	35,430 (78,300 lbs)[1]	53,030 kg (117,200 lbs)[1]
Engine Size	156,800 N st (35,000 lbs)	197,120 N st (44,000 lbs)	156,800 N st (35,000 lbs)
SFC at Cruise	1.0	1.3	1.3
Cruise Altitude	16,768 m (55,000 ft)	20,120 m (66,000 ft)	20,120 m (66,000 ft)
Wing Loading	85	86	86
T/W at Takeoff	.31	.25	.32
Cruise L/D	8.18	11.13	10.74
Wing Area	697 m^2 (7,500 ft^2)	767 m^2 (8,250 ft^2)	474 m^2 (5,100 ft^2)
AC Elevation	Bottom of Fuselage	Bottom of Fuselage	Middle of Fuselage
Aspect Ratio	3.0	2.89	2.64
Taper Ratio	.2	.2	.17
t/c_{root}	.02	.02	.02
t/c_{tip}	.02	.02	.02
Sweep	38°	37.7°	38.5°
Takeoff Field	2,000 m (6,570 ft)	1,895 m (6,217 ft)	1,680 m (5,500 ft)
Landing Field	3,360 m (11,010 ft)	3,321 m (10,890 ft)	3,510 m (11,500 ft)
A/C Mfr Cost	$338 million[2]	$362 million[2]	$1.12 billion[3]

[1]Payload includes propane, tank, injection system, and refueling system weight allowances. See Section 8.3.2 for propane payload weights.

[2]A fleet of 400 was assumed to be the market demand in the year 2005 (General Electric, 1993.) All costs in 2005 dollars.

[3]Cost was based on a total fleet of 44. Cost is in 2005 dollars.

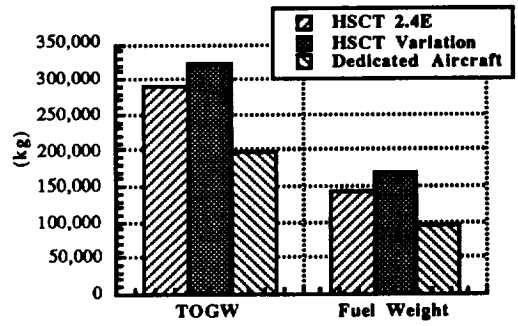

Figure 8.3.3-2a
TOGW and Fuel Weight Comparisons

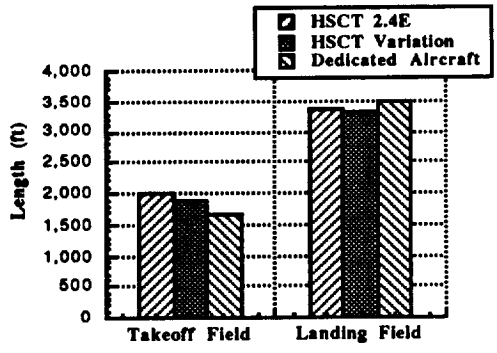

Figure 8.3.3-2b
Field Lengths Comparison

C-2

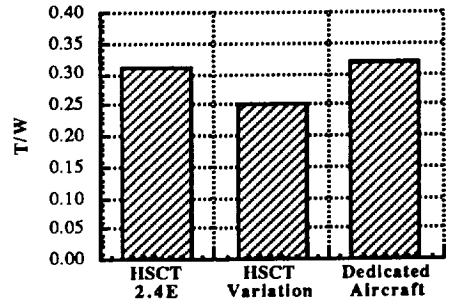

Figure 8.3.3-2c
T/W Comparison

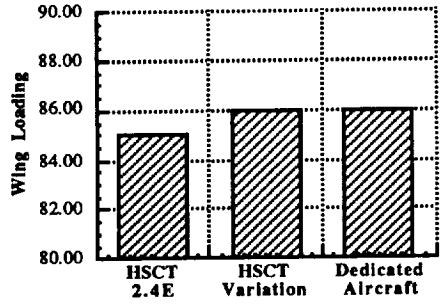

Figure 8.3.3-2d
Wing Loading Comparison

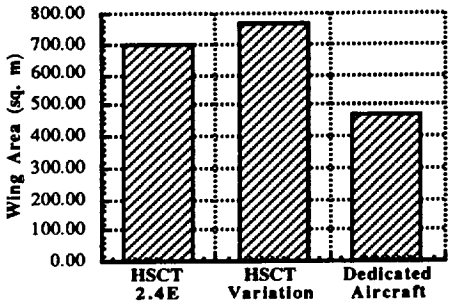

Figure 8.3.3-2e
Wing Area Comparison

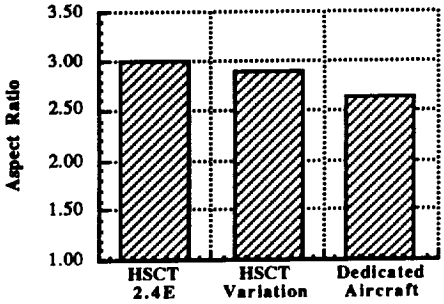

Figure 8.3.3-2f
Aspect Ratio Comparison

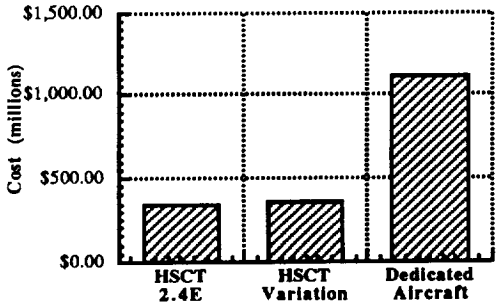

Figure 8.3.3-2g
Manufacturing Cost Comparison

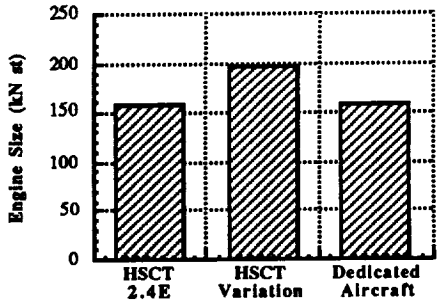

Figure 8.3.3-2h
Engine Size Comparison

Before running the optimization model for the HSCT variation and dedicated aircraft concepts, several parameters were changed from the models described in Section

8.2.4. The propane payloads were changed to accommodate the optimum mission selections presented in Section 8.3.2. The cruise SFCs were kept at 1.3 for each concept unlike in the modeling results described in Section 8.3.1. Figures 8.3.3-3a-b show the theta-averaged area distribution for each concept superpositioned over the desired Sears-Haack theta averaged profile. These plots show the ACSYNT geometry for each concept could be refined to reduced wave drag using area ruling. A wave drag factor of 0.85 was applied to each ACSYNT model to compensate for ACSYNT's inability to directly model area ruling.

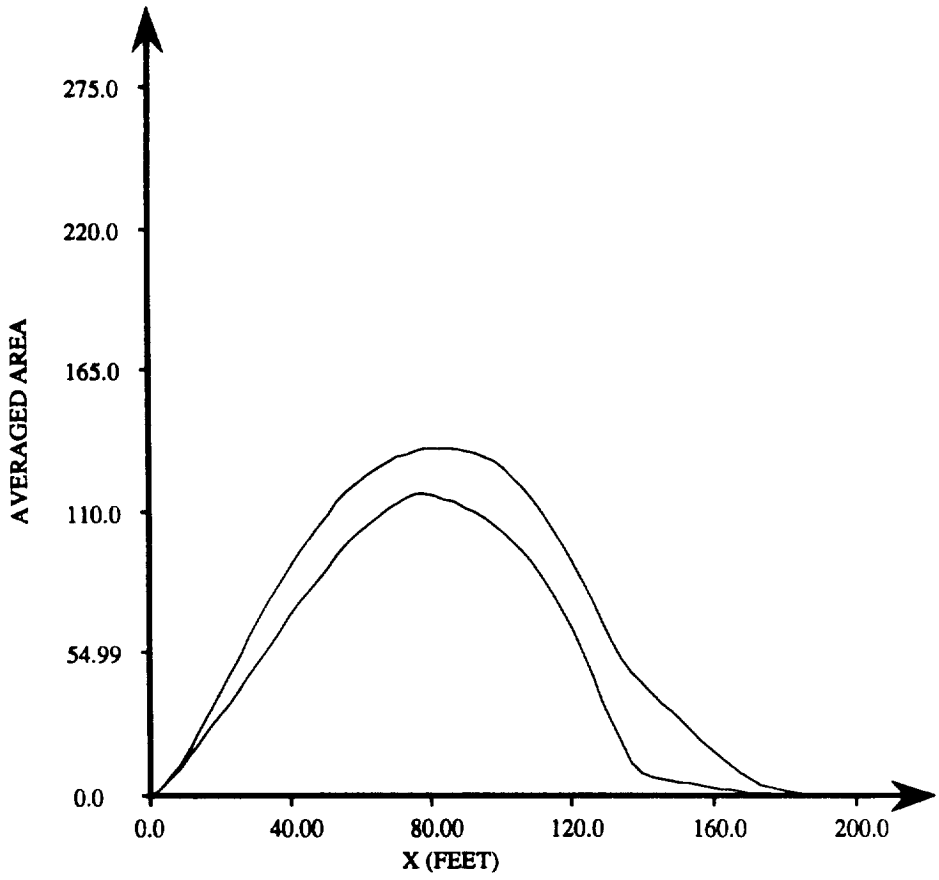

Figure 8.3.3-3a
Theta Averaged Area Rule Plot of HSCT Variation Area vs. Sears-Haack Plot

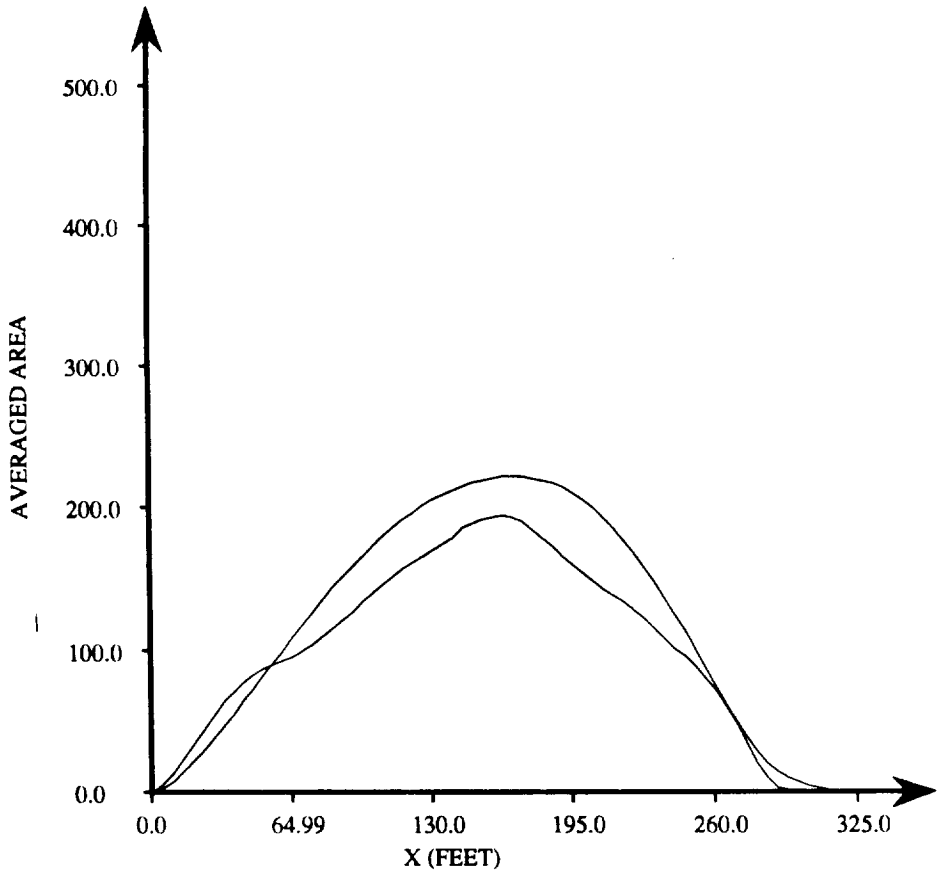

Figure 8.3.3-3b
Theta Averaged Area Rule Plot of Dedicated Aircraft Area vs. Sears-Haack Plot

As a result of the COPES optimization, the total gross weight and fuel weights of the HSCT variation were reduced. COPES only significantly varied aspect ratio and wing area of the HSCT variation concept. It did not vary sweep, root chord thickness, tip chord thickness, or taper ratio. The initial results of the optimization could not keep the T/W of the HSCT variation at or above 0.25. The engines had to be sized up by 25% to bring the T/W of the HSCT variation to 0.25.

The COPES optimization of the dedicated aircraft concept generated an aircraft comparable in size and weight to the North American XB-70 (see Table 8.1.2-1.) The optimization for minimum fuel generated a dedicated aircraft concept with a wing loading of only 76.5 and a thrust to weight at takeoff of 0.28. Therefore, the optimized model was further modeled to bring the dedicated aircraft concept back towards the lower left corner of the carpet plot in Figure 8.2.3-1 where W/S=86 and T/W=.25. The wing area was reduced by 93 m^2 (1000 ft^2) to accomplish this task. Lowering the wing area reduced TOGW of the dedicated aircraft by 452 kg (1000 lbs) to what is shown in Table 8.3.3-2.

8.4 Productivity Index Studies

In order to measure how effectively the optimized HSCT variation concept (described in Table 8.3.3-1 and shown in Figure 8.3.3-1) performs the USRA mission with respect to mission performance and cost, the productivity index (PI) in Equation 8.5-1 was defined.

$$PI = \frac{\text{(Aircraft Velocity) x (Propane Payload)}}{\text{(Fuel Weight + Empty Weight) x (\# of A/C) x (Effective A/C Cost)}} \qquad \text{[Equation 8.5-1]}$$

The general philosophy behind developing Equation 8.5-1 was to place quantities that hurt the mission and aircraft in the denominator. The quantities that make the mission and aircraft more efficient are placed in the numerator. A higher productivity index indicates a more effective delivery vehicle for the USRA mission.

In Equation 8.5-1, *(# of A/C)* is the size of the fleet required to complete the USRA mission scenario selected for an aircraft concept. *(Effective A/C Cost)* term in Equation 8.5-1 is defined by Equation 8.5-2.

Effective A/C Cost = Manufacturer Cost + USRA Fuel Cost - Revenue [Equation 8.5-2]

Manufacturer cost and revenue earned was determined for each concept using the ACSYNT cost module developed by Brett Malone (Malone, 1993.) USRA fuel cost was calculated by assuming each concept would have a life of twenty years and calculating the cost of all the fuel used by each concept over that twenty year period. When calculating revenue earned for the HSCT variation it was assumed that the aircraft would fly as a commercial transport for nine months of the year, be down for one month before and after the USRA mission, and fly the USRA mission for one month. The revenue for the dedicated aircraft concept was set at zero. All the costs in Equation 8.5-2 are calculated in 2005 dollars.

When initially calculating the productivity index for the HSCT variation, it was shown that if a market demand 400 in the year 2005 was assumed the HSCT variation could be built cheaply enough that its revenue would pay for its USRA mission fuel and manufacturing cost (General Electric, 1993.) The following calculation shows the costs calculated by ACSYNT when assuming a fleet of 400. The ACSYNT cost module determined the HSCT variation could earn 6 cents per average seat mile when transporting passengers.

Effective A/C Cost = $362 million + $206 million - $875 million

Effective A/C Cost = -$307 million

Therefore, if HSCT variations could be purchased at this manufacturing cost which assumes a fleet of 400, each HSCT variation could make money.

After determining the HSCT variation could make money if purchased at $362 million dollars per aircraft, the point at which the *(Effective A/C Cost)* is zero was

identified. It was determined that if the HSCT variation could be built at a cost of $669 million dollars there would have to be a demand for a fleet of 166 HSCT aircraft in the year 2005.

After looking at the predicted fleet demand, the worst scenario was investigated and compared to the dedicated aircraft productivity index. The worst scenario was defined to be a situation in which the world wants no HSCT aircraft in 2005 and only 83 are built due to the USRA mission. If this were the case, effective cost would be the following:

Effective A/C Cost = $842 million + $206 million - $875 million

Effective A/C Cost = $173 million

In other words, if the HSCT variation was built at a cost that corresponds to manufacturing costs when the total HSCT fleet size is 83, the manufacturing cost of the HSCT variation would be $842 million dollars. The productivity index of the HSCT variation manufactured at $842 million dollars was calculated to be the following:

$$PI_{HSCT} = \frac{(2{,}550 \text{ km/h}) \times (27{,}680 \text{ kg})}{(169{,}570 \text{ kg} + 123{,}980 \text{ kg}) \times (83) \times (\$173 \text{ million})}$$

$$\mathbf{PI_{HSCT} = 168 \times 10^{-4} \text{ km/h/\$}}$$

After calculating the productivity index for the HSCT variation assuming the worst fleet scenario, the productivity index was calculated for the dedicated aircraft basing its cost on a fleet of 44 which is required by its optimum mission selection in Section 8.3.2. The following calculations show this result:

$$PI_{Dedicated} = \frac{(2{,}550 \text{ km/h}) \times (43{,}250 \text{ kg})}{(62{,}510 \text{ kg} + 93{,}850 \text{ kg}) \times (44) \times (\$1{,}120 \text{ million})}$$

$$\mathbf{PI_{Dedicated} = 143 \times 10^{-4} \text{ km/h/\$}}$$

The productivity index shows that dedicated aircraft is 20% less productive even if only the fleet of HSCT aircraft required for the USRA mission are built.

A final productivity index calculation was done without including the *(Effective A/C Cost)* term. The results were:

$$PI_{HSCT} = 28.9 \times 10^{-1} \text{ km/h}$$

$$PI_{Dedicated} = 160.3 \times 10^{-1} \text{ km/h}$$

This shows that the HSCT variation is only 20% as effective when performing the USRA mission. A bar chart of the productivity index results is in Figure 8.4-1. (Note that the scale is 10^{-2} with cost values and 10^{-4} without cost values.)

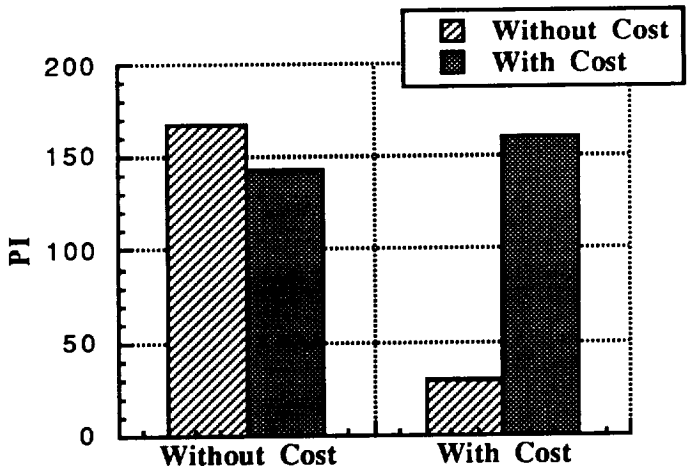

Figure 8.4-1
Comparison of Productivity Index Results

The dedicated aircraft is so much more effective because it can carry a payload that allows it to deliver more propane per nautical mile it flies. As shown in Table 8.3.2-1, the payload capability of the dedicated aircraft allows it to have a mission scenario with a plume radius that cuts delivery levels in the vortex from three to two. The payload capability of the HSCT variation only allows it to have a mission scenario with a plume radius that requires three delivery levels. The injection mass per unit distance traveled ratio is 36%

less for HSCT variation than it is for the dedicated aircraft concept. These key mission parameters are compared in Table 8.4-1.

Table 8.4-1 Comparison of Key Mission Parameters

	HSCT Variation	*Dedicated Aircraft*
Propane Payload	27,680 kg (61,175 lbs)	43,250 kg (95,583 lbs)
Plume Radius	1200 m (3,940 ft)	1500 m (5,580 ft)
Delivery Levels	3	2
Injection Mass/Range	2.30 kg/km (9.41 lb/nmi)	3.59 kg/km (14.7 lb/nmi)
Fleet Required	83	44

8.5 Conclusions With Respect to Objective of ACSYNT Analysis

The answers to the questions presented in Section 8.2.2 were determined by performing ACSYNT and COPES analysis on the HSCT variation and dedicated aircraft concepts. The first question asked how the HSCT 2.4E design would have to be altered to perform the USRA mission. The range of HSCT 2.4E would have to be extended by 1850 km (1,000 nmi.) This required a 70 m^2 (750 ft^2) increase in wing area and 25% increase in engine size. These modifications increased TOGW by 33,030 kg (73,000 lbs.) The increase in manufacturing cost for a fleet of 400 was $24 million dollars per aircraft. The total operating cost of the aircraft when performing commercial transport increased from eight to nine cents per average seat mile. There would be a significant cost impact if an entire fleet of HSCT aircraft were built according to the HSCT variation design.

The second question asked how the USRA mission would suffer by flying an HSCT variation aircraft instead of a dedicated aircraft. If a dedicated aircraft were flown, the USRA mission would only require a fleet of 44 aircraft that are 121,615 kg (268,000 lbs) lighter than the HSCT variation. (The USRA mission requires a fleet of 83 HSCT variations.) The dedicated aircraft performs the mission much more efficiently since

its fuselage does not have excess internal volume and the elevation of its wing was placed at the middle of its fuselage. As a result, the dedicated aircraft generates much less drag than the HSCT variation when flying the USRA mission. This allowed the dedicated aircraft to have a much greater payload capability and a much greater injection mass to injection range ratio, hence the lower number of aircraft required.

The dedicated aircraft concept looks very attractive from a mission performance point of view, but since there exists no aircraft in the world with its capabilities, the manufacturing cost of the dedicated aircraft would be $1.12 billion dollars per plane. Since market predictions indicate a demand for a fleet of 400 HSCT aircraft by the year 2005, the cost of building the HSCT variation concept would be much lower at $362 million dollars per aircraft (General Electric, 1993.) In addition, the dedicated aircraft does not have the capability to earn revenue like the HSCT variation. Using Malone's ACSYNT cost module, it was calculated that the HSCT variation concept could earn $53 million dollars a year while not flying the USRA mission (Malone, 1993.) The lower manufacturing cost and revenue earning capability of the HSCT variation compensates for its lack of mission performance when compared to the dedicated aircraft.

8.6 Summary and Recommendations

The answers determined in Section 8.5 illustrate an HSCT variation concept would be a intelligent choice for the USRA mission. A dedicated aircraft concept would deliver more propane per nautical mile flown during the USRA mission but it does not, by definition, have an alternate revenue earning function as does the HSCT variation. The HSCT variation performs the USRA mission fairly effectively and can earn revenue as a commercial transport the remainder of the year, making it more cost effective and thereby more productive than the dedicated aircraft concept. However, the first answer discussed

in Section 8.5 showed that there would be significant cost impacts if the overall HSCT design was modified to accommodate the USRA mission requirements. This indicated the HSCT variation should be configured as a HSCT 2.4E, or industry baseline aircraft, that could be feasibly modified into an HSCT variation on the assembly line (e.g. installation of larger engines as opposed to a modification of wing taper ratio.)

The productivity index calculations in Section 8.5 clearly illustrated with respect to mission performance and cost effectiveness that the HSCT variation concept was a good design for the USRA mission. However, some of the ACSYNT modeling techniques employed to generate data for evaluating the HSCT variation's performance were only approximate in nature. Specifically, the dedicated aircraft should be sized taking off with minimal fuel since it can refuel at the edge of the vortex with a minimal loss of time. The optimization of both aircraft concepts should include engine parameter variation. The wave drag assumptions used in the modeling process should be more vigorously calculated for each aircraft concept, and furthermore, ACSYNT does not directly support area ruled geometry. Finally, the HSCT variation needs to be sized as an HSCT 2.4E, or the current industry baseline design, that can be mechanically altered to fly the USRA mission.

9.0 CONCLUSIONS

The 1993/1994 design objectives were:

1) To re-evaluate the key assumptions of the 1992/1993 design team, in addition to reviewing the team's results.
2) To develop a matrix of baseline vehicle concepts as candidates for the delivery vehicle.
3) To develop a selection criteria and perform quantitative trade studies to use in the selecting the vehicle concept.

To complete the first objective, an investigation into ozone replenishment techniques and the current understanding of the ozone problem was completed. The findings of this analysis concur with last year's findings that a hydrocarbon injection scheme currently provides the best intervention method.

An evaluation of the previous year's mission analysis modeling technique indicated possible shortcomings of their modeling methods. Therefore, a new modeling method (coverage pattern) was developed to utilize the aircraft's range to its fullest potential. Incorporated in this new modeling method was the ability to determine the best combination of refuelings, injection plume radius, ground time, and Mach that would minimize the number of aircraft required while not exceeding an aircraft's payload capacity. It was determined that for the HSCT variation concept, the lowest number of aircraft required for the mission while still meeting payload capacity requirements was 83. This mission consists of one refueling per sortie, 1200 meter plume radius, 4 hour ground time, and a delivery velocity of Mach 2.4. In addition, recommendations were made for the use of airports on only one continent and provisions for multiple tanker support have been incorporated.

Distribution of the propane from the delivery vehicle was achieved using a nozzle with swirl vanes. The propane plume was analyzed using Classical Diffusion Theory to achieve a 1200 meter plume radius as defined in the mission analysis. The nozzle was a 0.2 meter radius nozzle injecting propane at Mach 0.32. Supplementing this analysis was an investigation into propane storage systems. The investigation illustrated that a multiple tank storage system, constructed of composite materials would provide optimum use of storage space, while minimizing storage weight. In addition, a plan for tank and support structure integration with the aircraft was developed.

As a result of performing the aircraft configuration studies, a variation of the HSCT 2.4E design was modeled and optimized as a HSCT variation concept using ACSYNT. The propane storage tank studies calculated that with a payload of 35,430 kg (78,300 lbs), the HSCT variation would be capable of transporting tanks, tank supports, a refueling and injection system, and 27,680 kg (61,175 lbs) of propane. The mission analysis calculated that with the calculated propane payload, there would have to be a fleet of 83 HSCT variations delivering propane at a plume radius of 1200 m (3,940 ft.) After determining the characteristics and the mission scenario of the HSCT variation, the cost effectiveness and mission performance of the HSCT variation were compared to that of a dedicated aircraft concept sized solely for the USRA mission. It was determined that even though the HSCT variation does not inject as much propane per unit distance flown (the driving parameter in mission performance) as would a dedicated aircraft, the HSCT variation flew the mission more cost effectively. Since the HSCT variation performed the mission much more cost effectively than a dedicated aircraft concept, it was decided it would be an intelligent choice for the USRA mission.

The next stage of the aircraft configuration studies should involve acquiring an understanding of how the HSCT 2.4E, or current industry HSCT baseline design, could be modified on an assembly line into an HSCT variation. It was found that modifying the HSCT 2.4E design into the HSCT variation decreased the aircraft's revenue earning ability

significantly. Therefore, it would be unfeasible to modify the overall industry baseline HSCT design for the USRA mission. Also, the next stage of the aircraft configuration analysis needs to detail the design of the HSCT variation concept with respect to injection and refueling system configuration, stability and control, aerodynamic performance, propulsion system characteristics, and trajectory profile.

APPENDIX A - CALCULATIONS

Calculations of Mass Propane per Unit Length

First calculate the average propane concentration in terms of mass. (We need the concentration in terms of mass because that is what Classical Diffusion Theory uses)

C_{iave} - average plume concentration by mass
$MW_{C_3H_8}$ - molecular weight of propane
MW_{air} - molecular weight of air
ppbv - parts per billion of propane by volume

ppbv = (# molecules propane / # molecules air)
C_{iave} = (mass of propane / mass of air)

$C_{iave} = (MW_{C_3H_8} / MW_{air}) * ppbv$
$= (44 / 28.9) * 3.6 \times 10^{-9}$
$= 5.48 \times 10^{-9}$

Next, calculate the mass of propane per a plume unit length. This will be unique for each desired plume radius, here the calculations are performed for a desired plume radius of 1200m.

R_{plume} = 1200m
L_{plume} = 1m (unit length)

$V_{plume} = \pi * R^2_{plume} * L_{plume}$
$= \pi * (1200)^2 * (1)$
$= 4.524\ 10^6 m^3$

Mass air in Plume = $V_{plume} * \rho_{air}$
$= (4.524 \times 10^6) * (0.121)$
$= 547{,}391.1$ kg

Mass propane in Plume = Mass air in Plume * C_{iave}
$= 547{,}391.1 * 5.48 \times 10^{-9}$
= .00300 kg (remember, this is in a cylindrical volume of desired radius and unit length)

From the mass of propane in the plume (per unit length of plume), we can find the propane mass flow, m_{prop}, required to achieve the desired concentration. This calculation is shown for a Mach 2.4 (708 m/s) aircraft.

m_{prop} = Mass of propane * Aircraft velocity
$= (.00300$ kg/m) * (708 m/s)
$= 2.124$ kg/s

To calculate the mixing; nozzle specification, mixing time and desired plume radius must be specified. In the sample calculations the optimum nozzle specifications for a 1200m plume radius and a mixing time of 2 hours will be used. In doing the actual calculations many nozzle designs were investigated to find the one that achieved the optimum plume requirements defined in the mission analysis.

a	nozzle radius
t	mixing time
U_i	propane injection velocity
U_∞	free stream velocity (aircraft speed)
ρ_i	propane injection density
ρ_∞	free stream (air) density

First, determine the injection velocity for the nozzle radius, form the desired mass flow.

$$U_i = m_{prop} / (\rho_i * \pi * a^2)$$
$$= (2.124 \text{ kg/s})/(0.1806 \text{kg/m}^3 * 3.1416 * (0.2\text{m})^2)$$
$$= 93.6 \text{ m/s}$$

Unfortunitly, classical diffusion theory makes the assumption that the nozzle injection velocity is equal to the free stream velocity. As a result, in order for mass to be conserved between the injection nozzle, and the downstream plume an effective nozzle radius must be calculated and used.

$$m = \rho U A$$
$$m_{prop} = \rho_i U_i * \pi * a^2 = \rho_i U_\infty \pi * Reff^2$$

rearranging to solve for Reff

$$Reff^2 = a^2 U_i / U_\infty$$
$$= (0.2 \text{ m})^2 * 93.6\text{m/s} / 708 \text{ m/s}$$
$$= 0.00528$$
$$Reff = 0.0727 \text{ m}$$

Next, calculate the mixing constant using the effective nozzle radius

$$c = (0.025/0.8) * a * | 1 - (\rho_i U_i / \rho_\infty U_\infty) |$$
$$= (0.025/0.8) * 0.0727\text{m} * | 1 - (0.1806 \text{ kg/m}^3 * 93.6\text{m/s})/(0.121 \text{ kg/m}^3 * 708 \text{ m/s}) |$$
$$= 0.00182$$

Now the swirtl factor comes into play. It accounts for the increased mixing due to the swirl vanes. The swirl factor simply multiptlies the mixing constant by another constant (sf). From conversations with Dr. Schetz, a reasonable swirl factor is 10.

$$c = c * sf$$
$$= 0.00182 * 10$$
$$= 0.0182$$

Calculate the values required for the P-function table analysis.

$\sigma^2 = 2cx$
$= 2c\ U_\infty\ t$
$= 2^*\ 0.0182\ ^*\ 708\ m/s\ ^*\ 7200s$
$= 185552.6$

so $\sigma = 430.76$

now,

$a/\sigma = 0.0727m / 430.76$
$= 0.000169$
assume equal to zero

$C_{center\ line} = 1 - \exp(-a^2/2\sigma^2)$
$= 1 - \exp(-(0.0727m)^2/(2^*185552.6))$
$= 14.2^*10^{-9}$
$= 14.2$ ppbm

With these values, use the P* definition to calculate P*

$P^* = C_{iave} / C_{center\ line}$
$= 5.48$ ppbm / 14.2ppbm
$= 0.386$

Using the P-function Table II, for $P^* = 0.386$, and $a/\sigma = 0.0$, we get

$r/\sigma = 1.48$

then,

$r = (r/\sigma)\ ^*\ \sigma$
$= 1.48\ ^*\ 430.76$
$= 637.5m$

APPENDIX B

```
      PROGRAM MISSION

* This program is designed to determine the total mission range and
* total number of missions required for the mission profile developed
* by the VPI & SU 1993-94 USRA Senior Design Team.
*  The code was written by Daniel L. Youngblood
*   Spring 1994.
*  Last Modified:  4/21/94
**************************
*    VARIABLE DEFINITION: (ALL UNITS ARE SI UNLESS OTHERWISE STATED)
*
*       BASRNG : RANGE OF AIRCRAFT WITHOUT REFUELING
*       REFEXT : RANGE ADDED TO AIRCRAFT WITH EACH REFUELING
*       TR     : RANGE OF AIRCRAFT WITH REFUELING
*       PVR    : POLAR VORTEX RADIUS
*       AIRPAVGR: AVERAGE RANGE FROM AIRPORT TO S. POLE
*       REFTM  : TIME FOR TOTAL REFUELING IN MIDAIR
*       REFUEL : # OF TIMES PLANE WILL REFUEL IN MIDAIR
*       GTHR   : GROUND TIME IN HOURS
*       PLMRAD : PROPANE PLUME RADIUS
*       MACH   : FLIGHT MACH OF DELIVERY VEHICLE
*       BASRNG : RANGE OF AIRCRAFT (WITHOUT REFUELING) IN METERS
*       REFEXT : RANGE EXTENSION OF 1st REFUELING
*       REFHLD : VALUE USED FOR CALCULATIONS IF REFUEL = 0
*       FLAG1  : =1 IF REFUEL = 0; ELSE =0
*       A      : SPEED OF SOUND AT ALTITUDE
*       VEL    : VELOCITY OF DELIVERY VEHICLE (=MACH*A)
*       SUBVEL : VELOCITY OF DELIVERY VEHICLE WHEN SUBSONIC
*       N      : LOAD FACTOR WHEN TURNING
*       G      : ACCELERATION DUE TO GRAVITY
*       MINRAD : MINIMUM TURN RADIUS BASED ON MACH AND N
*       TRNRAD : TURN RADIUS NECESSARY FOR FULL COVERAGE OF
VORTEX
*       TRNDIA : TURNING DIAMETER BASED ON TRNRAD
*       TIME   : 3 WEEK DELIVERY PERIOD IN SECONDS
*       GT     : GROUND TIME IN SECONDS
*       TRNDST : DISTANCE COVERED IN 180 deg. TURN
*       EFFPLM : EFFECTIVE PLUME RADIUS W/OVERLAP TAKEN INTO
ACCOUNT
*       SWPNUM : # OF PLANES REQUIRED TO COVER ONE SWEEP
*       KOUNT  : COUNTS THE TOTAL # OF SORTIES REQUIRED
*       TMR    : TOTAL DISTANCE COVERED BY ALL PLANES IN ALL MISSIONS
*       YSTART : Y- COORDINATE WHERE SWEEP BEGINS
*       XSTART : X- COORDINATE WHERE SWEEP BEGINS
*       THETAS : ANGLE (IN POLAR COORDINATES) WHERE SWEEP BEGINS
*       YEND   : Y- COORDINATE WHERE SWEEP ENDS
*       XEND   : X- COORDINATE WHERE SWEEP ENDS
*       DIN    : DISTANCE THE PLANE FLIES TO THE VORTEX
*       DOUT   : DISTANCE THE PLANE FLIES FROM THE VORTEX
*       DIST   : DISTANCE FLOWN BY THE AIRPLANE ON THAT SORTIE
```

```
*       REFS   : COUNTING VARIABLE FOR REFUEL LOOP
*       SECT   : 2 * THE NUMBER OF LAYERS REQUIRED
*       AC     : # OF AIRCRAFT REQUIRED
*       SPD    : SORTIES PER DAY REQUIRED
*       SUBMR  : DISTANCE THE AIRCRAFT MUST FLY SUBSONIC
*       LIMIT  : PAYLOAD LIMIT
*************************************************************

      INTEGER KOUNT,MISSION,FLAG1
      DOUBLEPRECISION TR,PVR,AIRPAVGR,PI,TMR,REFUEL,
     $             XSTART,YSTART,XEND,YEND,THETAS,THETAE,
     $              DIST,DIN,DOUT,MACH,A,TIME,AC,SUBMR,GT,BASRNG,
     $              REFEXT,TRNRAD,VEL,N,G,EFFPLM,MINRAD,TRNDIA,
     $              TRNDST,PLMRAD,SWPNUM,GTHR,SECT,REFTM,
     $              REFS,REFHLD,BEST(30),MA(30),REF(30),PRAD(30),
     $             GHR(30),MAX,DR,PAYLOD,MAXPLD,PLD(30),LIMIT


      OPEN(2,FILE='(C)CON')
*     OPEN(2,FILE='A:ANALDAT.DAT')
      OPEN(4,FILE='(C)CON')

      WRITE(4,*)'  MISSION ANALYSIS 1994 by DAN YOUNGBLOOD'
       WRITE(4,*) ' '
        WRITE(4,200)'MACH','REFUEL','PLUME RAD', 'GROUND TIME',
     $   '# AC','MAX. PLD'

      PI = ACOS(-1.0D0)

      DO 150, I = 1,30
        BEST(I) = 1000.0D0
150    CONTINUE

      DO 1000, MACH = 2.0,2.5,.2
      DO 1010, PLMRAD = 800,1500,100
       DO 1020, GTHR = 3.0,5.0,1.0
       DO 1030, REFUEL = 1.0, 3.0, 1.0

*      REFUEL = 1.0D0
*      GTHR   = 4.0D0
*      PLMRAD  = 1000.0D0
*      MACH   = 2.40D0

*      LIMIT IS IN lbs
*      LIMIT = 63147.0D0
      LIMIT = 138000.0D0
*      CONVERT LIMIT FROM lbs TO kgs
      LIMIT = LIMIT/2.20D0

*     BASRNG = 6600 nmi
     BASRNG = 12231014.0D0

*     REFEXT ~ 800 nmi
     REFEXT = 1482547.0D0
```

```
      REFTM   = 30.0D0 * 60.0D0

      IF (REFUEL.EQ.0.0) THEN
        REFHLD =1.0
        FLAG1 = 1
      ELSE
        FLAG1 = 0
        REFHLD = REFUEL
      END IF

      IF (REFUEL.LE.1.0) THEN
       TR     = BASRNG + REFEXT*REFUEL
      ELSE
       TR     = BASRNG*REFUEL + REFEXT
      END IF

       PVR    = 2524067.0D0
       AIRPAVGR= 4204133.0D0
       A      = 295.0D0
       VEL    = MACH*A
       SUBVEL  = .80D0 * A
       N      = 2.0D0
       G      = 9.80D0
       MINRAD  = (VEL**2.0)/(G*SQRT(N**2.0 -1.0))
       TRNRAD  = PVR/(4.0*REFHLD*(INT(PVR/(4.0*REFHLD*MINRAD))))
       TRNDIA  = 2.0D0 * TRNRAD
       TIME    = 1814400.0D0
       GT      = GTHR * 3600.0D0
       TRNDST  = PI*TRNRAD

       EFFPLM  = PLMRAD - (.134*PLMRAD)
       SWPNUM  = TRNRAD/EFFPLM

       KOUNT   = 0
       TMR     = 0.0D0

* Begin mission analysis


      YSTART = TRNRAD
      YEND   = 0.0D0
      MAXPLD = 0.0D0

      WHILE ((PVR-YEND).GE.(TRNDIA)) DO

       THETAS = ASIN(YSTART/PVR)
       XSTART = PVR*COS(THETAS)
       YEND   = YSTART + TRNDIA
       THETAE = ASIN(YEND/PVR)
       XEND   = PVR*COS(THETAE)

       DIN    = SQRT(((AIRPAVGR-XSTART)**2.0D0) + (YSTART**2.0D0))

       DIST = DIN+3.0D0*PVR*SIN((PI/2.0D0-THETAS))
```

```
$       +PVR*SIN((PI/2.0D0-THETAE))+TRNDST

 DR = 2.0D0*PVR*SIN((PI/2.0D0-THETAS))
$      + 2.0D0*PVR*SIN((PI/2.0D0-THETAE))

  IF (REFUEL.GT.1.0) THEN
   DO 400, REFS = 2.0,REFUEL,1.0

    YSTART = YEND + TRNDIA
    THETAS = ASIN(YSTART/PVR)
    XSTART = PVR*COS(THETAS)
    YEND   = YSTART + TRNDIA
    THETAE = ASIN(YEND/PVR)
    XEND   = PVR*COS(THETAE)

    DIST = DIST + 2.0D0*REFTM*SUBVEL
$         +3.0D0*PVR*SIN((PI/2.0D0-THETAS))
$         +PVR*SIN((PI/2.0D0-THETAE)) + 2.0D0*TRNDST


  DR = DR + 2.0D0*PVR*SIN((PI/2.0D0-THETAS))
$      + 2.0D0*PVR*SIN((PI/2.0D0-THETAE))
400   CONTINUE

  END IF

   DOUT   = SQRT(((AIRPAVGR-XEND)**2.0D0) + (YEND**2.0D0))
   DIST = DIST + DOUT
   TMR  = TMR+DIST*SWPNUM

   KOUNT = KOUNT + NINT(SWPNUM)
   PAYLOD = DR*(PI*PLMRAD**2.0D0)*6.09E-10

   IF (PAYLOD.GT.MAXPLD) THEN
    MAXPLD = PAYLOD
   END IF

  IF (DIST .GT. TR) THEN
    WRITE(4,*)' '
    WRITE(4,430)'REFUEL = ',REFUEL,'=> Insufficient aircraft range.'
    WRITE(4,440) 'NEED ADDITIONAL ', (DIST-TR), ' METERS RANGE.'
   GOTO 1030
  END IF
430  FORMAT(1X,A9,F3.1,A32)
440  FORMAT(1X,A20,F12.2,A14)

   YSTART = YEND + TRNDIA
  END WHILE

   IF (PLMRAD.GT.1428) THEN
      SECT = 4.0
    ELSE
      SECT = 6.0
   END IF
```

```
      TMR     = TMR*SECT
      MISSION = KOUNT*SECT

*     CONVERT MAXPLD AND LIMIT FROM kg TO lbs
      MAXPLD = 2.20D0*MAXPLD
      LIMIT  = 2.20D0*LIMIT

      IF(FLAG1 .EQ. 1) THEN

       AC = (TMR/(VEL*TIME)+GT*MISSION/TIME)*1.1
       SPD = MISSION/(21.0D0*AC)

*       WRITE(4,'(A31,F4.0)')' NUMBER OF AIRCRAFT REQUIRED = ',AC
*       WRITE(4,'(A28,F4.2)')' SORTIES PER DAY REQUIRED = ',SPD

      ELSE IF (FLAG1 .EQ. 0) THEN
       SUBMR = (REFEXT+(REFUEL-1.0D0)*REFTM*SUBVEL)*MISSION
       AC = (SUBMR/(SUBVEL*TIME)+(TMR-SUBMR)/(VEL*TIME)+
     $      GT*MISSION/TIME)*1.1
       SPD = MISSION/(21.0D0*AC)

*       WRITE(4,*)'REFUEL .GE.1'
*       WRITE(4,'(A31,F4.0)')' NUMBER OF AIRCRAFT REQUIRED = ',AC
*       WRITE(4,'(A28,F4.2)')' SORTIES PER DAY REQUIRED = ',SPD

      END IF

      MAX = 0.0D0
      DO 640, I = 1,30
         IF(BEST(I).GT.MAX) THEN
          MAX = BEST(I)
          LOC = I
         END IF
  640 CONTINUE

      IF ((AC.LT.BEST(LOC)).AND.(MAXPLD.LT.LIMIT)) THEN
         BEST(LOC) = AC
         MA(LOC)   = MACH
         REF(LOC)  = REFUEL
         PRAD(LOC) = PLMRAD
         GHR(LOC)  = GTHR
         PLD(LOC)  = MAXPLD
         GOTO 680
      END IF
  680   WRITE(4,*)

*       WRITE(4,*) 'MACH = ',MACH
*       WRITE(4,*)'TMR = ',TMR,'   MISSIONS = ',MISSION

       WRITE(4,210) MACH,REFUEL,PLMRAD,GTHR,AC,MAXPLD

  210    FORMAT(1X,F11.3,F11.1,F11.3,F11.2,F11.0,F11.0)
```

```
200   FORMAT(1X,6A11)

1030 CONTINUE
1020 CONTINUE
1010 CONTINUE
1000 CONTINUE

   DO 1100, I = 1,30
   WRITE(2,1150) NINT(BEST(I)),MA(I),REF(I),PRAD(I),GHR(I),PLD(I)
1100 CONTINUE

1150 FORMAT(1X,I8,2F8.3,F8.1,F5.1,F10.0)

 99  STOP
     END
```

REFERENCES

ACSYNT Analysis User Guide, NASA Ames Research Center, November 1992.

Airport Capacity and Delay, Advisory Circular, U.S. Department of Transportation, 1983.

Beer, F. and E. Johnston, *Mechanics of Materials*, McGraw Hill, N.Y., 1981. p.325.

Boeing Aircraft Company, "Airport Locations And Runway Lengths", 1992.

Bowersox, Rodney D. W., "Compressible Turbulence in a High-Speed High Reynolds Number Mixing Layer," Dissertation, Virginia Polytechnic Institute & State University, Blacksburg, VA, 1992.

Bowersox, Rodney D. W., Telephone Conversation, Dec. 7, 1993.

Carslaw, H.S. and J.C. Jaeger, *Conduction of Heat in Solids*, Oxford University Press, 1959. p.260.

Chipperfield, M., "Satellite Maps Ozone Destroyer," *Nature*, Vol. 362, Apr. 15, 1993. p. 30.

Cicerone, R.J., S. Elliot, and R.P. Turco, "Reduced Antarctic Ozone Depletions in a Model with Hydrocarbon Injections," *Science*, Vol. 254, pp. 1191-1194.

Coen, P., Electronic Mail Memorandum, Oct. 18, 1993.

Fowler, W.T., Project Advisor. "Feasibility Study of Methods for Stopping the Depletion of Ozone Over Antarctica Final Report." NASA-CR 184583. May 1988.

Gourlay, A., *The World's Great Stealth and Reconnaissance Aircraft*, Aerospace Publishing, 1991.

Hamrill, P. and O. Toon, "Polar Stratospheric Clouds and Ozone Hole," *Physics Today*, Dec. 1991. pp.34-42.

High Speed Civil Transport - Vital Investiment in America's Future, Advertisement Pamphlet, NASA.

Hutchinson, M.G., Mason, W.H., Grossman, B., and Haftka, R.T., "Aerodynamic Optimization of an HSCT Configuration Using Variable-Complexity Modeling," AIAA Paper 93-0101, 1993.

Jane's All The World's Aircraft, 1968-69, 77-78, 80-81, 88-89,91-92, Jane's Publishing Company Inc., New York, New York.

Jones, Robert, *Mechanics of Composite Materials*, Hemisphere Publishing, 1975. p. 72.

Kay, Jacob, "A Review of the Stratospheric Ozone Depletion Problem and Considerations for the Development of Vehicle-Based Intervention

Schemes," VPI-Aero-191, College of Engineering, Virginia Polytechnic Institute and State University. Aug. 24, 1992.

Lee, Mario, and W.C. Reynolds, "Bifurcating and Blooming Jets," Fifth Symposium on Turbulent Shear Flows, Ithaca, NY, 1985.

Lipske, Michael, "Living Under an Angry Sun," *National Wildlife*, Aug./Sept. 1992. pp. 30-33.

Madronich, S., "Skin Cancer and UV Radiation," *Nature*, Vol. 366, Nov. 4, 1993. p23.

Malone, Brett, and Mason, William, "Aircraft Concept Development Using the Global Sensitiivity Approach and Algebraic Technology Models" VPI-Aero-184, College of Engineering, Virginia Polytechnic Institute and State University, Dec. 10, 1991.

Megyesy, Eugene F., *Pressure Vessel Handbook*, Tulsa, Oklahoma, Pressure Vessel Handbook Publishing Inc., 1983. p. 23.

Mims, Forrest M., III, "Ozone Layer," *Science PROBE!*, Nov. 1992. p. 34.

Nicolai, L.M., *Fundamentals of Aircraft Design*, MERS, San Jose, 1975.

Parekh, D. E., and W. C. Reynolds, "Bifurcating Air Jets at Higher Subsonic Speeds," Sixth Symposium on Turbulent Shear Flows, Foulouse, France, 1987.

Prather, M. and R. Watson, "Stratospheric Ozone Depletion and Future Levels of Atmospheric Chlorine and Bromide," *Nature*, Vol. 344, Apr. 19, 1990. pp. 729-731.

Raymer, O., Aircraft Design, AIAA, Washington, 1989.

Representatives of Southwestern Virginia Gas Service Corp., Telephone Conversations, 1993.

Reynolds, W.C., and J.D. Powell, "Entrainment Control in Blooming Jets," Department of Mechanical Engineering, Stanford University, Stanford, CA, 1986.

Roskam, J., *Airplane Design I*, Roskam Aviation and Engineering Corporation, Ottowa, Kansas, 1985.

Sarin, S. C., Professor of Industrial Systems Engineering, Virginia Tech, Personal Conversations, Feb 17, 1994.

Schetz, Joseph A., *Boundary Layer Analysis*, Prentice-Hall, Inc., 1993. p. 378.

Schetz, Joseph A., *Injection and Mixing in Turbulent Flow*, AIAA, N.Y., N.Y., 1980. pp. 111-112.

Simpson, R. L., Professor of Aerospace and Ocean Engineering, Personal Conversations, Virginia Tech, 1993.

Soloman, S. and D. Albritton, "Time Dependent Ozone Depletion Potentials For Short - and Long-Term Forecast," *Nature*, Vol. 357, May 7, 1992. pp. 33-37.

Svitil, K. "Holey War," *Discover*, Jan. 1993. pp. 75-76.

USRA/NASA, Undergraduate Design Team, "Design of a Vehicle Based System to Prevent Ozone Loss," Virginia Polytechnic Institute and State University, Blacksburg, VA, 1993.

Virginia Tech Aircraft Structures Course Notes, 1990.

Virginia Tech Thin Walled Structures Course Notes, 1991.

Wayne, Richard P., *Chemistry of Atmosphere 2nd Edition*, Clarendon Press, Oxford, 1991.

Zurer, Pamela, "Ozone Depletion's Recurring Surprises Challenge Atmospheric Scientists," *Chemical & Engineering News*, May 24, 1993. pp. 8-18.